LIFE TERRACESCAPE

"Employing Land Stewardship to transform terraced landscapes into green infrastructures to better adapt to climate change"

ACTION C5
Report on current climate of, and future projections for, the Aegean and Andros Island

Deliverable 1

Version 2 - January 2019

The LIFE16 CCA/GR/000050 project is implemented by the University of the Aegean, Municipality of Andros, Green Fund, National and Kapodistrian University of Athens, Hellenic Agricultural Organization – DEMETER and National Observatory of Athens with the financial support of the European Union.

Table of Contents

FIGURES

TABLES

EXECUTIVE SUMMARY

This report is the first deliverable of action C.5, entitled «**Current climate & future projections**». Action C.5 is headed by the National Observatory of Athens (NOA) and runs from July 2018 until September 2021. Here we examine the potential future climate changes in Andros Island (fine resolution) and the wider Aegean (coarse resolution), using projections derived by state-of-the-art Regional Climate Model (RCM) simulations developed within the framework of EURO-CORDEX at a horizontal resolution of approximately 12km.

The RCA4 regional climate model SMHI with boundary conditions from the global HadGEM-ES model of the Met Office Hadley Centre (MOHC) was found to give the best results for the Aegean region; accordingly, this model was selected for providing simulations.

Fine-resolution projections for Andros Island: approach. Model output of daily temperature and daily total precipitation for the closest model grid point to the study region of Andros Island were extracted. Results are presented for the control period (1971-2000) and the near- and distant future periods (2031-2060 and 2071-2100, respectively). Two new IPCC emissions scenarios are implemented in the future simulations, the weak climate change mitigation scenario (RCP4.5) and the non-mitigation business as usual scenario with high emissions (RCP8.5).

The bias-correction procedure of the climate model uses the general Cumulative Distribution Function transform method (CDFt). Long-term meteorological data sets are essential for this bias-correction procedure. The Aegean islands are not covered by the daily gridded pan-European E-OBS meteorological dataset, while long-term meteorological records are lacking for Andros Island. Detailed assessment proved that the long-term (1964-2014) Naxos meteorological station data may be used for the bias-correction procedure.

Coarse-resolution projections for the Aegean region: approach. Geographical maps for the Aegean depicting changes in coarse-resolution climatic indices at the horizontal resolution of ~12km were constructed based on model simulations. These model results could not be bias-corrected as the wider Aegean is not covered by the European gridded observational E-OBS database. Therefore, model data spanning 1950 to 2098 were split into a control period (1971-2000) and two future periods (2031-2060 and 2069-2098) under two IPCC emissions scenarios, namely the RCP4.5 and the RCP8.5, that were compared and evaluated.

For this report, climatic changes related to temperature and precipitation were studied using the following climatic indices: [1] Mean temperatures (absolute index), [2] Number of days with maximum temperature Tmax > 30 ^{o}C (threshold index; hot days), [3] Number of days Tmax> 35 ^{o}C (threshold index; heatwave), [4] Number of days with minimum temperature Tmin> 20 ^{o}C (threshold index; tropical night), [5] Total Precipitation -PR (absolute index, [6] Highest 1-day precipitation amount (absolute index), [7] Highest 5-day precipitation amount (absolute index), [9] Heavy precipitation days (PR>10mm/day; threshold index) and [10] Maximum length of dry spell (consecutive days PR<1mm; duration index).

First we summarise the simulation results for **Andros Island**, giving paired numbers: the first number refers to RCP4.5 and the second to RCP8.5.

Temperature increases in the near- and distant future are statistically significant under both emission scenarios, with the largest increases projected under the RCP8.5 scenario. T_{max} increases by 2-2,4 ^{o}C (near future) and 2,9-4,4 ^{o}C (distant future), and T_{min} by 2,2-2,7 ^{o}C (near future) and 3-4,9 ^{o}C (distant future). Seasonally, the largest temperature (T_{max} and T_{min}) increases are projected for summer and autumn; increases for winter and spring are about 1 ^{o}C lower under both emission scenarios.

The amount of **hot days** (T_{max}>30^{o}C) and **tropical nights** (T_{min}>20^{o}C) also incur statistically significant increases in the near- and distant future. Hot days increase in the near future by 23-32 days/year, and by 45-75 days/year in the distant future. Tropical nights, increase in the near future by 43-51 days/year, and by 57-82 days/year in the distant future. **Heatwaves** (T_{max}>35^{o}C) increase from 0,5 days/year to 2-6 days/year in the near future and 4-15 days/year in the distant future. The increase in heatwaves (T_{max}>35^{o}C) takes mainly place over future summers. Hot days (T_{max}>30^{o}C) over the control period are ~10/year; projected increases will mainly occur in summer, although 5-10 hot days/year may occur over autumn in the distant future. Of the ~85 tropical nights (T_{min}>20^{o}C) per year over the control period, ~70 occurred in summer and a~15 in autumn. In the near- and distant future, tropical nights will take place over the whole summer, and 10-20 days in spring to 40-60 days in autumn.

Total annual precipitation is set to decrease statistically significantly over the coming century under both emission scenarios. Annual precipitation over the control period (~450mm/year) is highly variable; future variability is set to increase. Total precipitation is projected to decrease by 17,7-13,2% in the near future, and by 18,9-23,8% in the distant future. Precipitation is set to decrease most over winter and autumn (25-34%). Spring precipitation (~60mm over the control period) is projected to decrease by ~10mm in the distant future. Total summer precipitation decreases from ~15mm to ~5mm in the near- and distant future, and becomes much more erratic.

Extreme precipitation events are not set to change statistically significantly in the future. However, the future variability of extreme precipitation events becomes greater. The relative magnitude of such events is increasing given the overall decrease in annual / seasonal precipitation.

Future simulations show **large, statistically significant, increases in the maximum length of dry spells** (with precipitation-PR < 1mm). Annually, the maximum average length of a dry spell was ~59 days over the control period. There are projected increases of 73 - 60 days in the near future, and of 72 - 83 days in the distant future. When there is a seasonal breakdown of dry spells, their length is 20 to 80 days in summer, and 5-30 days in all other seasons over the control period. In the near- and distant future period, dry spells in summer lasts 90 days (i.e. the entire season), while the length of dry spells in spring vary from 20-90 days, and 10-50 days over winter and autumn.

Coarse-resolution simulation results for the wider Aegean Region show similar changes in selected climate indices as summarized above for Andros Island, although specific values vary considerably across the region.

The annual averaged **maximum** and **minimum temperatures** are set to increase across the wider Aegean region in the near- and distant future, especially under the RCP8.5 climate change scenario. Temperature increases are in the range of 4-6^{o}C, and are largest in the E Aegean and least in the north. All extreme temperature indices are projected to increase considerably in the future. **Hot days** (T_{max}>30^{o}C) are to increase three- to six-fold, reaching up to 75-80 days/year in the E-N Aegean in the distant future. **Heatwave** days (T_{max} >35^{o}C) show also large increases, counting 30-50 days/year in the distant future; lowest values are registered for the Cyclades / Crete and the highest for the Dodecanese / N Aegean. **Tropical nights** (T_{min}>20^{o}C) are to double and triple in the near- to distant future for all Aegean Islands.

Total **annual precipitation** is to decrease significantly in the distant future across the region, by 15-25%, while large differences remain between- and within islands determined by geographical position and mountain height. **Extreme** precipitation indices only show minor decreases in the near- and distant future, while the maximum 1-day precipitation amount even records a minor increase in the distant future. The maximum **length** of **dry spells** (PR<1mm) shows large increases across the Aegean under both RCP scenarios. This length will double in the N Aegean / Crete and increase by 50% in the SE Aegean.

Based on these simulations, it is recommended that heat and drought-resistant varieties of crops without the need for irrigation should be prioritized and promoted in climate-proof island agriculture.

1. INTRODUCTION

This report is the first deliverable of action C.5, entitled «**Current climate & future projections**». This action is headed by the National Observatory of Athens (NOA) and runs from July 2018 until September 2021.

This action aims to use state-of-the-art regional climate models for a climate change vulnerability assessment of Andros Island and other Aegean islands (Cyclades and Dodecanese), in order to identify regions most at risk to adverse climate change impacts and to prioritize future interventions / adaptations. Specific attention will be paid to climate change indices that are relevant to agricultural activities. Projections of current and future climate change will focus on the Aegean Islands (coarse resolution) and Andros Island (fine resolution).

Geographical maps for the Aegean depicting changes in coarse-resolution climatic indices at the horizontal resolution of ~12km will be constructed based on the simulations from a Regional Climate Model (RCM). These model results cannot be bias-corrected as Andros Island and the wider Aegean are not covered by the European gridded observational E-OBS database. Therefore, model data spanning 1950 to 2098 have been split into a control period (1971-2000) and two future periods (2031-2060 and 2069-2098) under two IPCC emissions scenarios, namely the RCP4.5 representing a medium mitigation scenario and the RCP8.5, representing a high emission scenario with no climate mitigation policies. Differences between control and future periods were analysed in order to identify changes in climate indices, which directly or indirectly affect agriculture in the examined areas.

Initially this study intended to employ statistical downscaling techniques to provide higher resolution output (in the order of 1km) of gridded observational data of temperature and precipitation for the island of Andros. However, in absence of gridded observational E-OBS data, and thus the impossibility to bias-correct the model data, this method is not feasible. Instead, it was decided to use the long-term climate record from the Naxos meteorological station supported by the short-term Andros meteorological station record for bias-correction of the model data. This approach significantly improves the future fine-resolution climate projections, but also means that results are presented in the form of graphs and tables instead of maps covering Andros Island.

The structure of this report is as follows: here, in Chapter 1 the general background to historical and future climate change in southern Europe and the east Mediterranean region, in particular, are presented. In chapter 2 the data and methods used in this study are discussed. Chapter 3 presents the fine-resolution simulation results, starting with an evaluation of historical climate conditions in the central-eastern Aegean region, and continuing with future climate projections for Andros Island. Subsequently, in chapter 4, coarse resolution climate simulations for the wider Aegean region are presented in maps covering the control-, near and distant future periods; the results are briefly discussed. Finally, chapter 5 summarises the main conclusions of this study.

1.1 Background to Mediterranean climate change

The wider Mediterranean region has been identified as one of the main climate change hot-spots (Giorgi, 2006), being one of the most responsive areas to climate change globally. A number of scientific initiatives and projects have been recently undertaken to assess the possible changes that anthropogenic global warming might induce in the climate of the Mediterranean basin. Scenario simulations aimed at quantifying the possible future climate change in the European and Mediterranean region have been designed and performed in the framework of EU funded projects such as FP6 PRUDENCE, ENSEMBLES and CIRCE.

Mediterranean temperatures are projected to rise significantly by the end of the 21st century, while precipitation-PR is set to decrease (Giorgi and Bi, 2005; Giorgi and Lionello, 2008; Zanis et al., 2009). Hertig and Jacobeit (2008) showed temperature increases for the whole Mediterranean area for all months of the year in the period 2071–2100 compared to 1990–2019. This projected temperature increase varied strongly, depending on region and season; substantial temperature changes of locally more than 4^{o}C by the end of the century were found. Kostopoulou et al. (2014) indicated a statistically significant future warming trend for the Eastern Mediterranean (EM) region over the final 30 years of the 21st century. The annual trend patterns for both minimum -T_{min} and maximum-T_{max} temperature showed warming rates of approximately 0.4 – 0.6 ^{o}C per decade.

Studies focusing on changes in temperature and rainfall extremes project that heat stress (Diffenbaugh et al., 2007; Kuglitsch et al., 2010) and the duration of drought periods (Goubanova and Li, 2007) will drastically increase in the Mediterranean region in the future. Hot summer conditions that rarely occurred in the reference period may become the norm by the middle and the end of the 21st century (Founda and Giannakopoulos, 2009; Tolika et al., 2009). Giannakopoulos et al. (2009) found that one week of additional dry days will be evident in 2031-2060 along the coast of the already dry southeastern basin. Moreover, Oikonomou et al. (2008) found that the highest increase of dry spell length is expected during the period 2071-2100 in winter and spring in the southern part of the EM basin. These changes are expected to have a significant impact on the region's ecosystems, as well as on a number of sectors and implications of human activity (e.g. health, agriculture, tourism, energy demand, natural disasters, loss of biodiversity, etc.).

Similar results have been found for the Cyprus area in the framework of LIFE CYPADAPT (LIFE10ENV/CY/000723) project. In particular, in the period 2021-2050, a continual, gradual and relatively strong warming of about 1.0 to 2.0 ^{o}C is projected compared to the reference period (1961- 1990), while maximum and minimum seasonal temperatures appear to increase most in the continental part of Cyprus. Heatwave days (Tmax>35 ^{o}C) are expected to increase up to one month per year in inland and mountain regions. Moreover, an increase of about 10 days in the number of dry days per year, as well as in the length of dry spell is expected (CYPADAPT, 2013). For the island of Crete, an increase of 10 days per year in the number of hot (daily maximum temperature greater than 30 ^{o}C) and dry (daily precipitation less than 1mm) days, by 2050 compared to the reference period (1961-1990), is projected by the EU FP7 CLIMRUN project using RACMO2 RCM projections under A1B IPCC emission scenario.

According to the European Environment Agency (EEA 2017 and references therein), annual precipitation since 1960 shows a decrease of up to 90 mm per decade in parts of southern Europe. Mean summer precipitation has significantly decreased by up to 20 mm per decade in most of southern Europe. Projected future changes in precipitation vary substantially across Mediterranean regions and seasons. Annual precipitation is generally projected to decrease, with the projected decrease strongest in summer.

Future changes in extreme hydrometeorological events are also of great concern for the society (Oki and Kanae, 2006; Pall et al., 2011; Min et al., 2011). Past trends suggests that extreme precipitation events have become more intense and more frequent in Europe on average, but there are important differences across regions, seasons, time periods, extreme precipitation indices and underlying datasets (González Hidalgo et al., 2003; Mudelsee et al., 2003; Moberg and Jones, 2005; Nastos and Zerefos, 2007; Karagiannidis et al., 2012; Zolina, 2012). For instance, Karagiannidis et al. (2012) studied the trends in extreme precipitation for the period of 1958–2000, finding decreasing trends in southern Europe and increasing trends on continental Europe as a whole from September to February. Tank and Können (2003) found indices of wet extremes increasing during the 1946–1999 period, although the spatial coherence of the trends was low. Moberg and Jones (2005) also found a significant increase in precipitation intensity over the 20th century during the winter.

Climate change is expected to strongly affect agriculture, as it directly depends on climatic factors such as temperature, sunlight and precipitation for its viability. In southern Europe and the Mediterranean region in particular, the negative impacts of climate change include reduced crop yields due to high temperatures, increased water demand for irrigation and reduced water availability due to prolonged periods of droughts and water scarcity which will in turn lead to conflicting water demands between agriculture and other usage. In the EU, as reported by the PESETA II (JRC, 2014) research project, crop production may, depending on the scenario, drop by 0-27% in Southern Europe. Negative effects on agriculture will be exacerbated by damages to crops caused by extreme weather events. Climate change may also impact on soil fertility, for example, through increased removal of soil organic matter due to rising temperatures and higher risk of soil erosion linked to droughts and extreme precipitation changes. Adverse impacts can also be expected from the likely proliferation of pests, diseases, and weeds due to higher temperatures and humidity.

2. DATA & METHODS

The Aegean islands are not covered by the daily gridded pan-European E-OBS meteorological dataset. Therefore, providing coarse-resolution simulations for the entire Aegean region would be futile as climate model simulations cannot be validated with historical data, except for the single long-term dataset from the Naxos Island meteorological station. Any model simulation covering the entire region would therefore provide the same pattern of climate change as it would be validated against the same record. This would be a pointless exercise. Given these limitations, and taking into account that only measurements of temperature and precipitation were available from meteorological stations of nearby areas, it has been decided that future climate simulations will only cover Andros Island.

2.1 Regional Climate Models (RCMs)

Data regarding precipitation and temperature were retrieved and evaluated from a set of four state-of-the-art RCM simulations carried out in the frame of **EURO-CORDEX** (Coordinated Regional Climate Downscaling Experiment), with a horizontal resolution of about 12km (0.11°). Specifically, these four regional climate model experiments are:

The RCA4 regional climate model of the Swedish Meteorological and Hydrological Institute (SMHI) driven by 3 different global climate models: **[1]** the CNRM-CM5 of the Météo France Institute, **[2]** the HadGEM-ES of the Met Office Hadley Centre (hereafter MOHC; UK), and, **[3]** the MPI-ESM-LR of the Max Planck Institute (hereafter MPI) for Meteorology (Germany). These three simulations are basically the SMHI regional climate model with boundary conditions from three different global models (CNRM, MOHC, and MPI), which makes the combined modeling systems substantially diverse so as to be considered as different models. **[4]** The regional climate model ALADIN (version 5.2) of the Météo France Institute driven by the CNRM-CM5.

Following the evaluation of all four climate simulations, it was decided to proceed with the model giving the best results for the Aegean region, namely the RCA4 regional climate model SMHI with boundary conditions from the global HadGEM-ES model of the Met Office Hadley Centre (MOHC). Model output of daily temperature and daily total precipitation for the closest model grid point to the study region of Andros Island were extracted. Results are presented for the control period (1971-2000) and the near future and distant future periods (2031-2060 and 2071-2100, respectively). Non-parametric boot-strap testing (with confidence intervals at the 95th percentile) were employed (for its robustness) to detect statistically significant changes between the data-sets from the reference period and the distant future (Diciccio 1996, Varotsos *et al*. 2013).

2.2 Meteorological data for model evaluation

There is a clear advantage in using daily gridded E-OBS meteorological data set for model evaluation in Europe due to its spatial and temporal coverage (Haylock et al., 2008). However, several studies have questioned the quality of E-OBS in regions of sparse station density and particularly regarding daily extremes (Bellprat et al., 2012a; Herrera et al., 2012; Hofstra et al., 2009, 2010; Kotlarski et al., 2014; Kyselý and Plavcová, 2010; Maraun et al., 2012; Rajczak et al., 2013). High deviations were found in areas with low density of stations and in areas with complex terrain where interpolation usually degrades (Hanel and

Buishand, 2011; Kyselý and Plavcová, 2010). One such area with complex terrain is the Aegean region, which our evaluation found not to be covered by E-OBS data.

As E-OBS data cannot be used as observational reference for evaluating simulated temperature and precipitation results, this study followed two different approaches: one for the coarse-resolution climate projections covering the Aegean and another one for the fine-resolution climate projections for Andros Island. The **coarse-resolution** analyses did not employ any form of bias-correction in the absence of gridded E-OBS data. These analyses are therefore entirely based on climate model data that are available for a continuous period spanning from 1950 to 2098. Geographical maps are used to present the results for the control period (1971-2000), and the "near future" period (2031-2060) and the ''distant future'' period (2069-2098) under two new IPCC emissions scenarios, namely the RCP4.5 and the RCP8.5.

The **fine-resolution** analyses covering Andros Island had to rely on data sets from local meteorological stations for bias-correction. Accordingly, model evaluation relied upon daily measurements of mean, maximum and minimum air temperature that were obtained from the National Meteorological Service (HNMS) and the National Observatory of Athens (NOA) for the Naxos and Andros stations, respectively, covering the periods 2011-2017 and 1964-2014. Both of the stations are located close to the seashore (Fig. 1). Andros is located directly east of the mainland and its climate is subjected to continental influences, while Naxos is located in the central Aegean and its climate is more representative for this region. The data-set from Andros is too short for model evaluation, which is why the Naxos data set was selected for this purpose. In order to assess whether data from this station are representative for Andros Island, the data from these stations –as well as data from Elliniko station- were correlated. The Elliniko meteorological station in eastern Attika (HNMS) has a long record (1964-2014) and is located directly east of Andros Island (Fig. 1). The good correlation of temperature and precipitation data between all of these stations means that the Naxos meteorological data set can be used for evaluation of the model simulations.

The Naxos meteorological station is located at the airport **(Lon:** 25.383, **Lat:** 37.100, **Alt:** 9m), on an open plain near the east-coast of the island. The Andros meteorological station is located at the port of Gavrio (Liopesi) on the top of a building (**Lon:** 24.739, **Lat:** 37.880, **Alt:** 16m), at the mouth of a deep valley in the mountainous east-coast of the island. Naxos climate is strongly affected by the sea breeze and Etesian winds, which are a dominant weather influence in the Aegean Basin. Finally, the Elliniko meteorological station (**Lon:** 23.736, **Lat:** 37.889, **Alt:** 43m) is located in on the mainland near Athens, in SE Attika. Figure 1 shows the location of the respective meteorological stations.

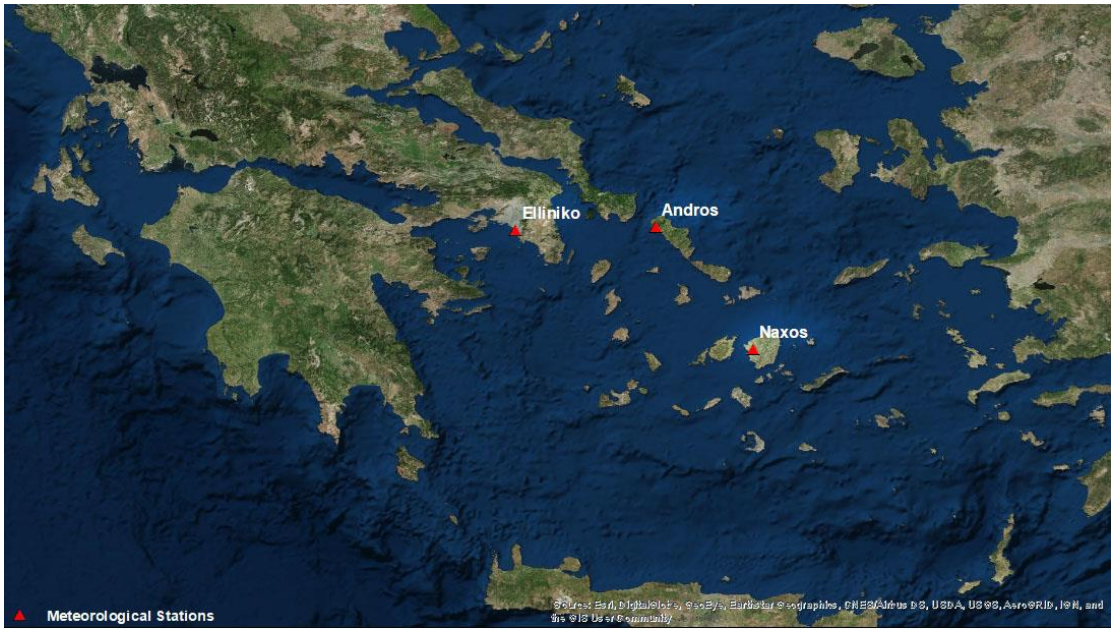

Figure 1 Map of southern Greece and the Aegean, showing the locations of the meteorological stations of Andros Island, Naxos Island and Elliniko (SE Attika).

2.3 Evaluation model and bias correction

Only the fine-resolution climate projection covering Andros Island was subjected to bias-correction (see explanation in section 2.2 above). The bias correction methodology used in this study is the general Cumulative Distribution Function transform method (CDFt), developed by Michelangeli et al. (2009). For detailed explanation of the method, see Vrac et al. (2012). CDFt assumes a reference period over which observational data are available. The reference period selected for this report is the historical period 1971 - 2000. Observational climate data, covering this period, are provided by the meteorological station of Naxos Island (section 2.2).

The CDFt method builds quantile transformations functions between future and historical simulations, and between historical simulation and observation - based data (https://cse.ipsl.fr/attachments/article/128/BCCORDEX.pdf).

2.4 RCP scenarios

Two new IPCC emissions scenarios are implemented in the future simulations (up to 2100), the weak climate change mitigation scenario (RCP4.5) and the non-mitigation business as usual scenario with high emissions (RCP8.5). With the Intergovernmental Panel on Climate Change's (IPCC) release of the Fifth Assessment Report (AR5; IPCC, 2013) the so-called representative concentration pathway (RCP) scenarios have been introduced which specify GHG concentrations and corresponding emission pathways for several radiative forcing targets.

The **RCP 4.5** was developed by the GCAM modeling team at the Pacific Northwest National Laboratory's Joint Global Change Research Institute (JGCRI) in the United States. It is a stabilization scenario in which total radiative forcing is stabilized shortly after 2100, without overshooting the long-run radiative forcing target level (Clarke et al. 2007; Smith and Wigley 2006; Wise et al. 2009). This scenario also suggests that various climate policies are implemented (Thomson et al., 2011).

The **RCP 8.5** was developed using the MESSAGE model and the IIASA Integrated Assessment Framework by the International Institute for Applied Systems Analysis (IIASA), Austria. This RCP is characterized by increasing greenhouse gas emissions over time, representative of scenarios in the literature that lead to high greenhouse gas concentration levels (Riahi et al., 2007). It represents a future state where no climate policies aiming at the reduction of GHG emissions are implemented (van Vuuren et al., 2011).

2.5 Climate Indices

Climatic changes related to temperature and precipitation will be studied using appropriately constructed climatic indices. There are three principal types of indices:

- **Absolute indices** (for example, mean seasonal temperature and annual total precipitation)
- **Threshold indices** (for example, number of days with maximum/minimum temperature greater/less than specific thresholds)
- **Duration indices** (for example, quantifying the number of consecutive wet or dry days)

For this report, the following indices were selected:

Temperature

- Mean temperatures (absolute index). Seasonal and annual sums;
- Number of days Tmax> 30 ^{o}C (threshold index; hot days). For daily maximum temperature (annual/seasonal);
- Number of days Tmax> 35 ^{o}C (threshold index; heatwave). For daily maximum temperature (annual/seasonal);
- Number of days Tmin> 20 ^{o}C (threshold index; tropical night). For daily minimum temperature (annual/seasonal);
- Number of days with Tmin<3°C (spring threshold index). Related to late frost and crop damage (seasonal; during spring).

Precipitation

- Total Precipitation (absolute index). Seasonal and annual sums
- Highest 1-day precipitation amount (absolute index). Maximum (annual/seasonal) precipitation sums for 1-day intervals
- Highest 5-day precipitation amount (absolute index). Maximum (annual/seasonal) precipitation sums for 5-day intervals.
- Heavy precipitation days (threshold index). Number of days (per year/season) with precipitation amount greater than 10 mm
- Very heavy precipitation days (threshold index). Number of days (per year/season) with precipitation amount greater than 20 mm
- Maximum length of dry spell (duration index). Maximum length of consecutive days with precipitation < 1 mm (per year / season)

3. RESULTS: fine-resolution projection for Andros Island

This section starts with the analyses of selected climate indices (section 2.5) from the meteorological stations of Naxos (record spanning 1964-2014) and Andros (record spanning 2011-2017). Subsequently, the temperature and precipitation patterns of different meteorological stations, spanning the central Aegean to eastern Attika, are compared to justify the use of the Naxos climate data for the bias-correction of the climate change model (sections 2.1 and 2.3). Finally, selected climate indices of the climate simulations are analysed.

3.1 Analysis of historical climate conditions

Annual, seasonal and extreme temperature and precipitation data have been evaluated for the Andros and Naxos climate records. Temperature data show a very similar pattern between stations, although actual values for Andros are higher. Precipitation data are much weaker correlated, but this is likely a function of the few years that are overlapping between the meteorological stations of Andros and Naxos islands. However, meteorological station data from Elliniko (Eastern Attika) prove that the longer-term precipitation patterns are similar between these islands.

3.1.1 Annual and seasonal temperature data

The pattern of average mean (TG), maximum (TX) and minimum (TN) air temperature of the meteorological stations of Naxos and Andros is quite similar, both on an annual (Fig. 2) and seasonal basis (Figs. 3-6). Higher temperatures in Andros Island, from springtime until autumn, are likely explained by the different station settings and available timeseries (section 2.2). The long-term temperature record from Naxos islands (first panel, Figs. 2-5) indicates a steady increase over all seasons over the period 1964-2014, in line with regional findings (see section 1 for discussion and references).

Mean Annual Cycle

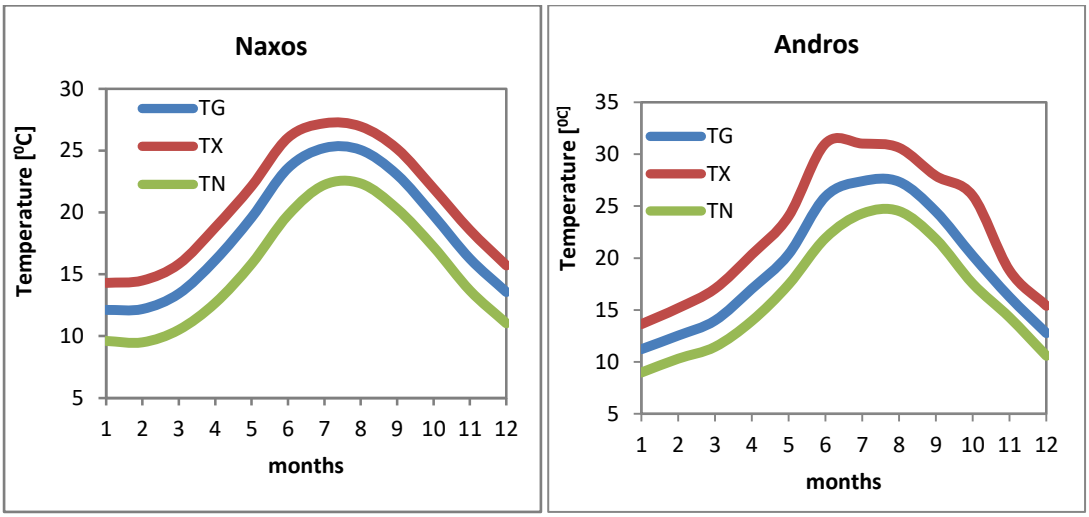

Figure 2 Observed monthly average air temperatures in Naxos station (left panel), and Andros station (right panel) for the period 1964-2014 and 2011-2017, respectively. Red, blue and green curves depict the maximum, mean and minimum temperature, respectively.

Seasonal Trends

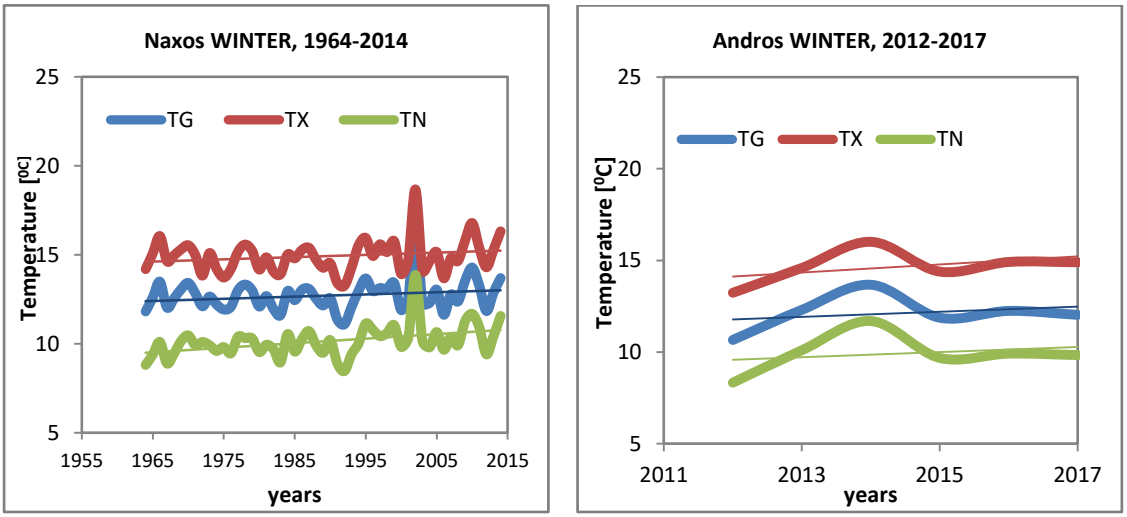

Figure 3 Average annual winter temperatures at Naxos station (left panel), and Andros station (right panel) during the period 1964-2014 and 2012-2017, respectively. Red, blue and green curves depict the maximum, mean and minimum temperature, respectively.

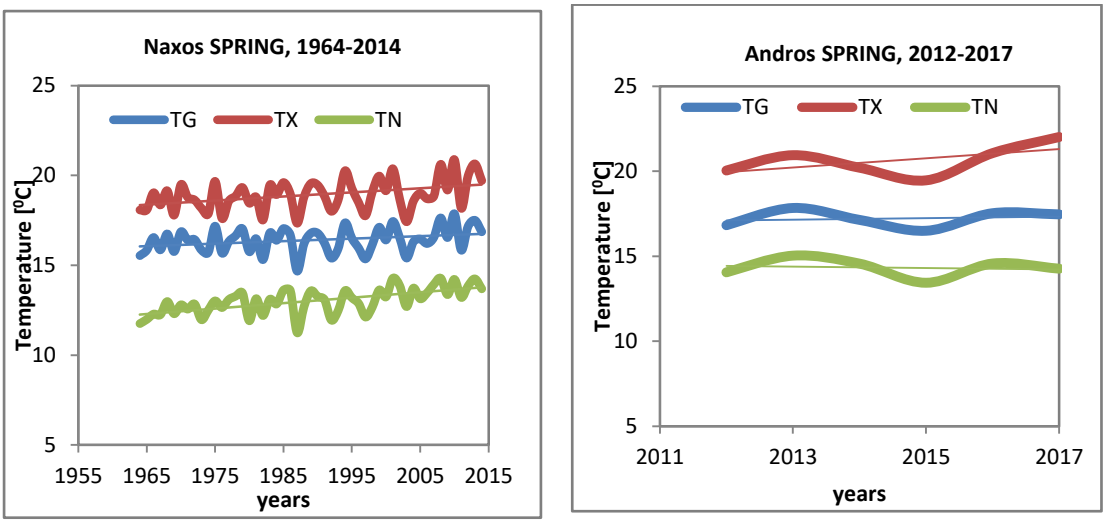

Figure 4 **Average annual spring temperatures at Naxos station (left panel), and Andros station (right panel) during the period 1964-2014 and 2012-2017, respectively. Red, blue and green curves depict the maximum, mean and minimum temperature, respectively.**

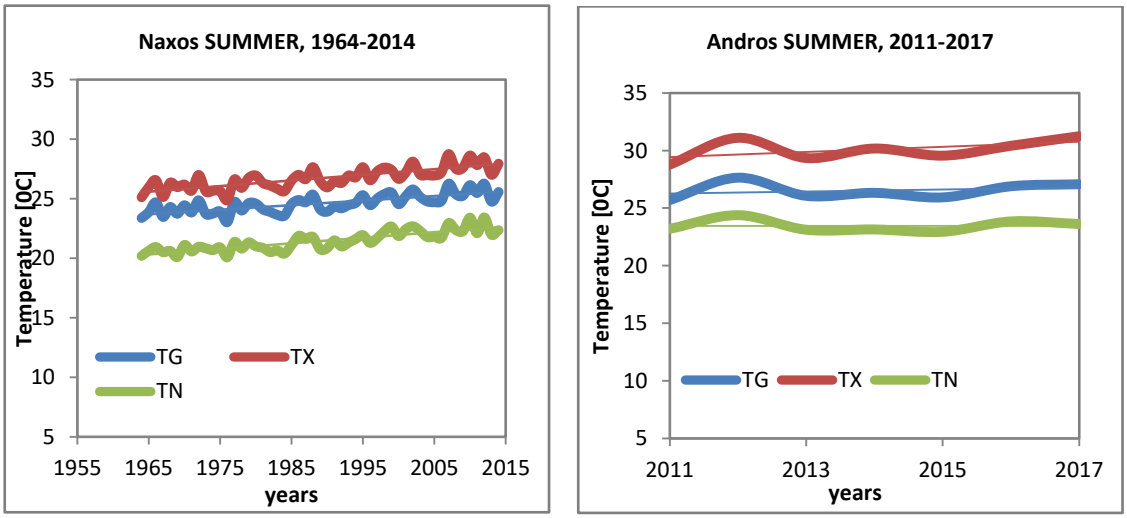

Figure 5 **Average annual summer temperatures at Naxos station (left panel), and Andros station (right panel) during the period 1964-2014 and 2011-2017, respectively. Red, blue and green curves depict the maximum, mean and minimum temperature, respectively**

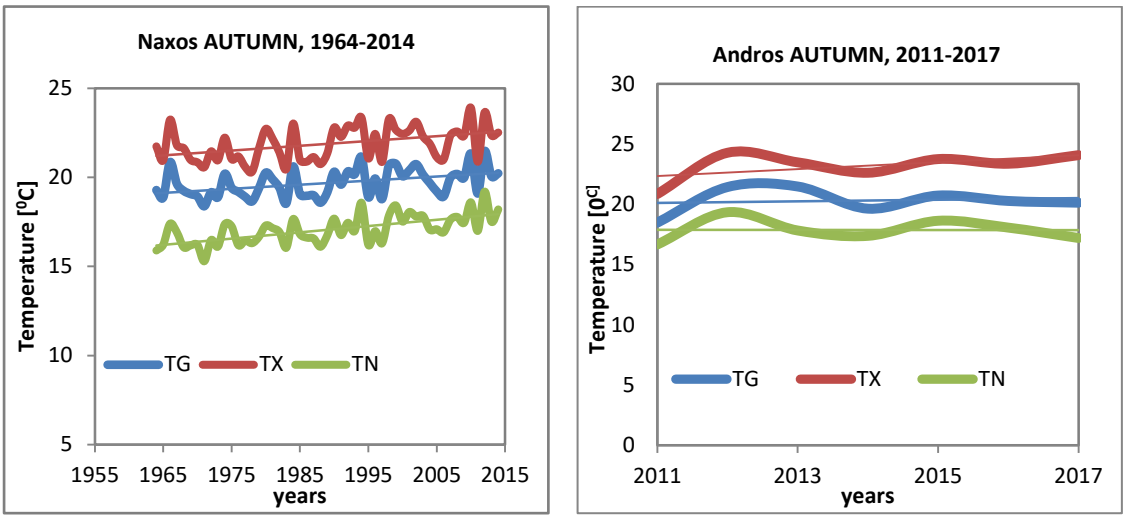

Figure 6 Average annual autumn temperatures at Naxos station (left panel), and Andros station (right panel) during the period 1964-2014 and 2011-2017, respectively. Red, blue and green curves depict the maximum, mean and minimum temperature, respectively.

3.1.2 Extreme temperature results

The number of hot days (Tmax > 30°C) are quite variable from year-to-year, but appear to increase over the long-term record (spanning 1964-2014) of Naxos Island (Fig. 7; Tables 1 & 2). The number of days characterized by a heatwave (Tmax > 35°C) is relatively small, and to few data are thus available for a meaningful statistical analysis of this index. Tropical nights (Tmin > 20°C) similarly appear to increase over the long-term (Fig. 8; Tables 1 & 2). Spring temperatures characterized by Tmin < 3°C (leading to crop damage) are virtually non-existent at the station sites; this index is only registered occasionally and not every year in winter (Tables 1 & 2). This index is therefore not relevant for further analyses.

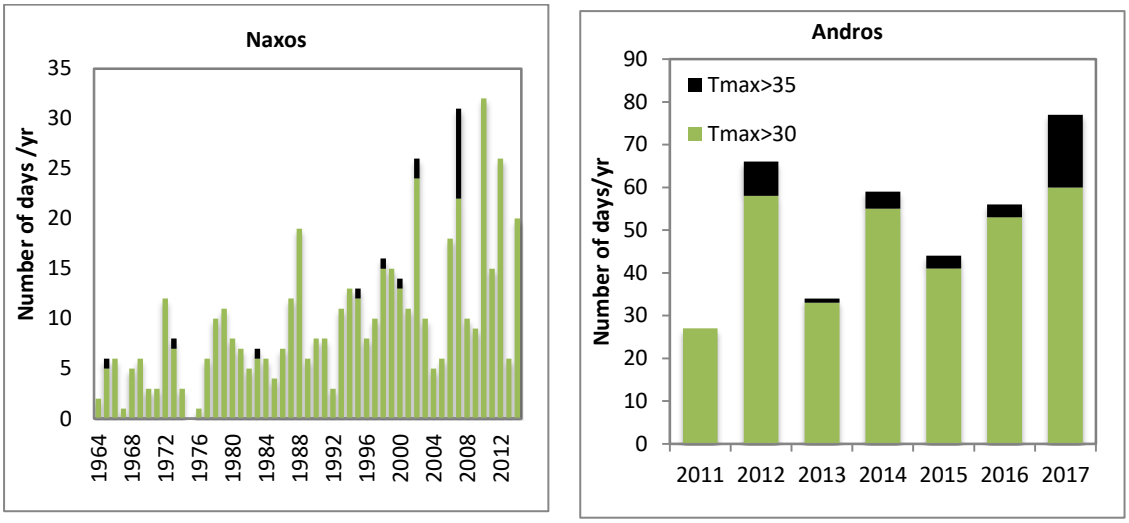

Figure 7 Annual number of daily maximum temperatures greater than 30^{O}C (green bars) and 35^{O}C (black bars) at Naxos station (left panel) and Andros station (right panel), during the period 1964-2014 and 2011-2017, respectively.

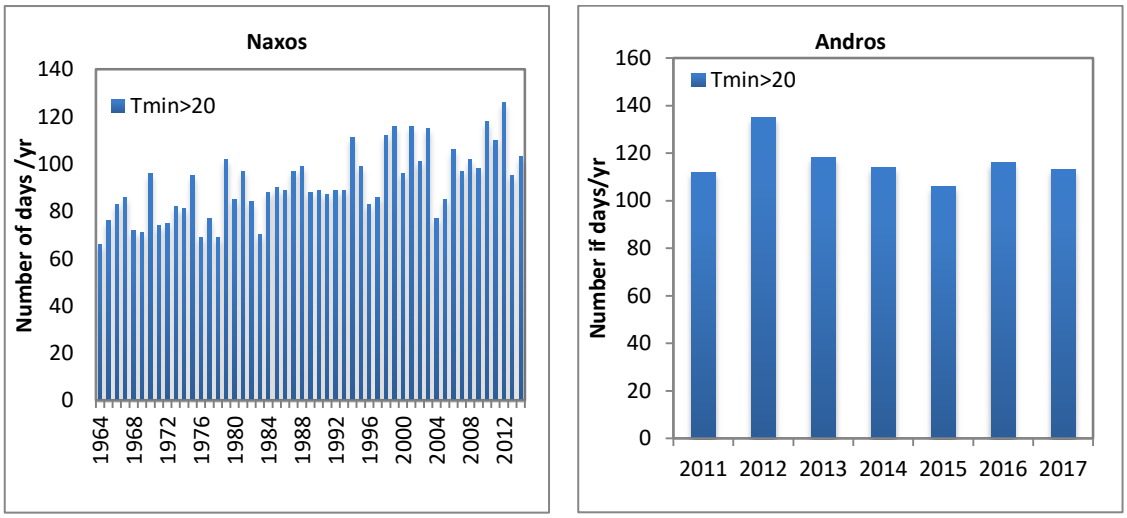

Figure 8 Annual number of daily minimum temperatures greater than 20^{O}C (at Naxos station (left panel) and Andros station (right panel), during the period 1964-2014 and 2011-2017, respectively.

Table 1 Annual number of days with temperatures exceeding specific indices for Andros Island (2011-2017)

Andros- Number of days/year with				
Year	Tmax>30°C	Tmax>35 °C	Tmin>20 °C	Tmin<3 °C
2011	27	0	112	0
2012	58	8	135	7
2013	33	1	118	2
2014	55	4	114	0
2015	41	3	106	9
2016	53	3	116	2
2017	60	17	113	3

Table 2 See next page: annual number of days with temperatures exceeding specific indices for Naxos Island (1964-2014)

NAXOS- Number of days/yr with				
Year	Tmax>30°C	Tmax>35 °C	Tmin>20 °C	Tmin<3 °C
1964	2	0	66	4
1965	5	1	76	1
1966	6	0	83	1
1967	1	0	86	6
1968	5	0	72	3
1969	6	0	71	0
1970	3	0	96	0
1971	3	0	74	0
1972	12	0	75	0
1973	7	1	82	0
1974	3	0	81	2
1975	0	0	95	0
1976	1	0	69	3
1977	6	0	77	0
1978	10	0	69	0
1979	11	0	102	0
1980	8	0	85	1
1981	7	0	97	1
1982	5	0	84	0
1983	6	1	70	6
1984	6	0	88	0
1985	4	0	90	1
1986	7	0	89	0
1987	12	0	97	6
1988	19	0	99	1
1989	6	0	88	0
1990	8	0	89	0
1991	8	0	87	0
1992	3	0	89	2
1993	11	0	89	0
1994	13	0	111	0
1995	12	1	99	0
1996	8	0	83	0
1997	10	0	86	0
1998	15	1	112	0
1999	15	0	116	0
2000	13	1	96	0
2001	11	0	116	0
2002	24	2	101	0
2003	10	0	115	1
2004	5	0	77	4
2005	6	0	85	0
2006	18	0	106	0
2007	22	9	97	0
2008	10	0	102	3
2009	9	0	98	3
2010	32	0	118	0
2011	15	0	110	0
2012	26	0	126	1
2013	6	0	95	0
2014	20	0	103	0

3.1.3 Annual and seasonal precipitation data

Annual precipitation patterns between Naxos and Andros Islands are broadly similar (Fig. 9). Overall, Andros Island appears to be dryer; however, this is a very tentative observation as there are few overlapping years and the respective location of the stations may strongly influence local rainfall patterns. There are clear seasonal differences in precipitation: most rain falls in winter, followed by autumn and spring, while summer rainfall is very low to non-existent over most years (Fig. 10). There are no clear changes in long-term rainfall, but inter-annual variation is very large.

Mean Annual Cycle

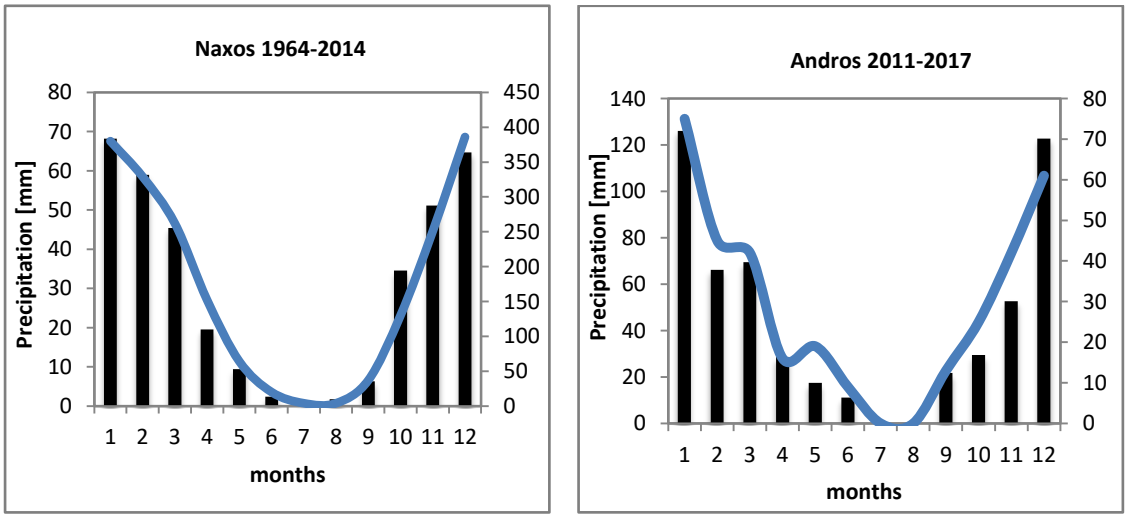

Figure 9 Monthly distribution of precipitation (black bars) and highest 1-day precipitation per month (blue curve) in Naxos (left panel) and Andros (right panel) meteorological stations, during the period 1964-2014 and 2011-2017, respectively.

Seasonal Trends

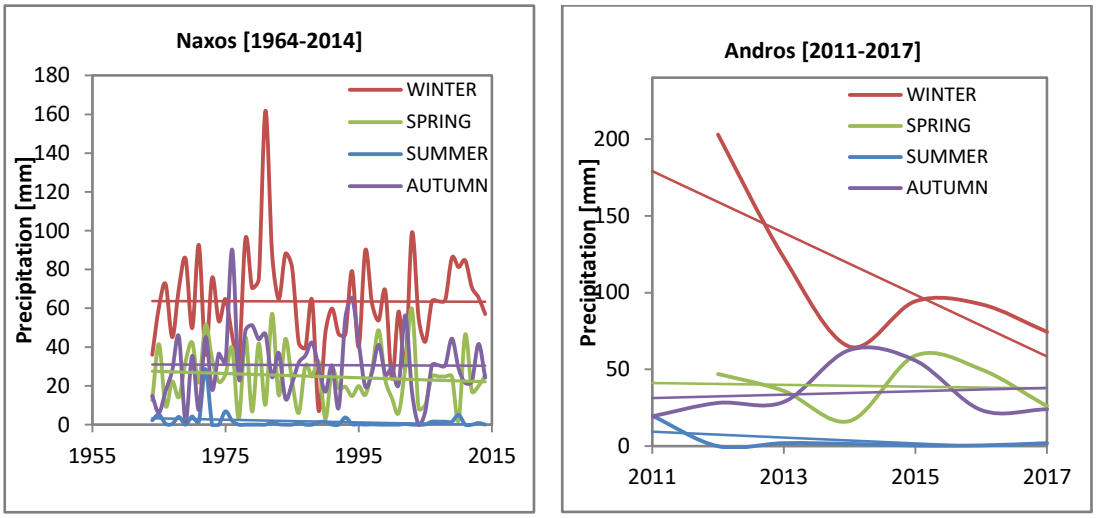

Figure 10 Seasonal trends for the total precipitation in Naxos (left panel) and Andros (right panel) over the periods 1964-2014 and 2011-2017, respectively.

3.1.4 Extreme precipitation results

Seasonal and extreme precipitation values are very different in Andros compared to Naxos for the years that the respective records overlap. This is no surprise, given the very high spatial precipitation variability in Greece, which is linked to its geography, topography and land-sea boundaries. This section focuses on extreme precipitation registered on Andros Island over the observation period.

The observational record of Andros is too short for a meaningful trend analysis. Extreme precipitation events have a high inter-annual (Fig. 11) and inter-seasonal (Figs. 12 & 13) variability. Indices registering maximum 5-day precipitation and days with very heavy precipitation (>20mm) show that such events are infrequent. Extreme precipitation events occur mainly in winter and occasionally in autumn and spring, and are very rare in summer (Figs. 12 & 13). The maximum amount of precipitation that may be falling over 1 day is quite similar across the autumn-winter-spring seasons, but much lower for the summer season (Fig. 12).

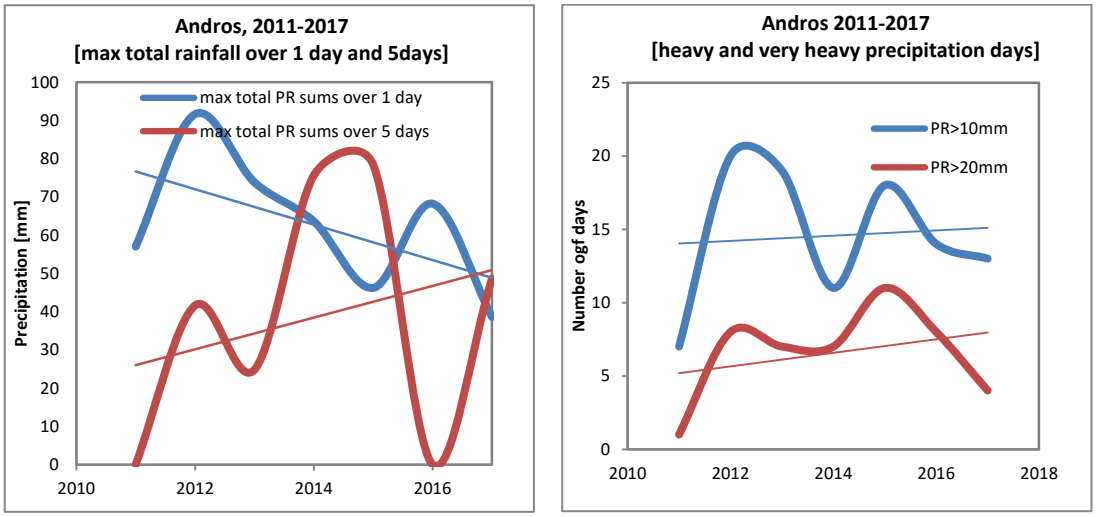

Figure 11 Left panel: Annual trends for the maximum total precipitation sums over 1 day (blue line, calculated slope s=-4.6) and 5 days (red line, calculated slope s=4.1) for Andros station during the period 2011-2017. Right panel: Annual trends for the number of days with precipitation greater than 10 mm (heavy precipitation days; blue line, calculated slope s=0.18) and 20mm (very heavy precipitation days; red line, calculated slope s=0.46) for Andros station during the period 2011-2017.

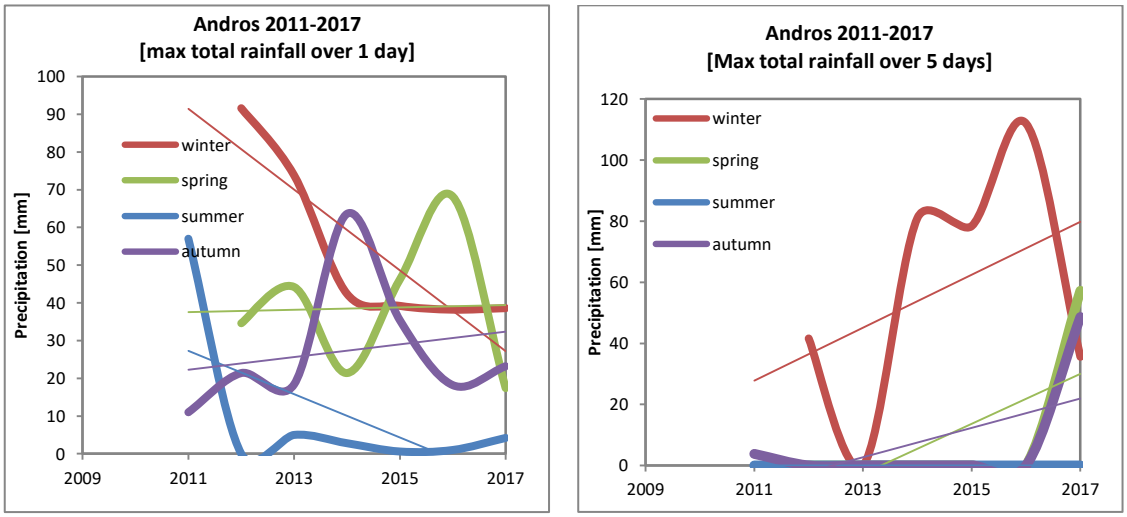

Figure 12 Left panel: Seasonal trends for the annual maximum total precipitation sums over 1 day for Andros station during the period 2011-2017 (calculate slopes: winter s=-10.7, spring s=0.3, summer s=-5.7, autumn s=1.7). Right panel: Seasonal trends for the annual maximum total precipitation sums over 5 day for Andros station during the period 2011-2017 (calculated slopes: winter s=8, spring s=8.1, summer s=0, autumn s=4.8).

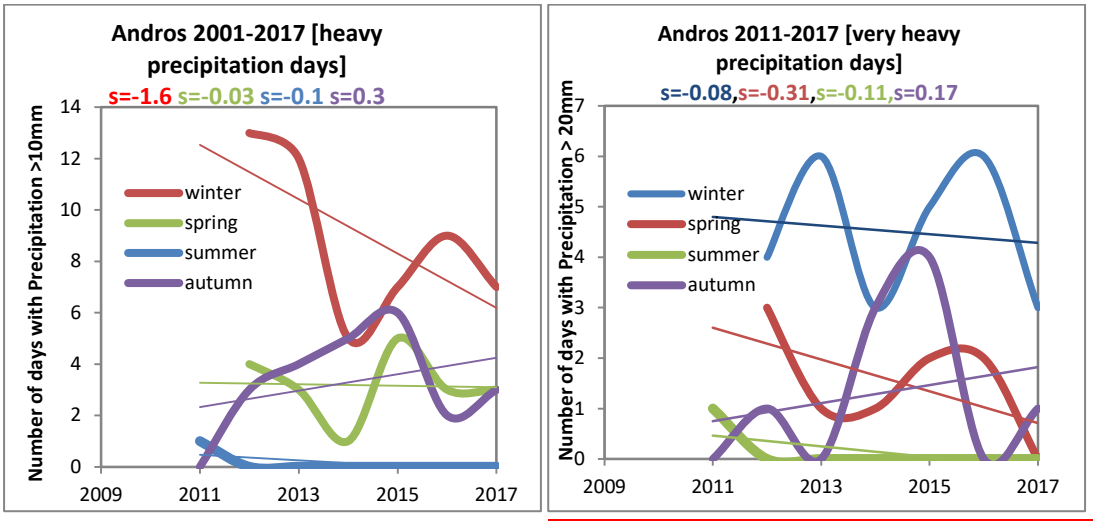

Figure 13 Seasonal trends for the annual number of days with precipitation amount greater than 10 mm (left panel) and 20 mm (right panel) for Andros station during the period 2011-2017. The colored numbers on the top indicate the calculated slopes for each one of the seasons.

3.1.5 Maximum duration of drought periods

The observational record of Andros is too short for a meaningful trend analysis of changes in the maximum length of annual dry spells (PR<1mm). Dry spells events have a high inter-annual variability (Fig. 14) and last between 80 to 140 days annually. These spells mostly cover summer and may incorporate part of spring and/or autumn. Dry spells in winter are rare; when occurring, they may last up to 30 days.

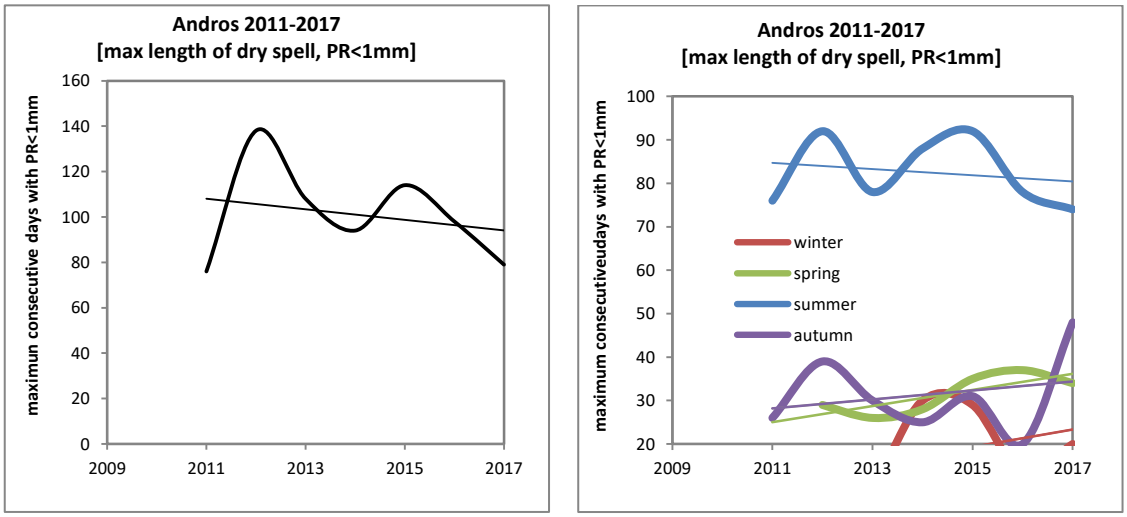

Figure 14 Left panel: annual trend for the maximum length of days with precipitation <1mm for Andros station during the period 2011-2017 (calculated slope: s=-2.3). Right panel: seasonal trends for the maximum length of days with precipitation < 1mm for Andros station during the period 2011-2017 (calculated slopes: winter s=2, spring s=1.8, summer s=-0.7, autumn s=1.04).

3.2 Comparison of meteorological station data

The bias correction of the chosen model (see sections 2.2 and 2.3) uses the long-term record of the Naxos meteorological station. The current section proves that this record is relevant for Andros Island given the similarities of the temperature and (long-term) precipitation patterns. Specifically, meteorological records from Naxos and Andros Islands, as well as precipitation data from the Elliniko meteorological station (section 2.2) are compared.

3.2.1 Observational temperature data: Naxos and Andros Islands

Overall, there is a good correlation between air temperatures on Naxos and Andros Islands. The average monthly mean temperature (Tmean) over the four seasons displays a similar pattern (Fig. 15). Temperatures that are registered at the meteorological station of Andros are higher during summer by up to 1,5°C, but close to the values registered at Naxos station during the other seasons. Correlations of seasonal averaged air temperature are good (R^2>0,88) across all seasons (Fig. 16). Correlations of seasonal maximum-T_{max} and minimum - T_{min} temperatures (Figs. 17 & 18) are also good, but have a slightly lower correlation coefficient. From autumn to spring T_{max} is well correlated (R^2>0,79), while showing a lower correlation value for summer (R^2=0,54). T_{min} also shows good correlations (R^2>0,70) from spring to autumn and is slightly lower for winter (R^2=0,62).

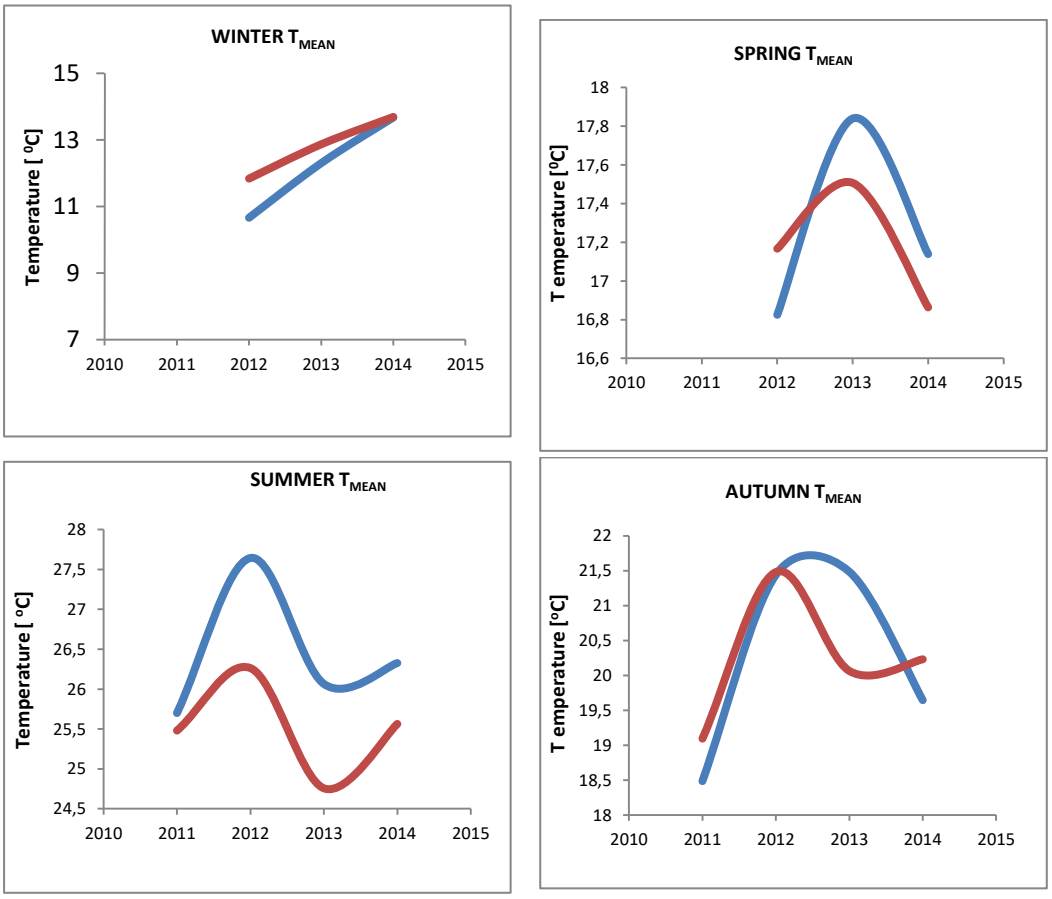

Figure 15 Comparison of the seasonal trends for the mean air temperature for Naxos (red lines) and Andros (blue lines) over the period 2011-2017.

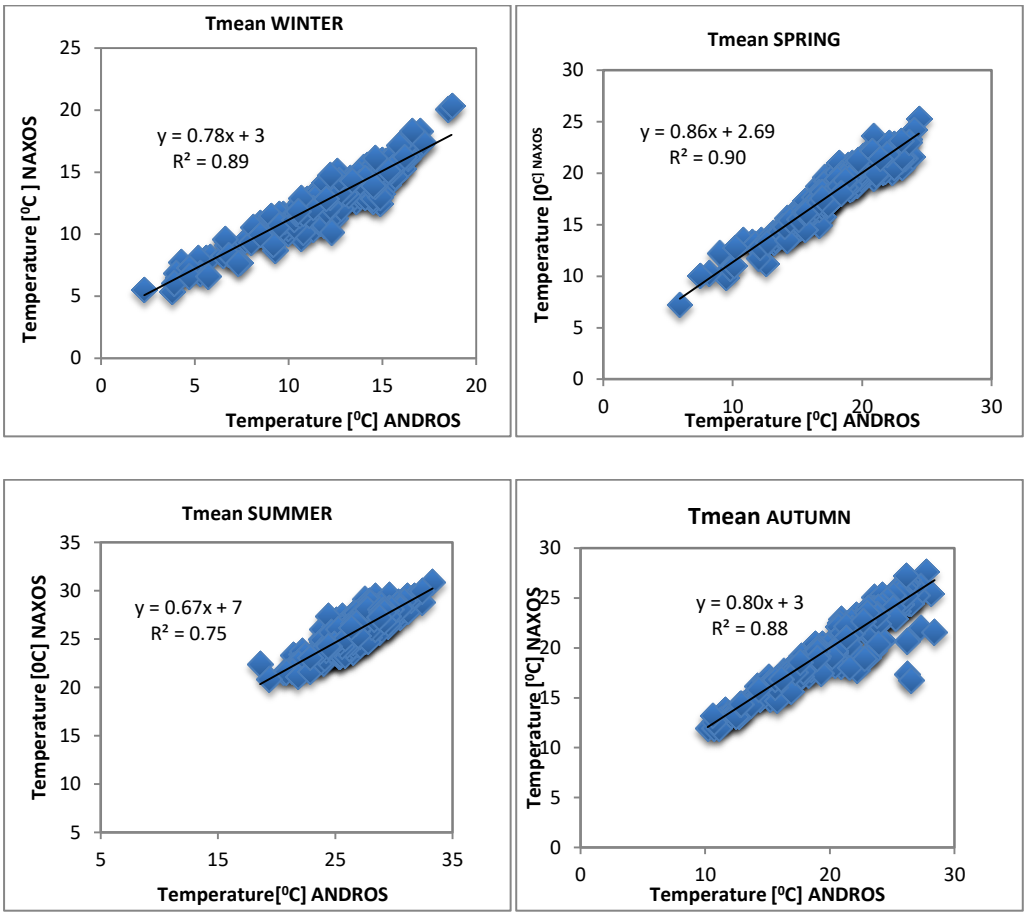

Figure 16 Correlation of the seasonal mean air temperatures of Naxos (y axis) and Andros (x axis) Islands over the period 2011-2017.

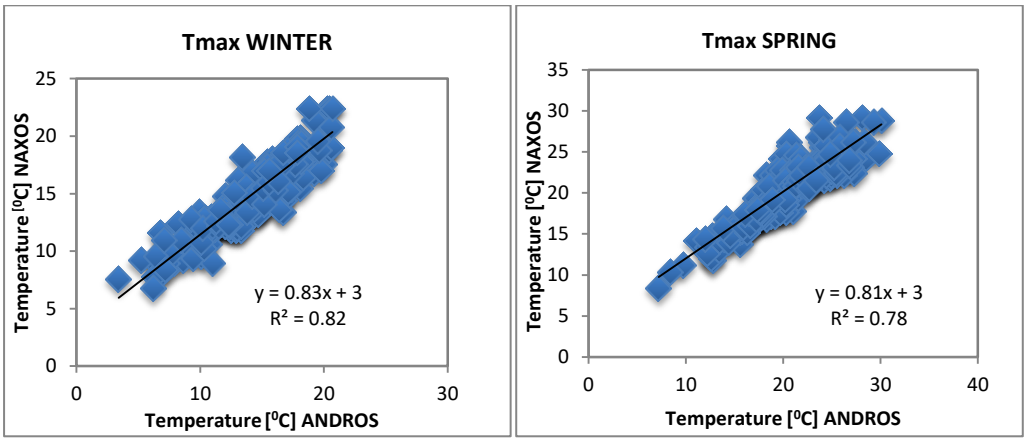

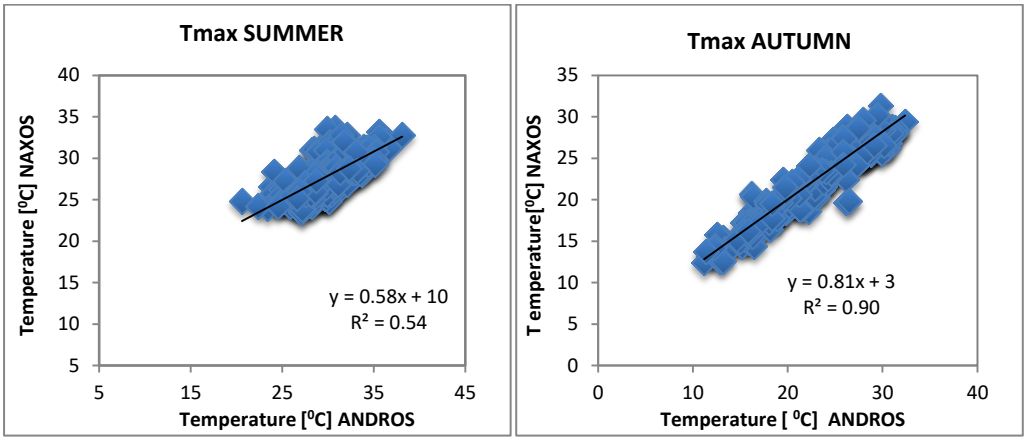

Figure 17 Correlation of the seasonal maximum air temperatures of Naxos (y axis) and Andros (x axis) Islands over the period 2011-2017.

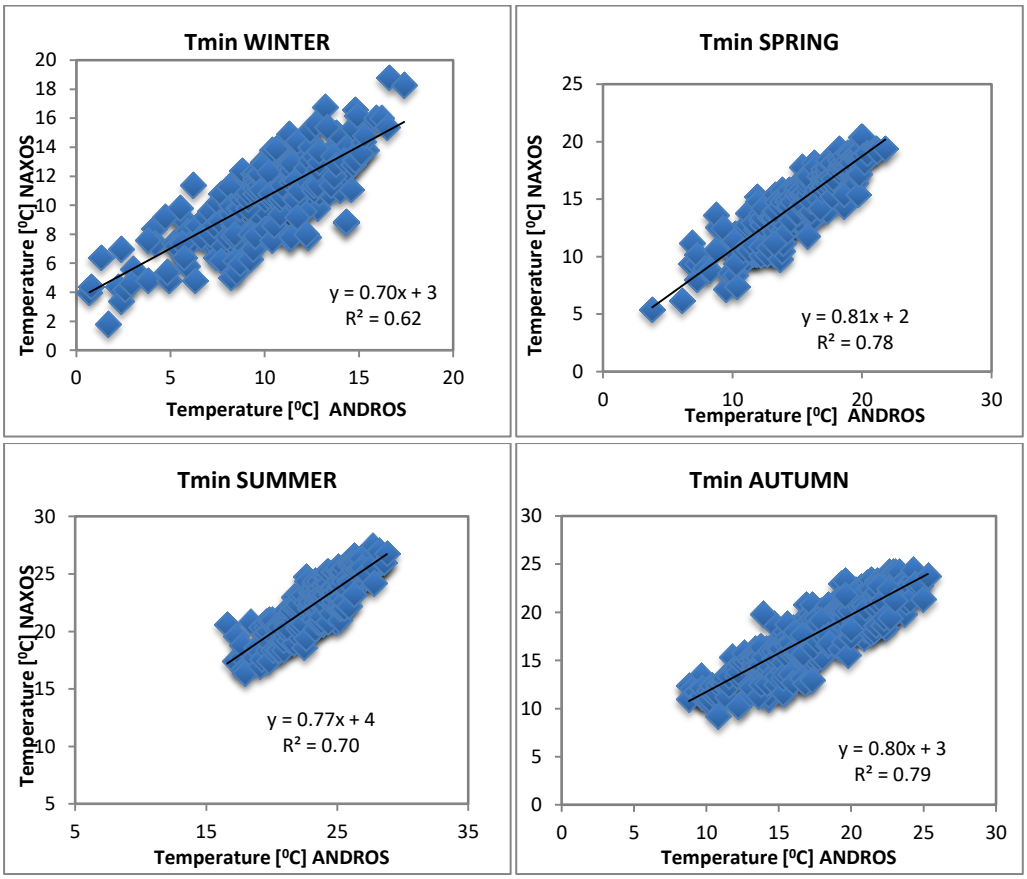

Figure 18 Correlation of the seasonal minimum air temperatures of Naxos (y axis) and Andros (x axis) Islands over the period 2011-2017.

3.2.2 Observed precipitation: Naxos and Andros Islands

Seasonal precipitation patterns of Andros and Naxos Islands show similar trends, but diverge substantially (Fig. 19). Correlation between seasonal precipitation is poor (Fig. 20). There are only few overlapping years that can be correlated, and seasonal variability in precipitation between Greek regions is known to be large. For more reliable comparisons it is better to compare annual to multi-annual (total or wet season) precipitation data, as random differences are evened out and the influence of large-scale weather systems (such as the North Atlantic Oscillation in winter) becomes more apparent (van der Schriek & Giannakopoulos 2017, *and references herein*). Therefore, longer-term datasets are required for meaningful correlation (see next, section 3.2.3).

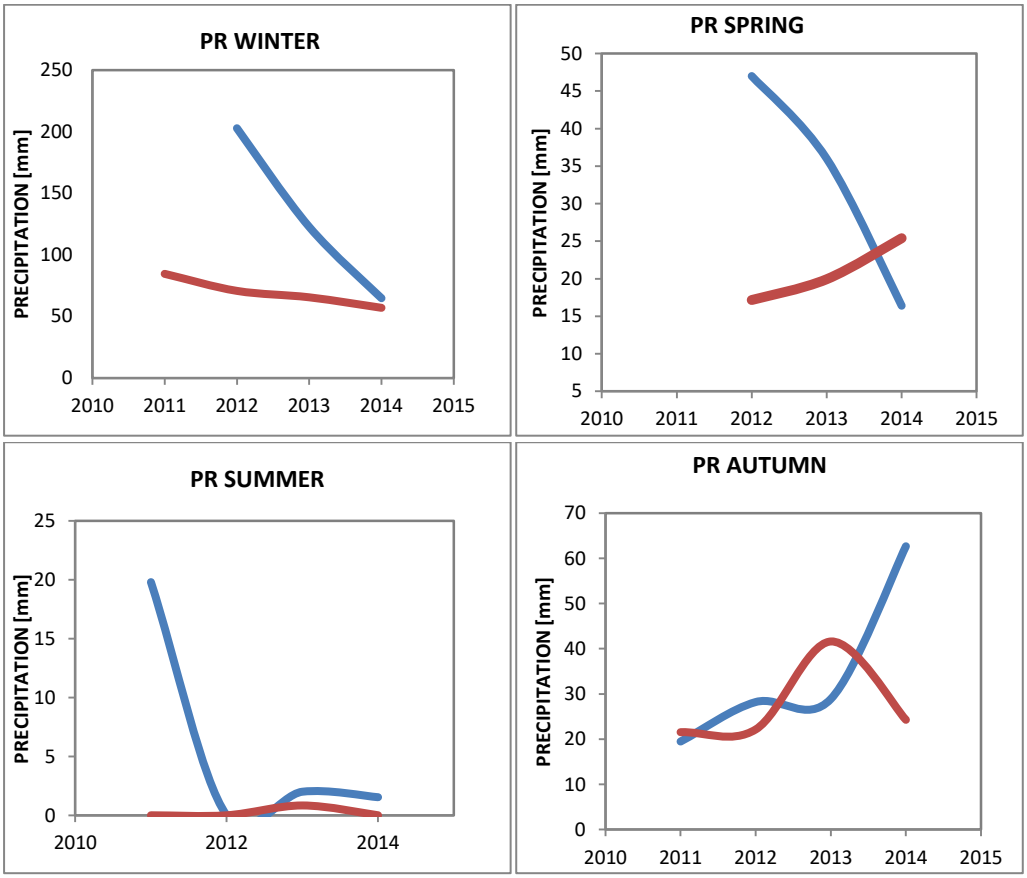

Figure 19 Comparison of the seasonal trends for the precipitation for Naxos (red lines) and Andros (blue lines) over the period 2011-2017

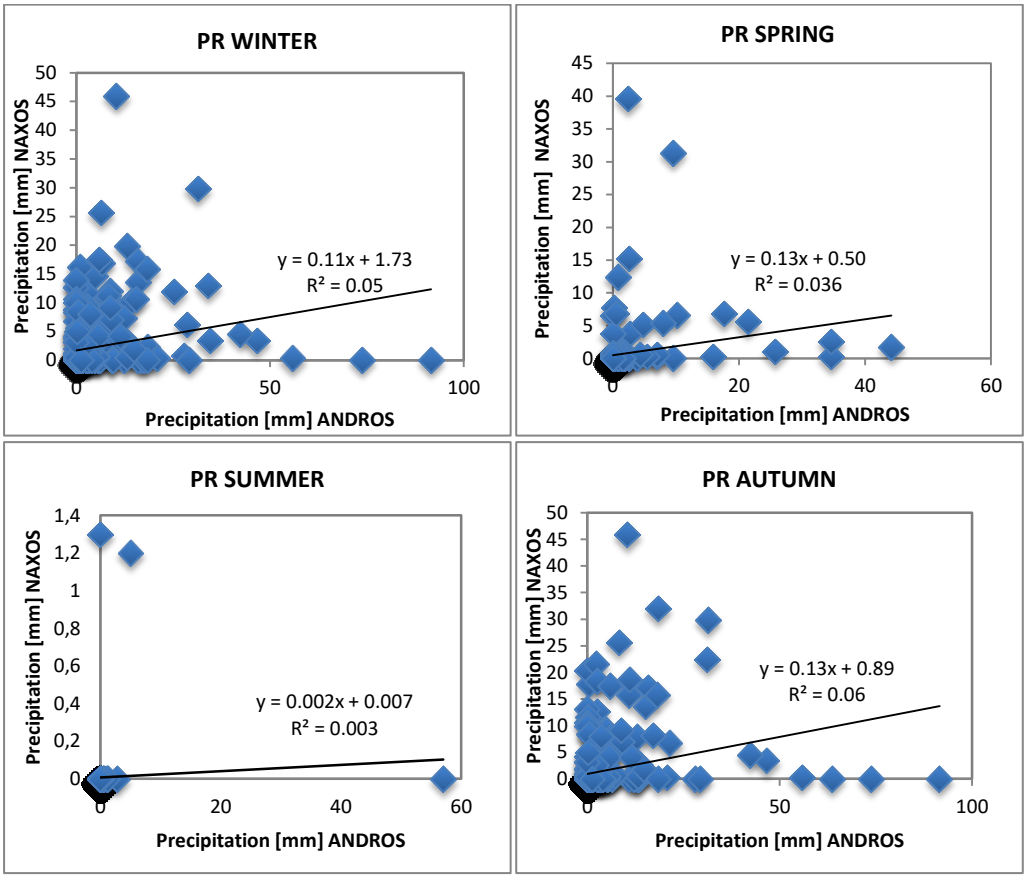

Figure 20 Correlation of the seasonal precipitation of Naxos (y axis) and Andros (x axis) Islands over the period 2011-2017.

3.2.3 Comparison of precipitation data from Naxos Island and Elliniko (eastern Attika)

The short overlap of the Andros- and Naxos Islands meteorological records may explain the poor correlation of precipitation data between the sites. It is expected that longer-term records offer better correlations (section 3.2.2). This report uses the Naxos Island meteorological record for bias-correction of the climate model. To prove the validity of this approach, we compared long-term precipitation records that are available for Naxos Island and Elliniko (eastern Attika; Fig. 1). Andros Island is located approximately halfway between these stations. By examining the long-term precipitation patterns between Elliniko and Naxos Island and establishing similarities, we could assume that the same similarities are displayed by Andros Island precipitation given its location between these two stations.

Comparison of the long-term precipitation patterns and trends (1964-2014) of Naxos Island and Elliniko reveal that these are similar between both sites (Fig. 21). Precipitation at both sites is fairly stable when looking at the 1964-2014 period. Annual precipitation is reasonably correlated (R^2=0,27; Fig. 22). However, the long-term monthly precipitation averages (1964-2014; Fig. 23) show that precipitation patterns and amounts are strikingly similar. Stronger correlation of precipitation between different regions is common in Greece, when using (multi-) decadal averages (van der Schriek & Giannakopoulos 2017, and references herein).

The similarity in precipitation patterns between these different sites means that it is possible to use the Naxos meteorological station data for the bias-correction procedure (section 2.2,) as its temperature record is already proven to be highly correlated to the Andros meteorological station data (section 3.2.2).

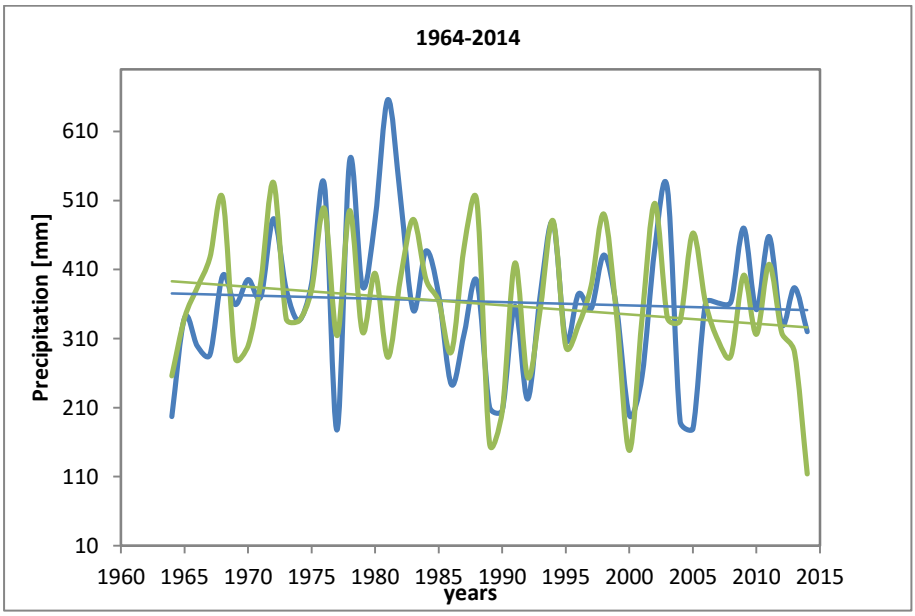

Figure 21 Comparison of the trends for the annual precipitation for Naxos (blue line) and Elliniko (green line) over the period 1964-2014

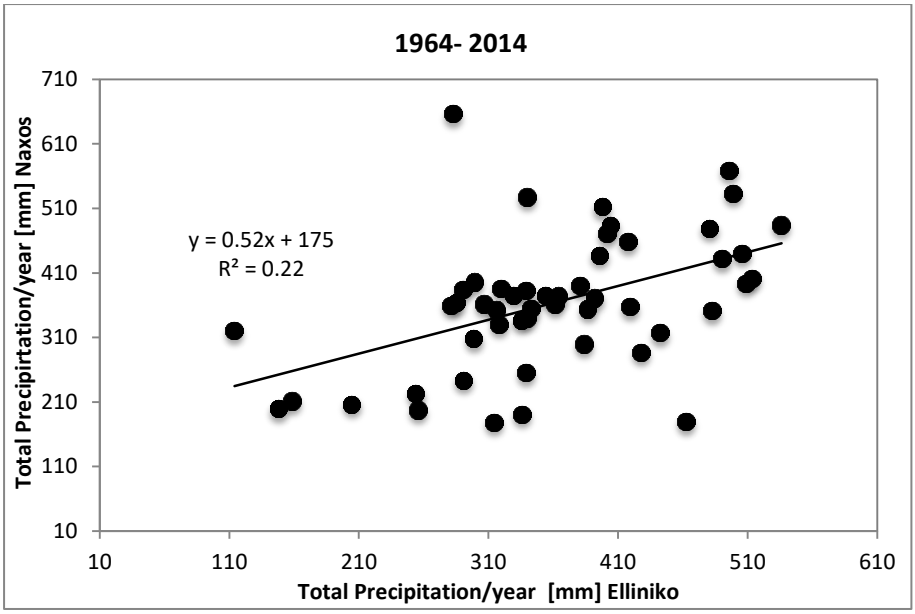

Figure 22 Correlation of the annual precipitation of Naxos Island (y-axis) and Elliniko, Attica, (x-axis) over the period 1964-2014

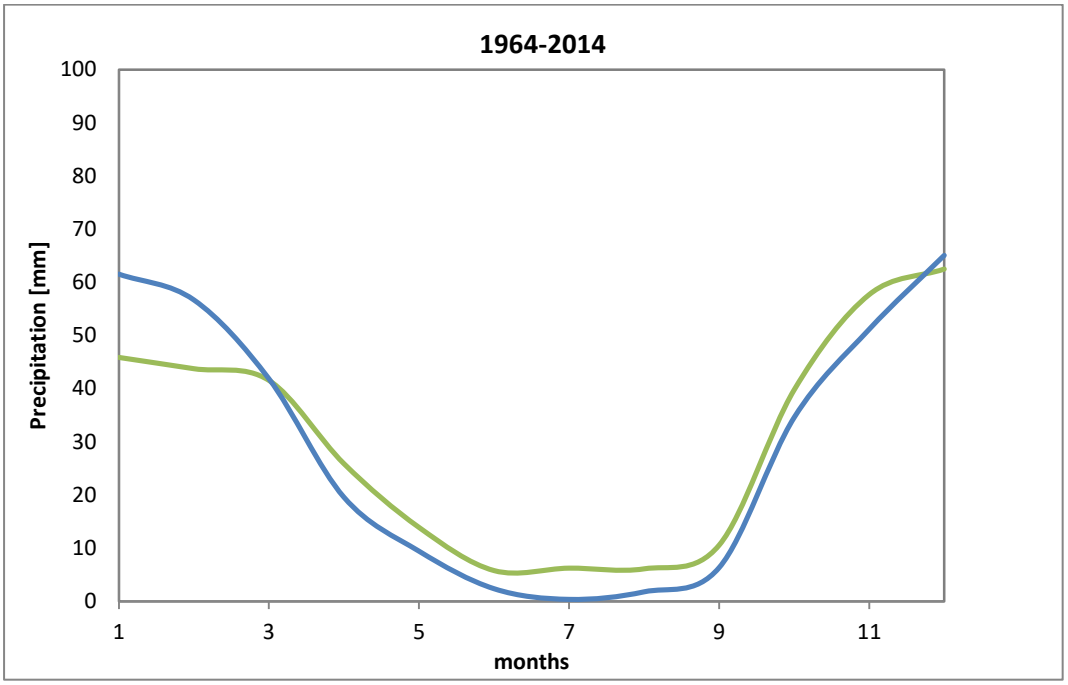

Figure 23 Annual precipitation patterns of Naxos Island (blue line) and Elliniko, Attica, (green line), based on mean monthly precipitation over the period 1964-2014

3.3 Future projections

This section presents climate simulations from the RCA4 regional climate model SMHI with boundary conditions from the global HadGEM-ES model of the Met Office Hadley Centre (MOHC); see section 2.1 for more details. Given the fact that the study region is not covered by E-OBS climate data (section 2.2), there is no point in providing bias-corrected simulations for the entire Aegean region – even with coarse resolution – as the model can only be corrected with the data from Naxos Island meteorological station. Any corrected model simulation would therefore provide the same pattern of climate changes across the Aegean region, rendering it a pointless exercise.

Here we present simulation-results for the location of Andros Island, extracted from the SMHI-MOHC model, with daily data for the period 1970-2100. Results are presented for the control period (1971-2000) and the near (2031-2060) and distant (2071-2100) future periods under emission scenarios RCP4.5 and RCP8.5 (section 2.4).

The evaluation of the historical climate data led to the selection of a smaller set of climate indices, as some of the initially selected indices did not occur or occurred too few times for any statistical analysis to be significant. Specifically, during spring there were no days with T_{min}<3°C (index related to late frost and crop damage); accordingly, this index was removed. Furthermore, one precipitation index was removed (*very heavy precipitation days with more than 20 mm precipitation*), as it did occur very few times.

To summarize, the following climate indices were used in the analyses of the future climate simulations:

Temperature

- Mean temperatures (absolute index). Seasonal and annual sums;
- Number of days Tmax> 30 ^{o}C (threshold index; hot days). For daily maximum temperature (annual/seasonal);
- Number of days Tmax> 35 ^{o}C (threshold index; heatwave). For daily maximum temperature (annual);
- Number of days Tmin> 20 ^{o}C (threshold index; tropical night). For daily minimum temperature (annual/seasonal);

Precipitation

- Total Precipitation (absolute index). Seasonal and annual sums
- Highest 1-day precipitation amount (absolute index). Maximum (annual/seasonal) precipitation sums for 1-day intervals
- Heavy precipitation days (threshold index). Number of days (per year/season) with precipitation amount greater than 10 mm
- Highest 5-day precipitation amount (absolute index). Maximum (annual/seasonal) precipitation sums for 5-day intervals
- Maximum length of dry spell (duration index). Maximum length of consecutive days with precipitation < 1 mm (annual/seasonal)

3.3.1 Future temperature data

This section presents the simulated temperature data on an annual and seasonal basis. The colored numbers indicate the calculated slopes for each one of the cases.

Mean Annual Maximum Temperatures

Modelled annual T_{max} show a rising trend-line over the historical (control) period, similar to meteorological station observations (section 3.2.1), with maximum average temperatures of around 20,5°C (Fig. 24). In the near future T_{max} rises to 22,3 °C (RCP 4.5) to 22,8 °C (RCP 8.5), while in the distant future T_{max} rises to 23,3 °C (RCP 4.5) to 25 °C (RCP 8.5).

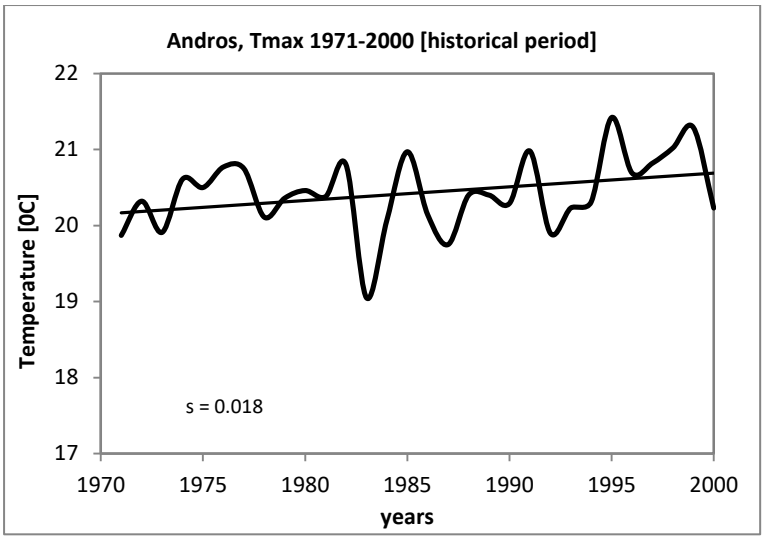

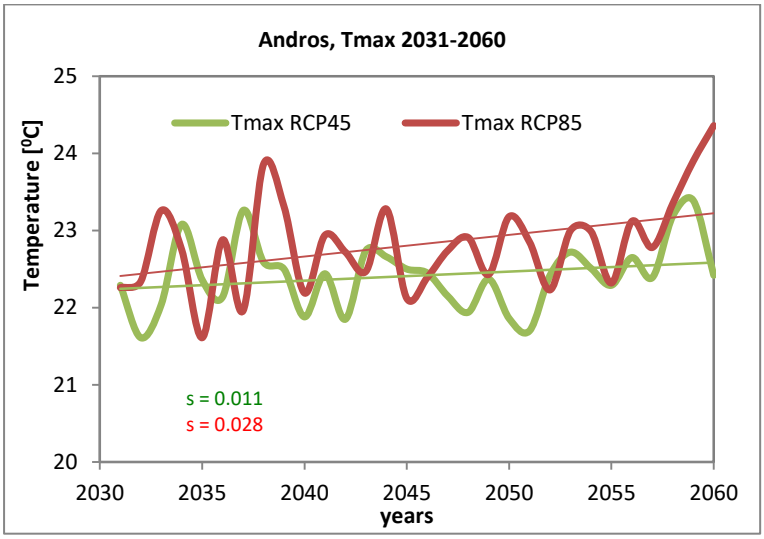

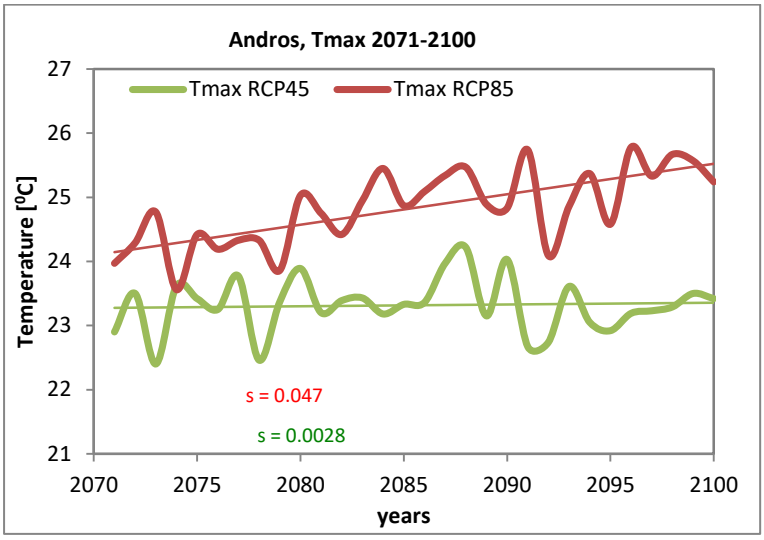

Figure 24 Maximum annual temperature predictions for Andros Island during the historical period 1971-2000 (top panel), the near future period 2031-2060 (middle panel) and the distant future period 2071-2100 (bottom panel), under the future scenarios RCP4.5 (green line) and RCP8.5 (red line).

Mean Annual Minimum Temperatures

Annual T_{min} also show a rising trend-line over the historical (control) period, similar to meteorological station observations (section 3.2.1), with temperature averages of around 15,2°C (Fig. 25). In the near future T_{min} rises to 17,3 °C (RCP 4.5) to 18,3 °C (RCP 8.5), while in the distant future T_{min} rises only under climate scenario RCP 8.5 to 20,4 °C (Fig. 25).

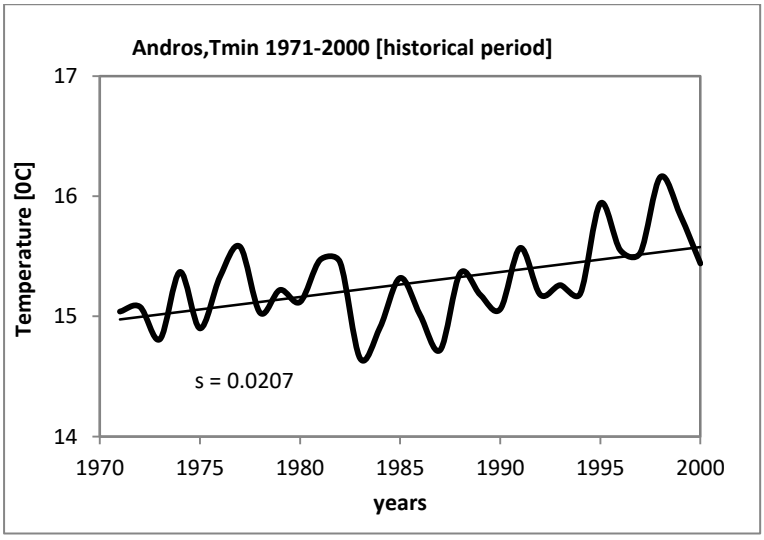

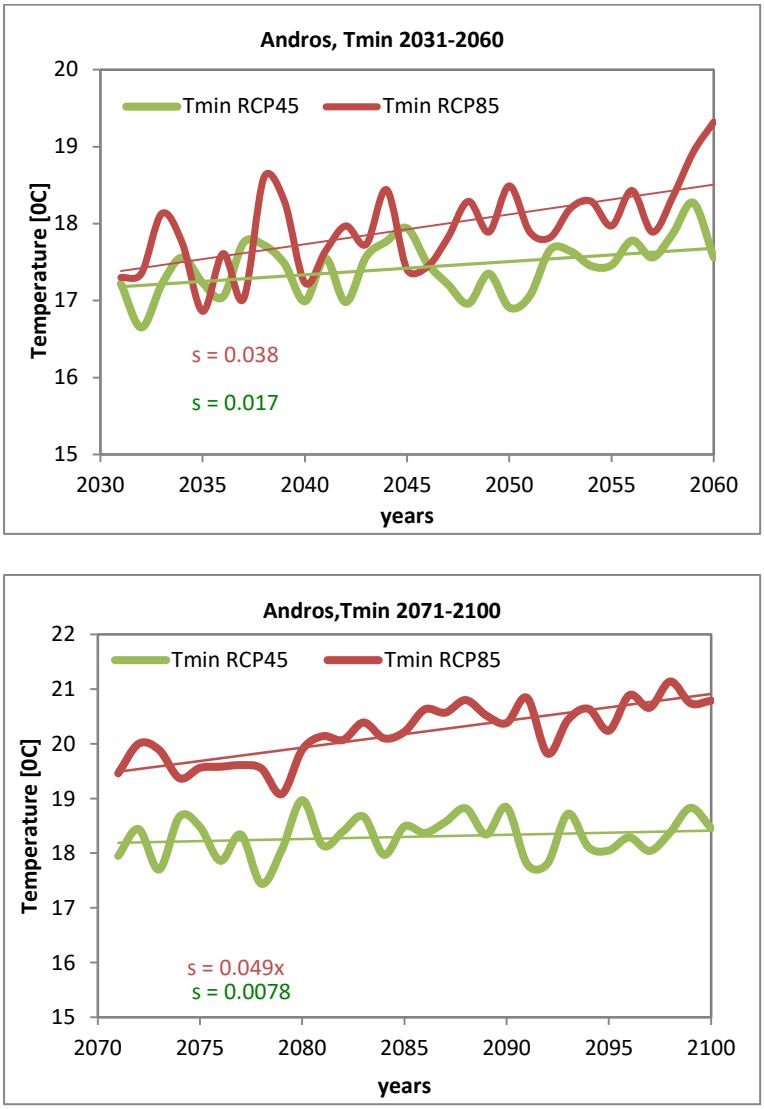

Figure 25 Minimum annual temperature predictions for Andros Island during the historical period 1971-2000 (top panel), the near future period 2031-2060 (middle panel) and the distant future period 2071-2100 (bottom panel), under the future scenarios RCP4.5 (green line) and RCP8.5 (red line).

Mean Seasonal Maximum Temperatures

Seasonal T_{max} changes in the near- to distant future are very similar to the annual pattern of projected temperature changes (Figs. 26-29). Compared to the control period, T_{max} rises by 2-3 ^{o}C in the near future and by 3-5 ^{o}C in the distant future. The largest rises are projected under the RCP 8.5 scenario. The largest temperature increases are projected for summer and autumn (Figs. 28-29), while increase for winter and spring are about 1 ^{o}C lower under both RCP scenarios (Figs. 28-29).

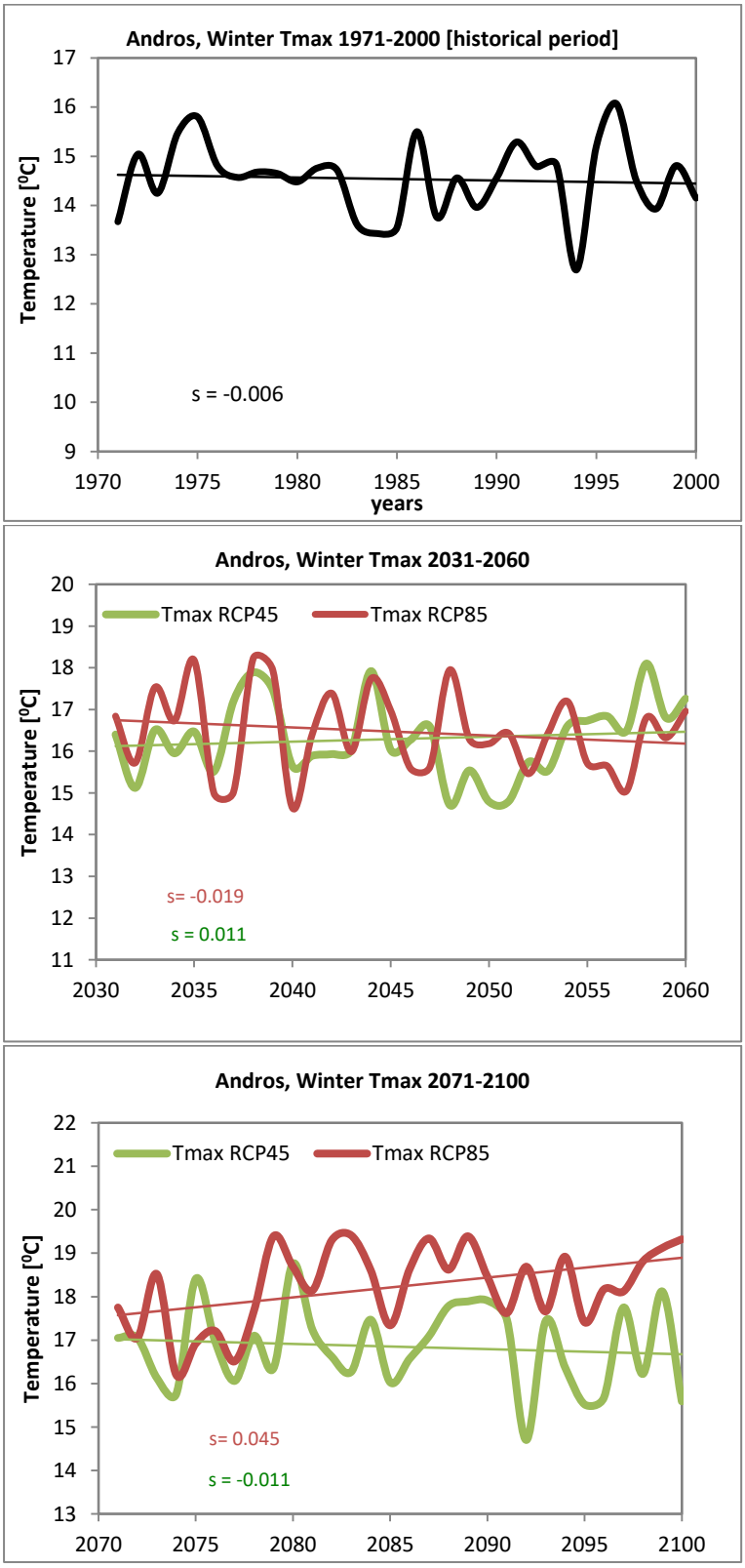

Figure 26 Maximum winter temperature predictions for Andros Island during the historical period 1971-2000 (top panel), the near future period 2031-2060 (middle panel) and the distant future period 2071-2100 (bottom panel), under the future scenarios RCP4.5 (green line) and RCP8.5 (red line).

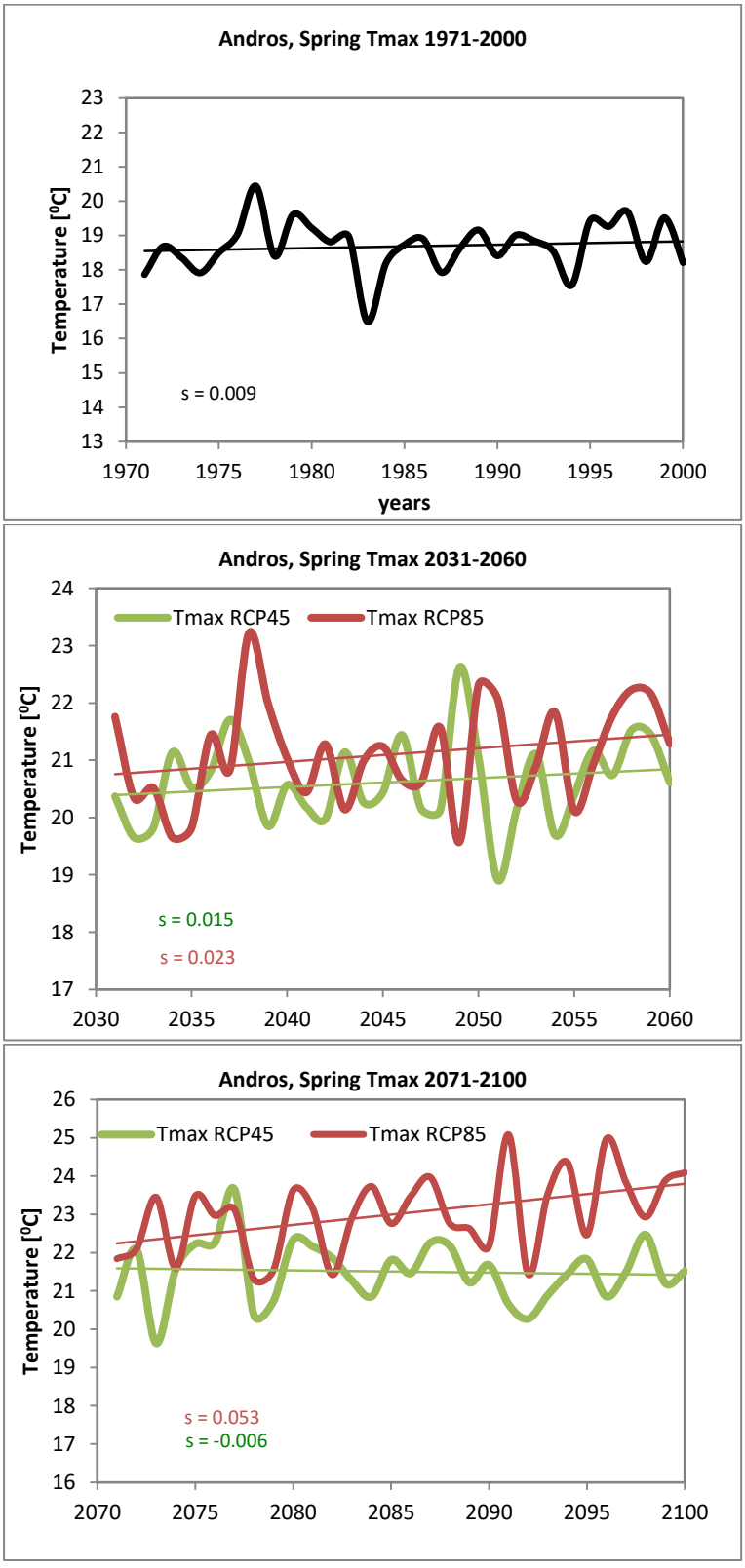

Figure 27 Maximum spring temperature predictions for Andros Island during the historical period 1971-2000 (top panel), the near future period 2031-2060 (middle panel) and distant future period 2071-2100 (bottom panel), under the future scenarios RCP4.5 (green line) and RCP8.5 (red line).

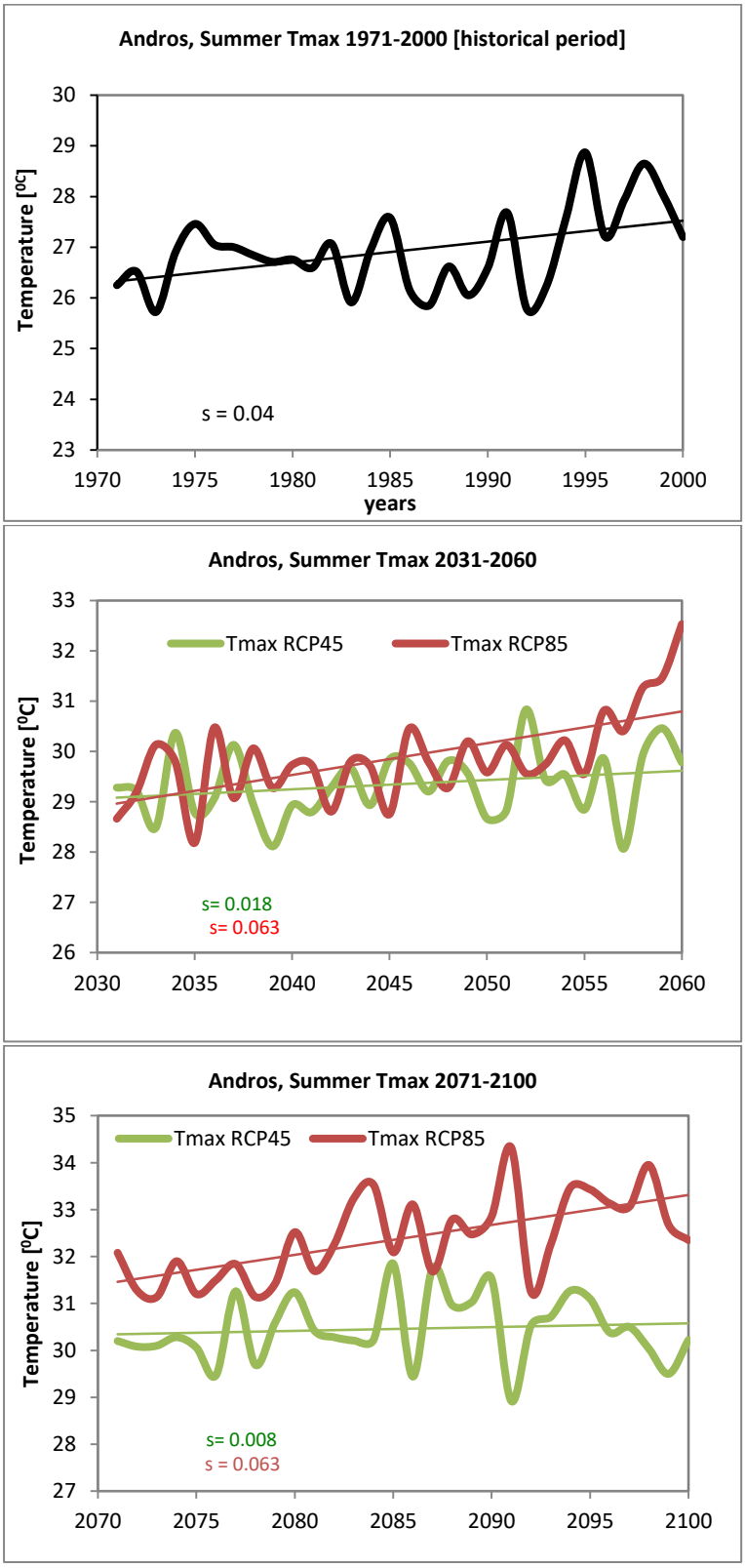

Figure 28 Maximum summer temperature predictions for Andros Island during the historical period 1971-2000 (top panel), the near future period 2031-2060 (middle panel) and the distant future period 2071-2100 (bottom panel), under the future scenarios RCP4.5 (green line) and RCP8.5 (red line).

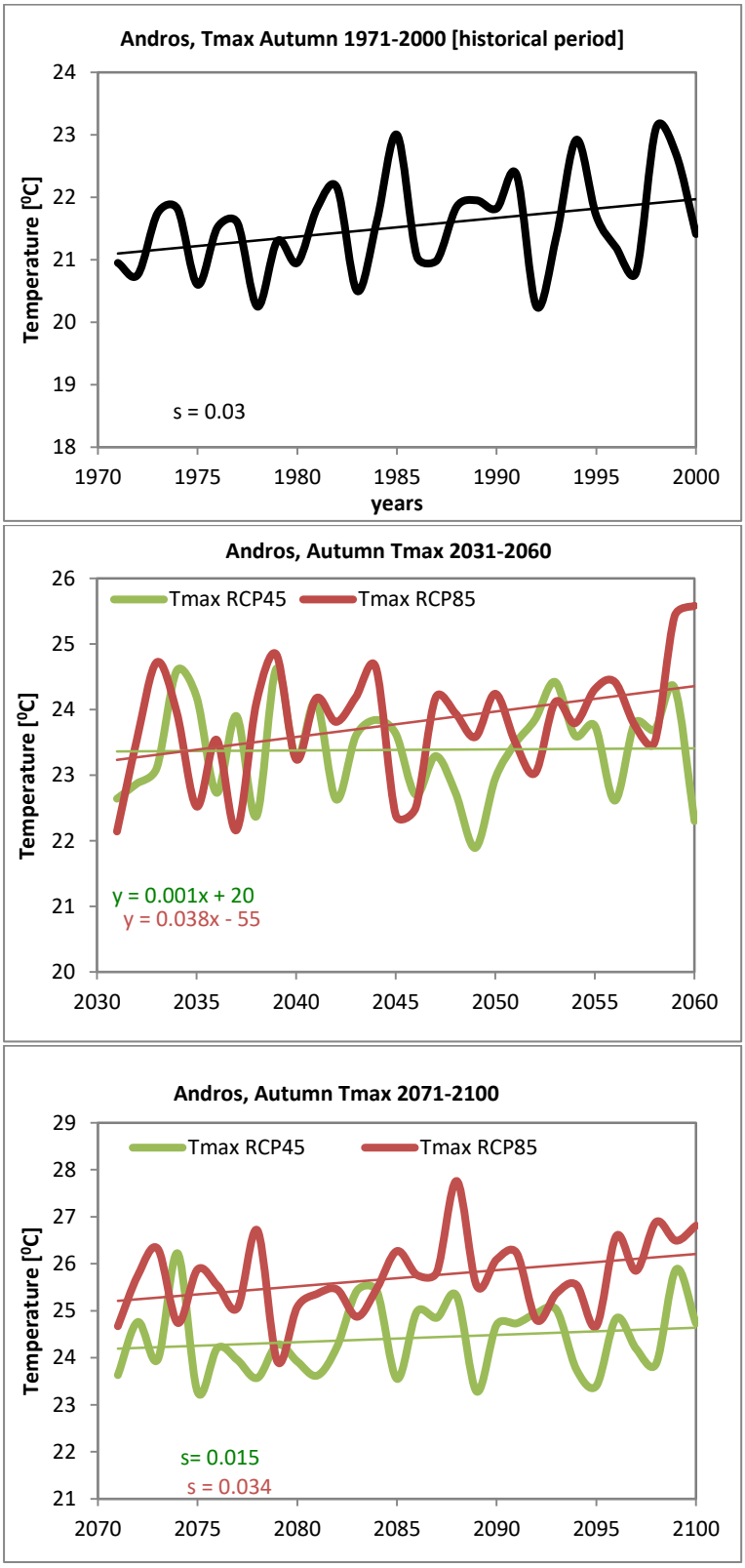

Figure 29 Maximum autumn temperature predictions for Andros Island during the historical period 1971-2000 (top panel), the near future period 2031-2060 (middle panel) and the distant future period 2071-2100 (bottom panel), under the future scenarios RCP4.5 (green line) and RCP8.5 (red line).

Mean Seasonal Minimum Temperatures

Seasonal T_{min} changes in the near- to distant future (Figs. 30-33) are very similar to the annual pattern of projected temperature changes. Compared to the control period, T_{min} rises by 2-4 °C in the near future and by 3-6 °C in the distant future. The largest rises are projected under the RCP 8.5 scenario. The projected temperature increases for summer (Fig. 32) are about 1 °C higher than the maximum projected increases for winter, spring and autumn under both RCP scenarios (Figs. 30, 31 and 33).

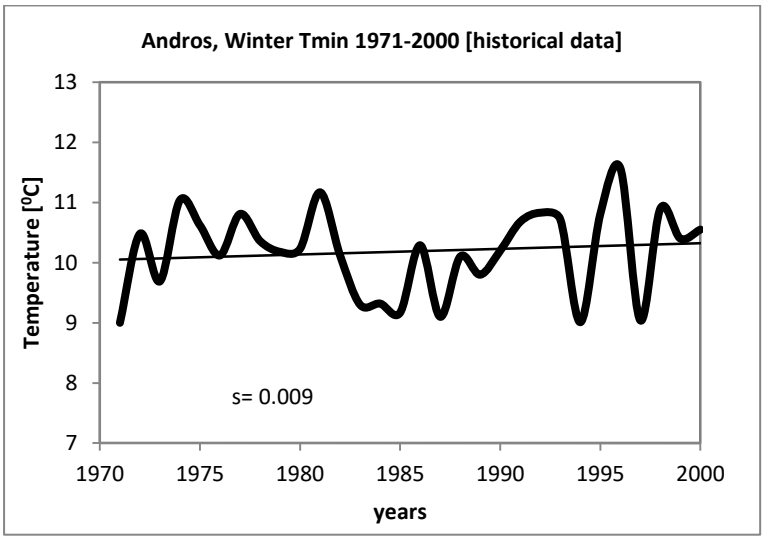

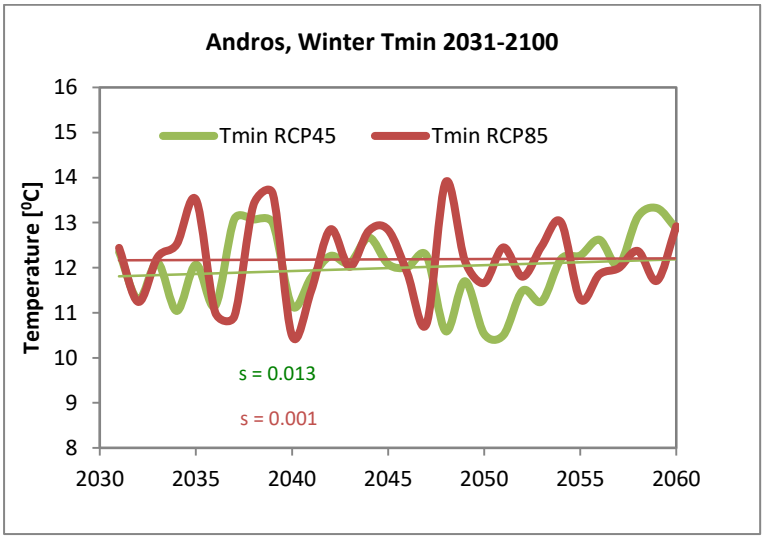

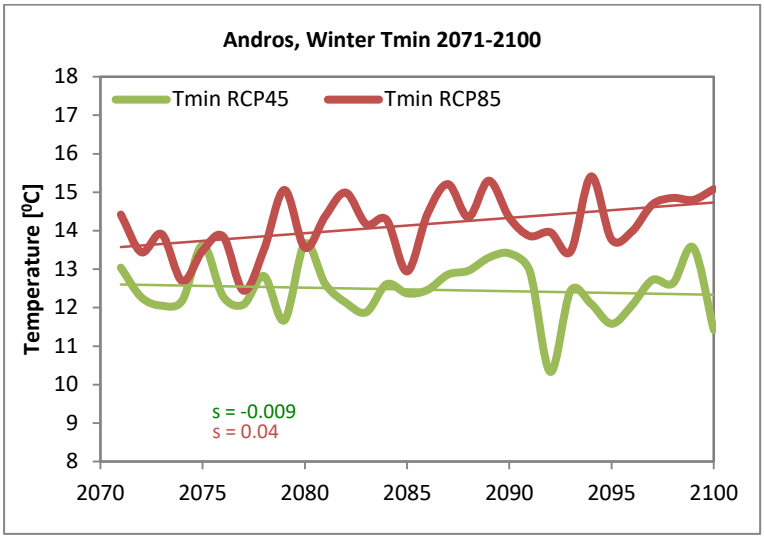

Figure 30 Minimum winter temperature predictions for Andros Island during the historical period 1971-2000 (top panel), the near future period 2031-2060 (middle panel) and the distant future period 2071-2100 (bottom panel), under the future scenarios RCP4.5 (green line) and RCP8.5 (red line).

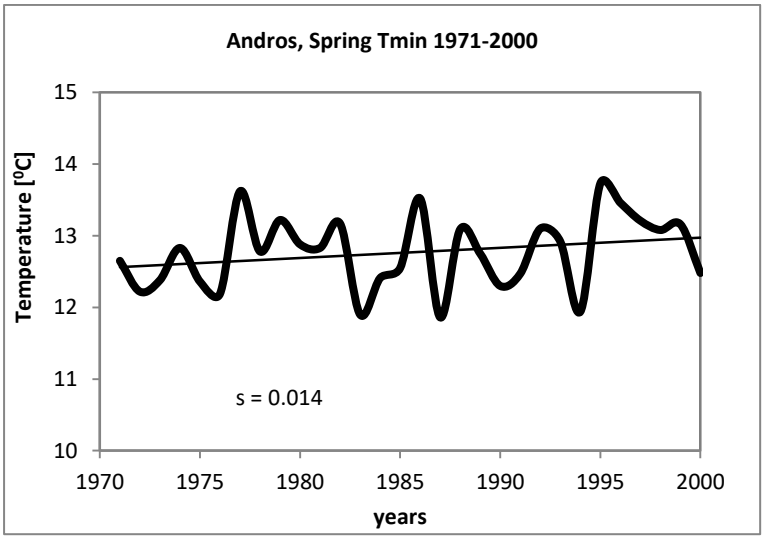

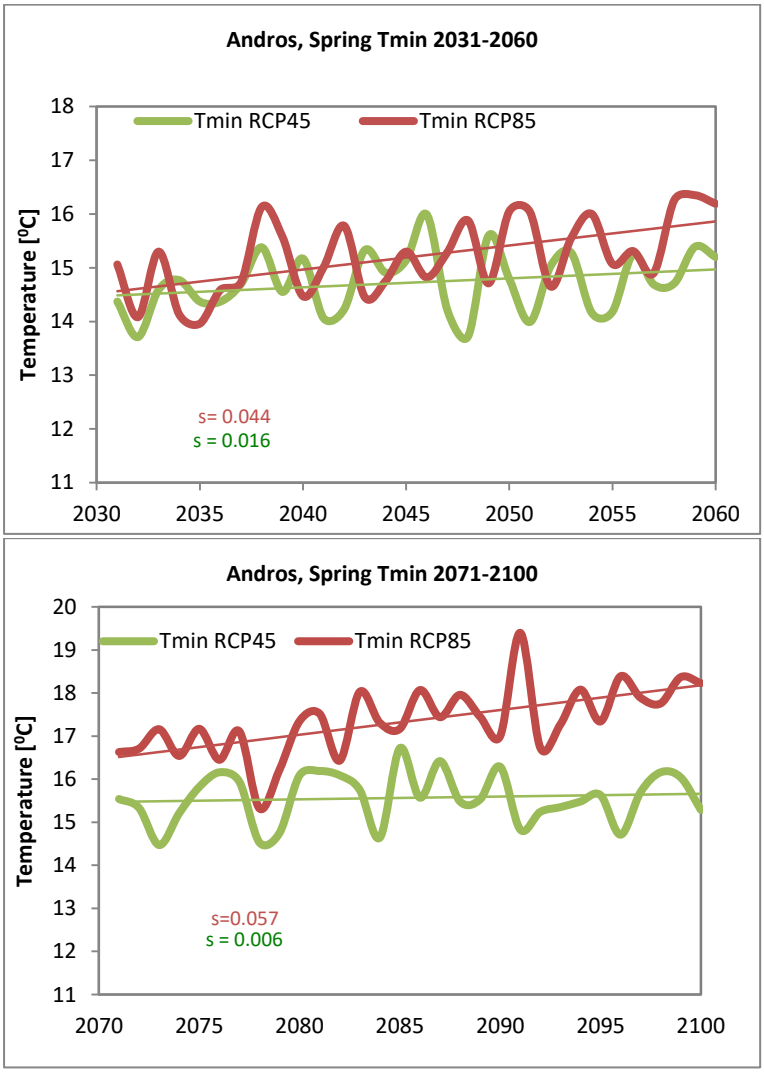

Figure 31 Minimum spring temperature predictions for Andros Island during the historical period 1971-2000 (top panel), the near future period 2031-2060 (middle panel) and the distant future period 2071-2100 (bottom panel), under the future scenarios RCP4.5 (green line) and RCP8.5 (red line).

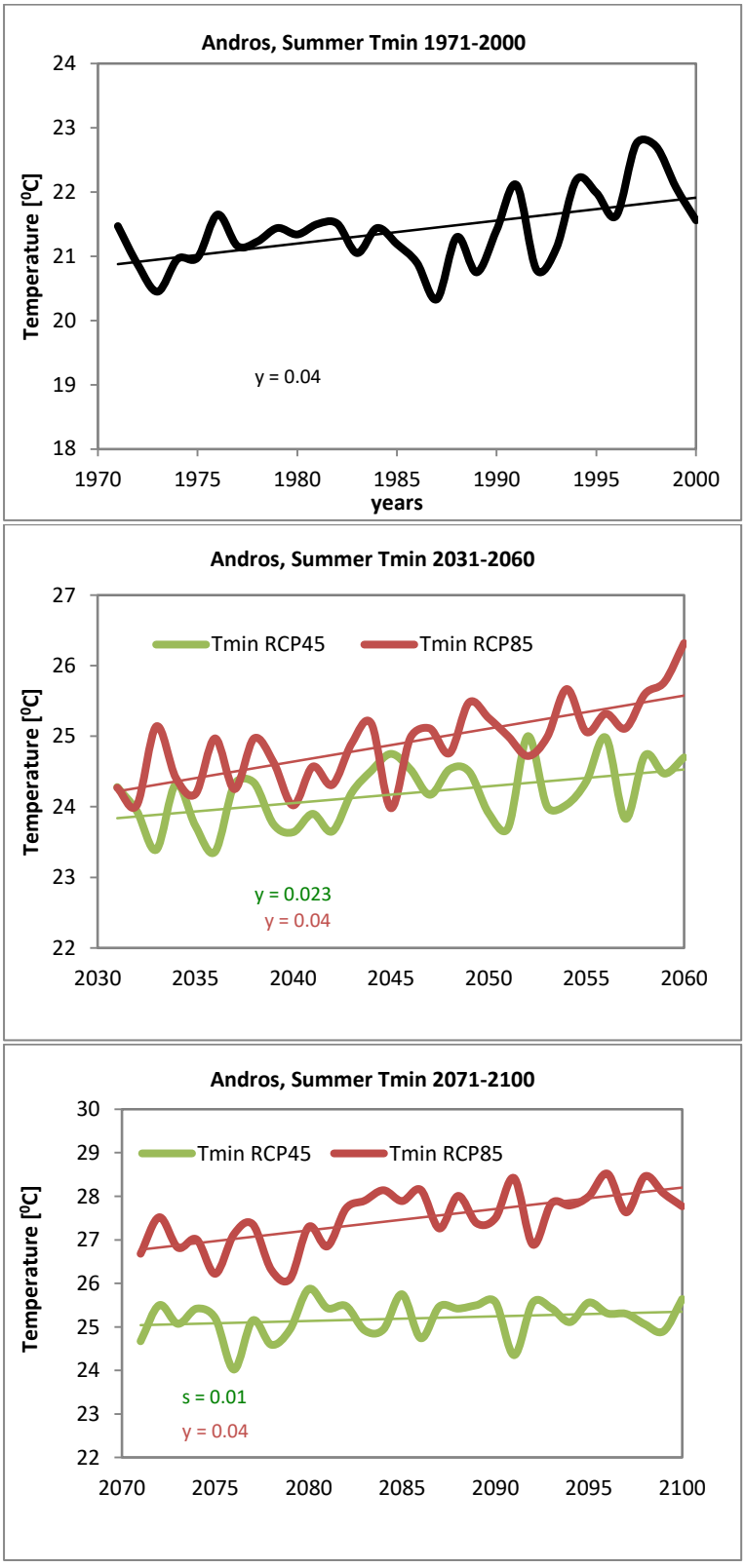

Figure 32 Minimum summer temperature predictions for Andros Island during the historical period 1971-2000 (top panel), the near future period 2031-2060 (middle panel) and the distant future period 2071-2100 (bottom panel), under the future scenarios RCP4.5 (green line) and RCP8.5 (red line).

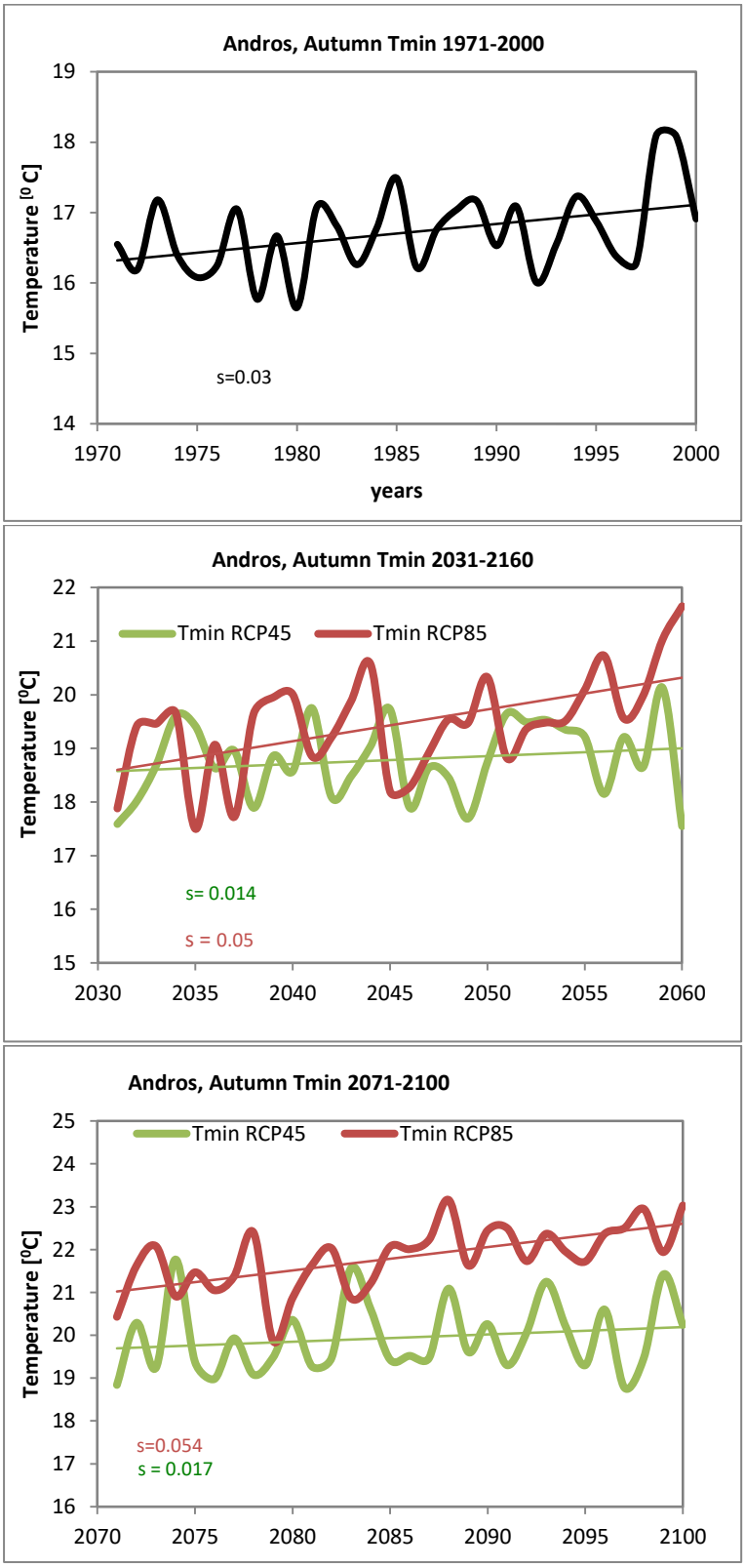

Figure 33 Minimum autumn temperature predictions for Andros Island during the historical period 1971-2000 (top panel), the near future period 2031-2060 (middle panel) and the distant future period 2071-2100 (bottom panel), under the future scenarios RCP4.5 (green line) and RCP8.5 (red line).

Extreme Temperatures Trends

Extreme temperature indices show large increases in the near- and distant future under both climate scenarios; the largest increases are projected under scenario RCP 8.5. Hot days (T_{max}>30°C) increase from 10 days/year to 30-40 days/year in the near future and 50-80 days/year in the distant future (Fig. 34). Heatwaves (T_{max}>35°C) increase from 0,5 days/year to 2-6 days/year in the near future and 4-15 days/year in the distant future (Fig. 35). Tropical nights (T_{min}>20°C) increase from 85 days/year to 132-140 days/year in the near future and 140-170 days/year in the distant future (Fig. 36).

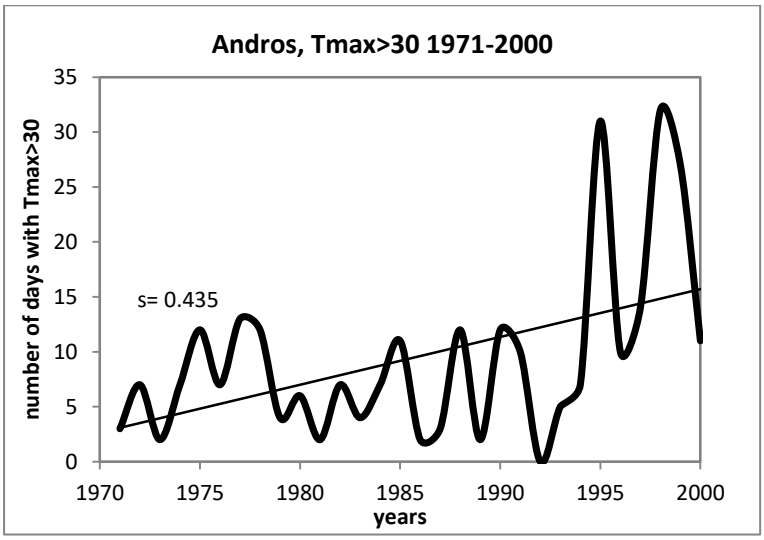

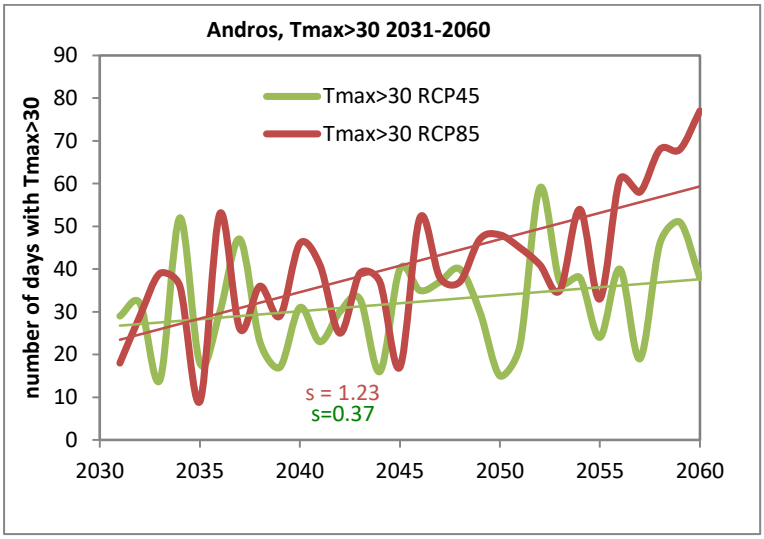

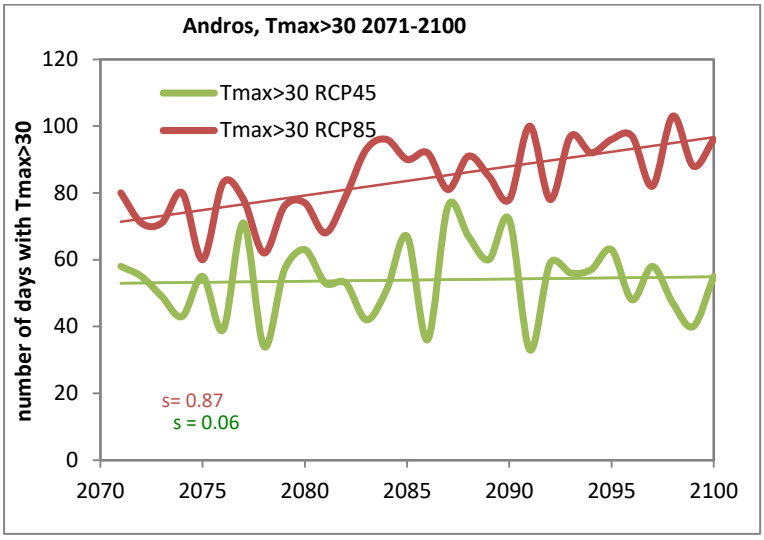

Figure 34 Average annual number of days with maximum temperature higher than 30^{o}C for Andros during the historical period 1971-2000 (top panel), the near future period 2031-2060 (middle panel) and the distant future period 2071-2100 (bottom panel), under the future scenarios RCP4.5 (green line) and RCP8.5 (red line).

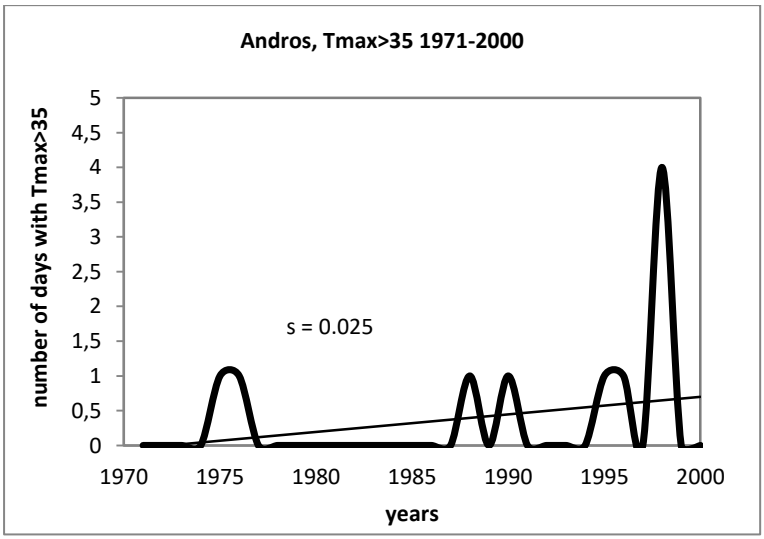

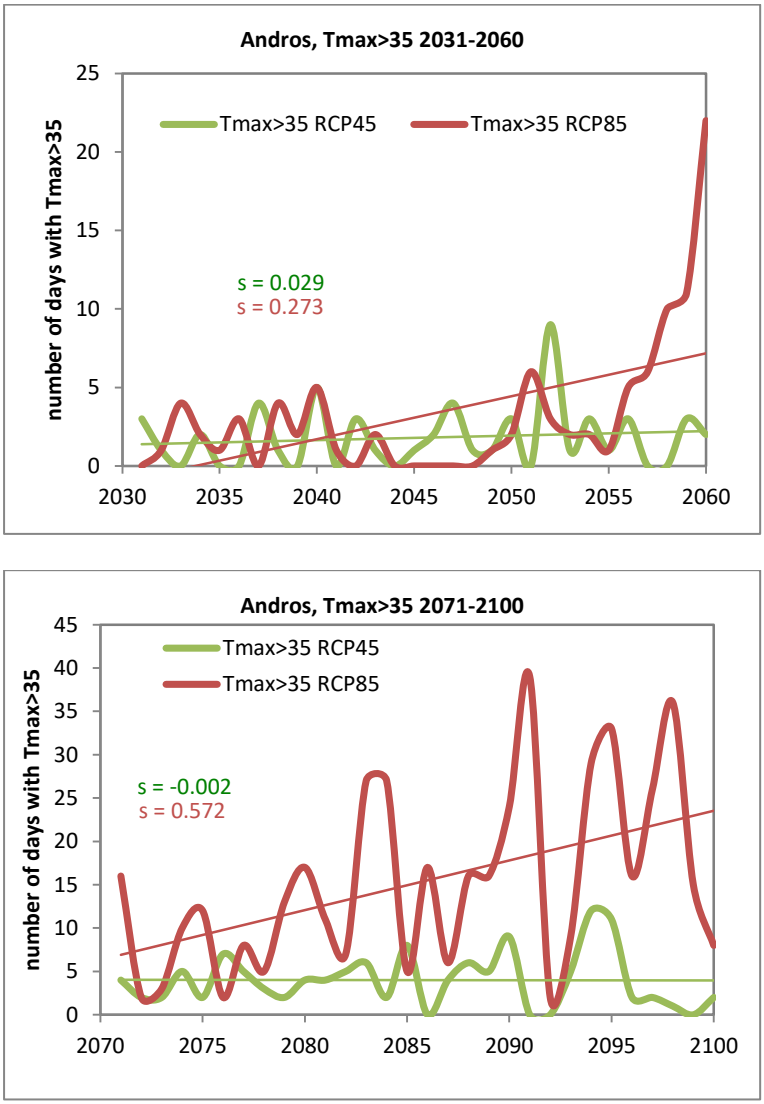

Figure 35 Average annual number of days with maximum temperature higher than 35^{o}C for Andros during the historical period 1971-2000 (top panel), the near future period 2031-2060 (middle panel) and the distant future period 2071-2100 (bottom panel), under the future scenarios RCP4.5 (green line) and RCP8.5 (red line).

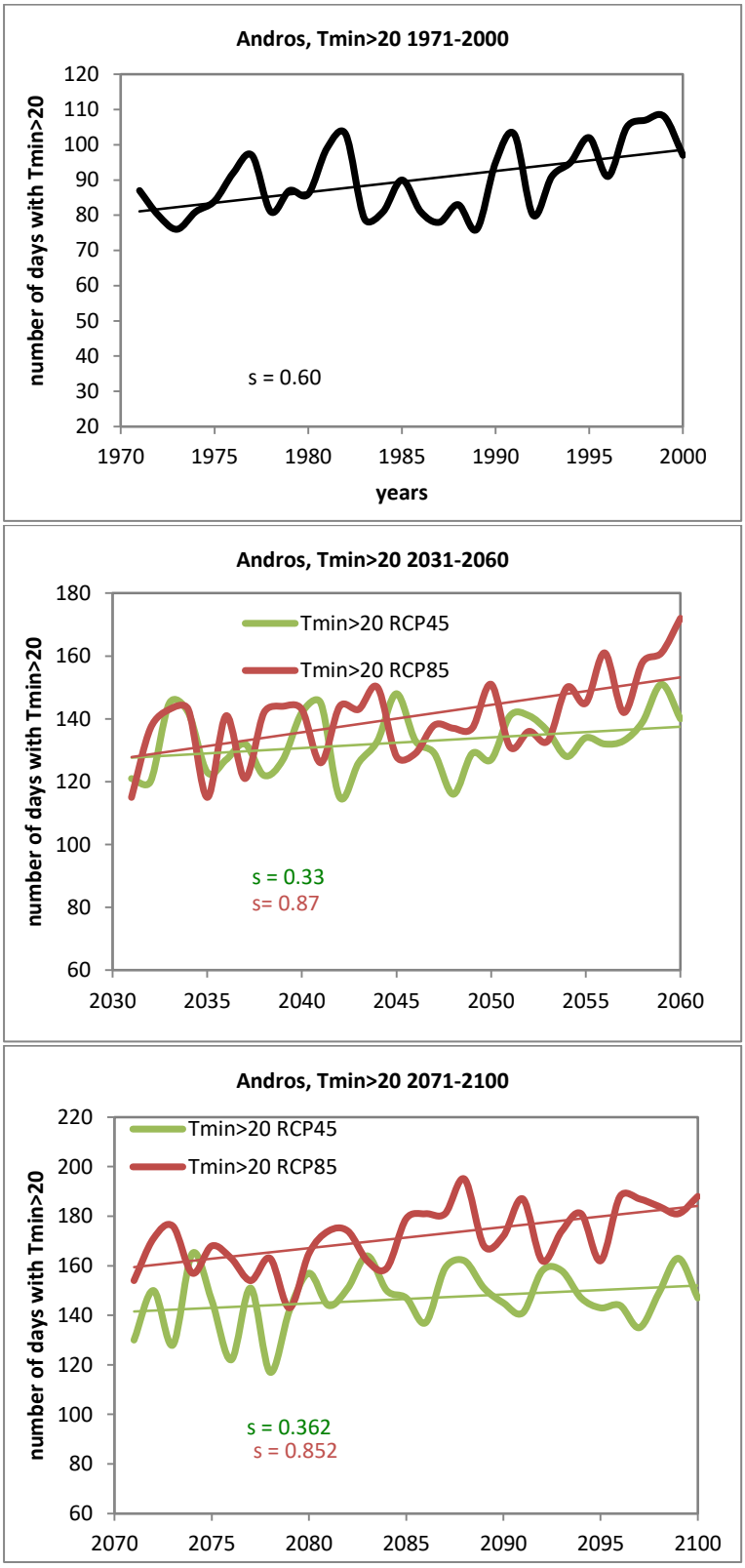

Figure 36 Average annual number of days with minimum temperature higher than 20^{o}C for Andros during the historical period 1971-2000 (top panel), the near future period 2031-2060 (middle panel) and the distant future period 2071-2100 (bottom panel), under the future scenarios RCP4.5 (green line) and RCP8.5 (red line).

Extreme Temperatures Trends – seasonal results

Extreme temperatures mainly occurred during summer over the historical (control) period. However, this is projected to change in the near- and distant future. The increase in heatwaves (T_{max}>35°C) takes mainly place over the summer (Fig. 35). About 10 days/year in summer are characterised as hot days (T_{max}>30°C) over the control period; projected increases will mainly occur in summer, although 5-10 hot days/year may occur in autumn in the distant future (Fig. 37). Of the about 85 tropical nights (T_{min}>20°C) that occurred per year over the control period, 70 happened in summer and about 15 in autumn. In the near- and distant future, tropical nights will take place over the whole summer, and 10-20 days in spring to 40-60 days in autumn (Fig. 38).

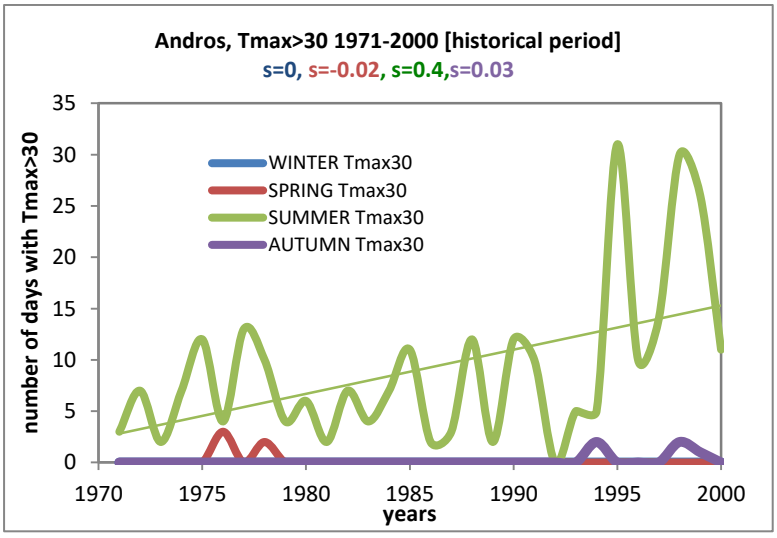

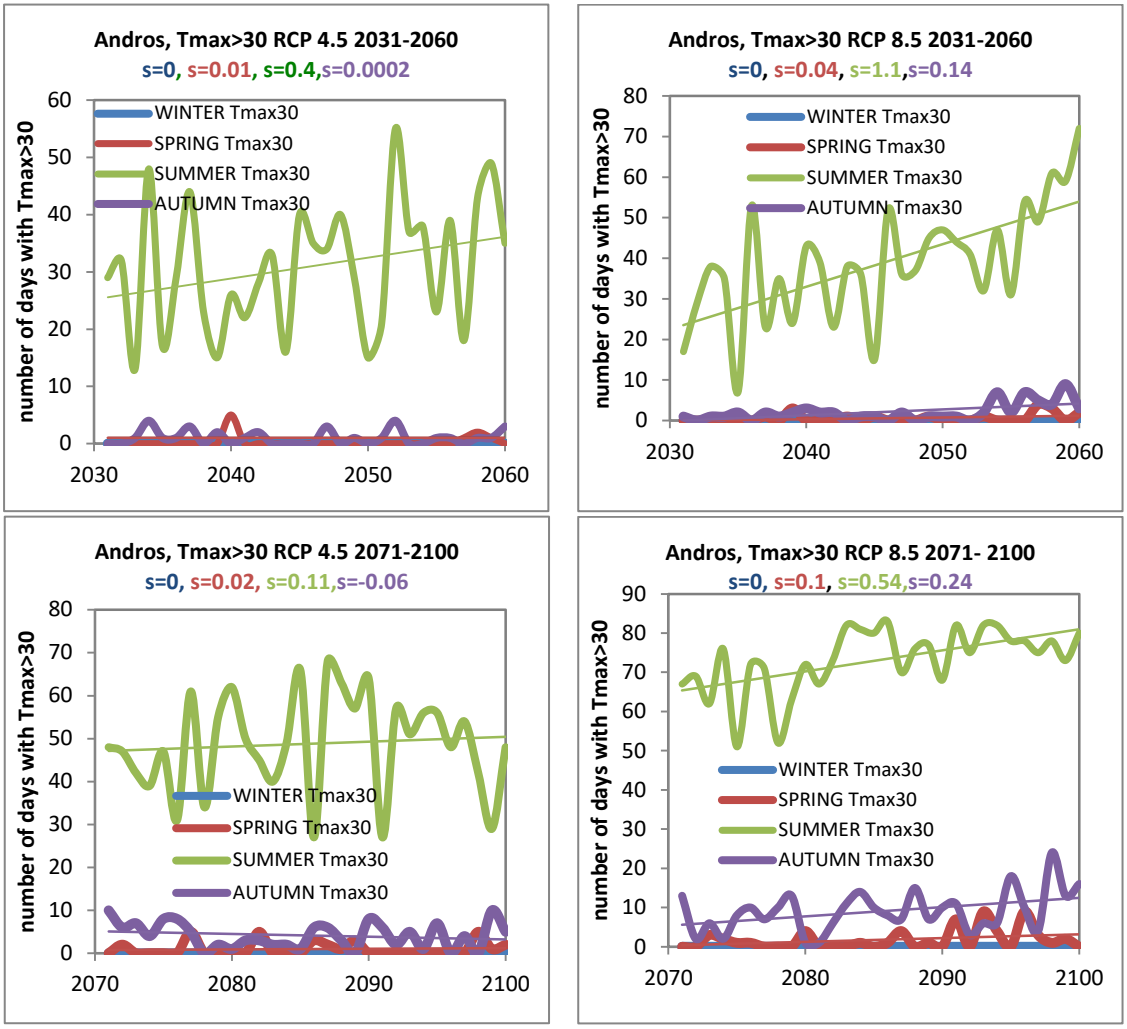

Figure 37 Seasonal trends for the annual number of days with daily maximum temperatures greater than 30^{o}C for Andros during the historical period 1971-2000 (top panel), the near future period 2031-2060 (middle panels) and the distant future period 2071-2100 (bottom panels), under the future scenarios RCP4.5 and RCP8.5 (left and right panel, respectively). The colored numbers on the top indicate the calculated slopes for each one of the seasons.

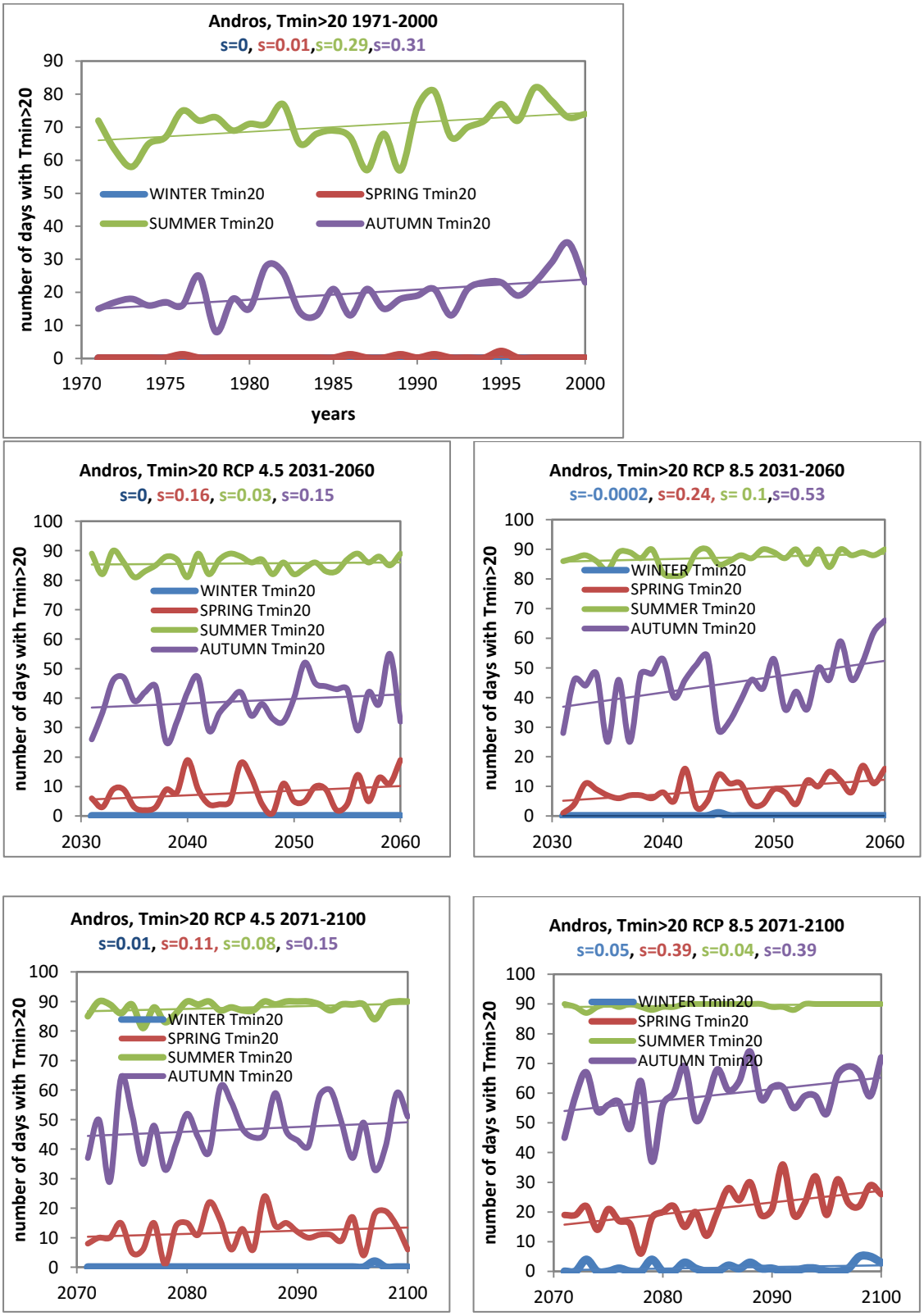

Figure 38 Seasonal trends for the annual number of days with daily minimum temperatures greater than 20^{O}C for Andros during the historical period 1971-2000 (top panel), the near future period 2031-2060 (middle panels) and the distant future period 2071-2100 (bottom panels), under the future scenarios RCP4.5 and

RCP8.5 (left and right panel, respectively). The colored numbers on the top indicate the calculated slopes for each one of the seasons.

3.3.2 Simulated precipitation

This section presents the simulated precipitation data on an annual and seasonal basis, as well as extreme precipitation indices. The colored numbers indicate the calculated slopes for each one of the cases.

Total Annual Precipitation

Total annual precipitation over the control period stands at about 450mm/year and is highly variable with a decreasing trendline. Over the near- and distant future this precipitation variability is set to increase, while total precipitation (PR) is projected to decrease to 350mm/year under both periods and climate scenarios (Fig. 39).

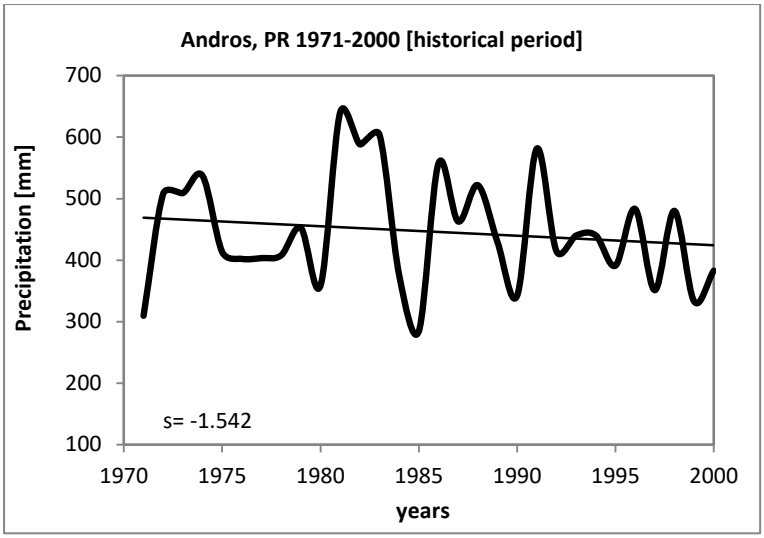

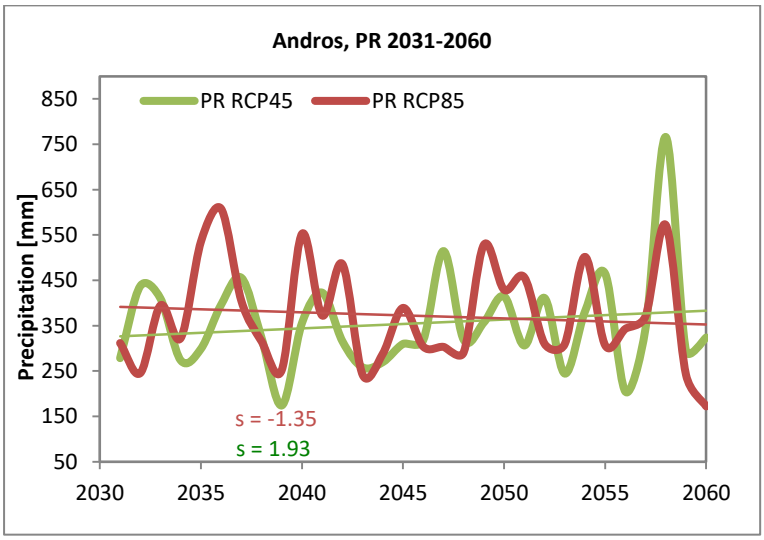

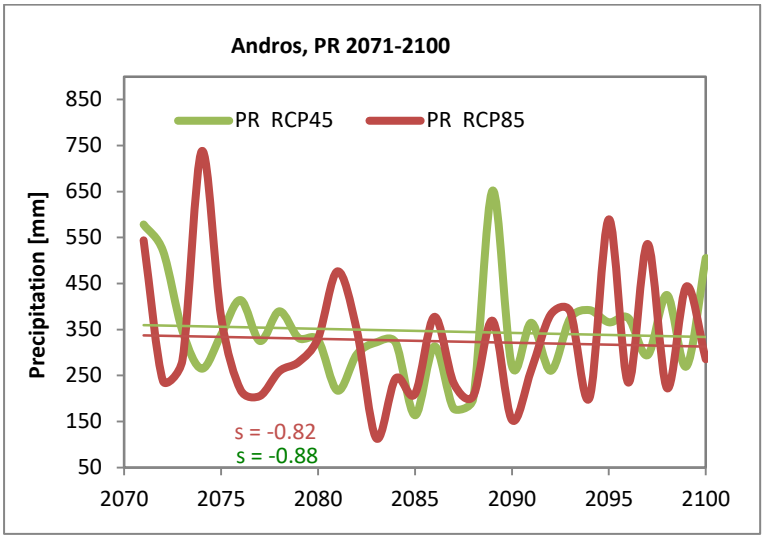

Figure 39 Total annual precipitation results for Andros Island during the historical period 1971-2000 (top panel), the near future period 2031-2060 (middle panel) and the distant future period 2071-2100 (bottom panel), under the future scenarios RCP4.5 (green line) and RCP8.5 (red line).

Seasonal total precipitation results

Total annual precipitation is projected to decrease to 350mm/year under both periods and climate scenarios (Fig. 39). A seasonal breakdown of projected precipitation indicates that precipitation is set to decrease most over winter and autumn (the "wet season"). Specifically, winter precipitation (at 200mm in the historical period) decreases by about 50mm in the near future and into the distant future (Fig. 40). Over spring, with 60mm in the historical period, there is a minor decrease of 10mm, focusing on the distant future (Fig. 41). Summer precipitation declines from 15mm to about 5mm in the near- and distant future, and becomes much more variable (Fig. 42). Finally, autumn precipitation decreases from 150mm to 135mm in the near future, and to 100-130mm in the distant future (Fig. 43).

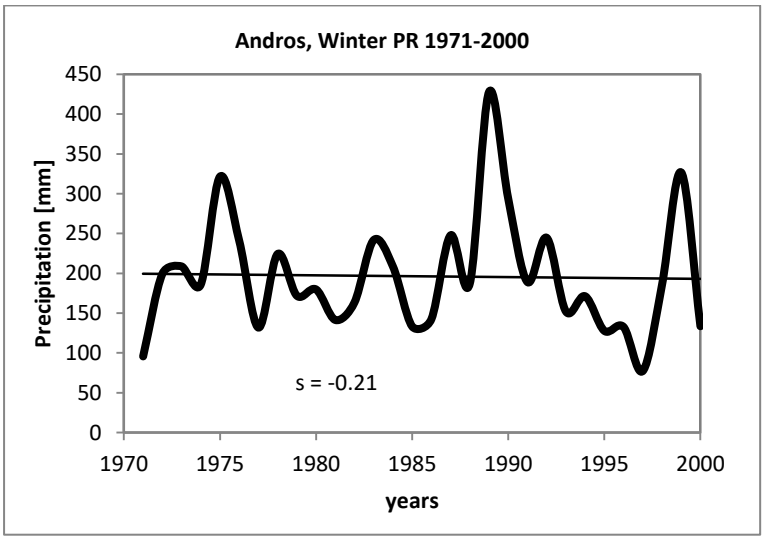

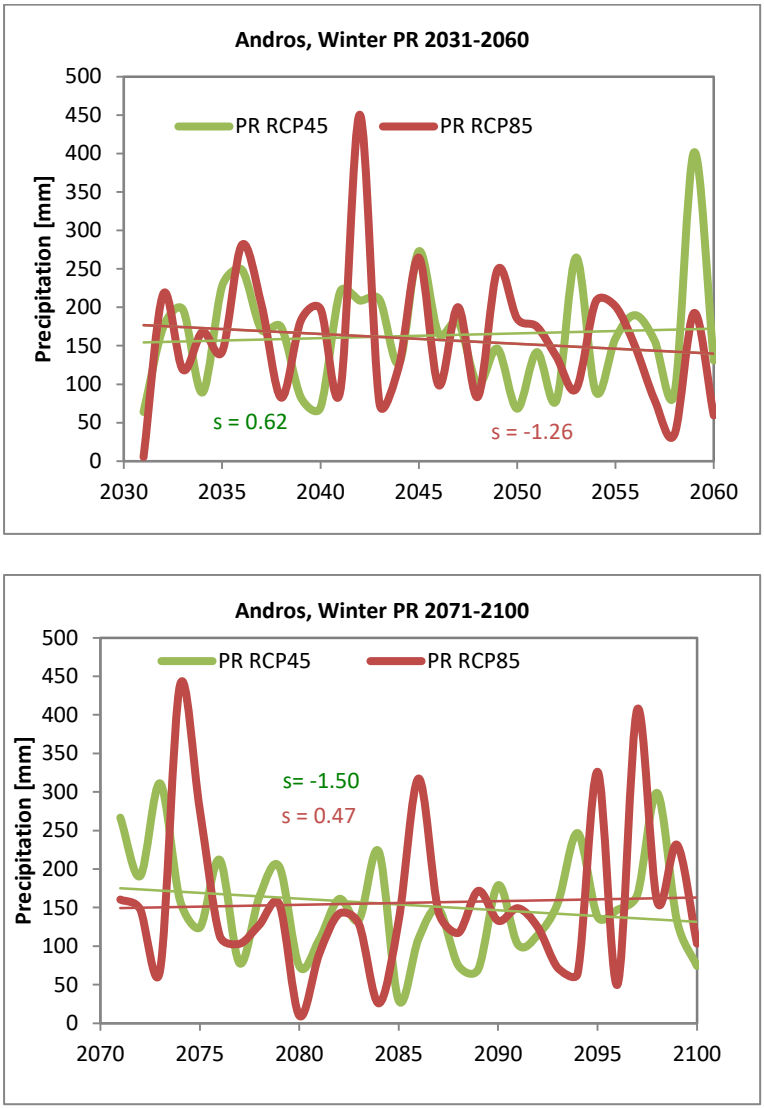

Figure 40 Total winter precipitation results for Andros Island during the historical period 1971-2000 (top panel), the near future period 2031-2060 (middle panel) and the distant future period 2071-2100 (bottom panel), under the future scenarios RCP4.5 (green line) and RCP8.5 (red line).

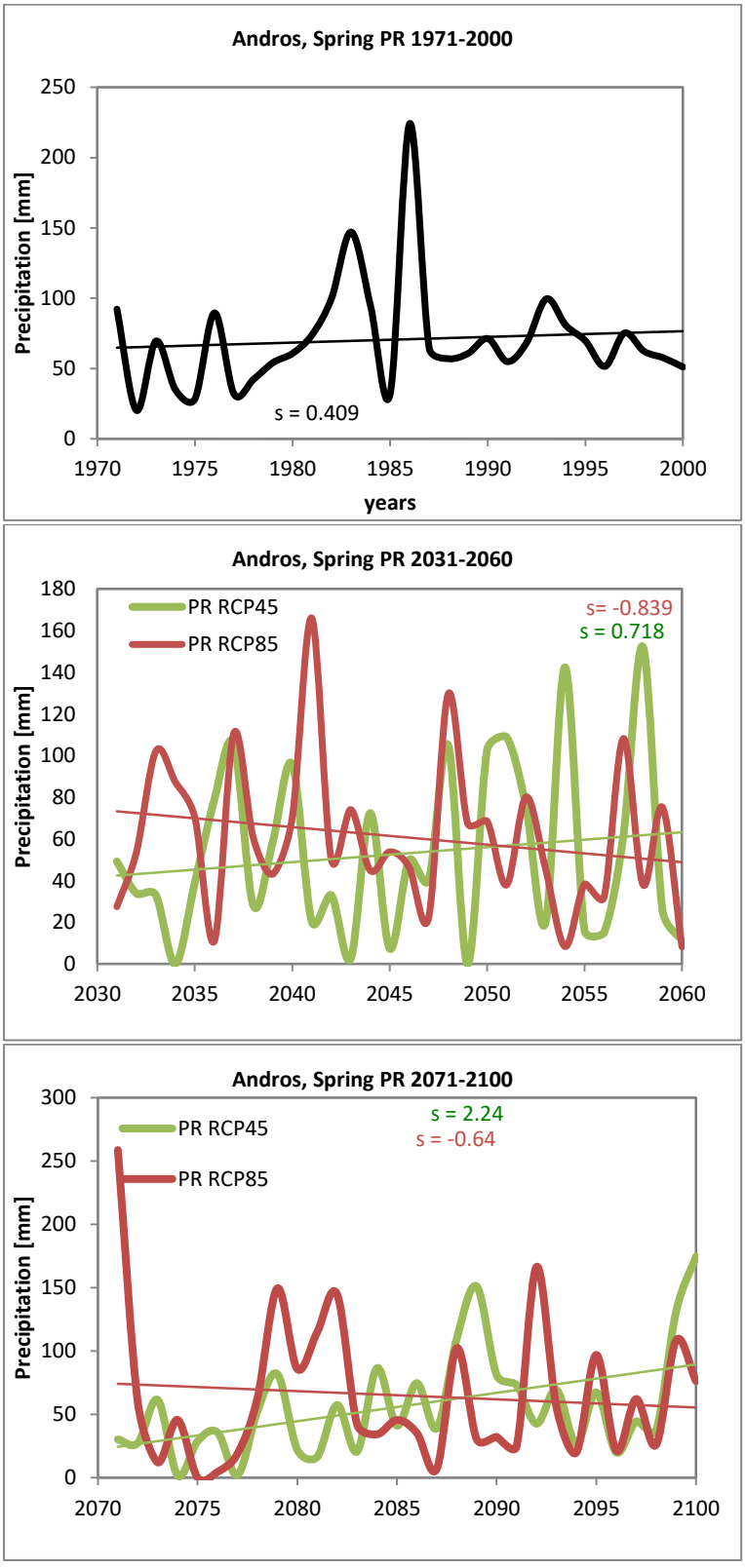

Figure 41 Total spring precipitation results for Andros Island during the historical period 1971-2000 (top panel), the near future period 2031-2060 (middle panel) and the distant future period 2071-2100 (bottom panel), under the future scenarios RCP4.5 (green line) and RCP8.5 (red line).

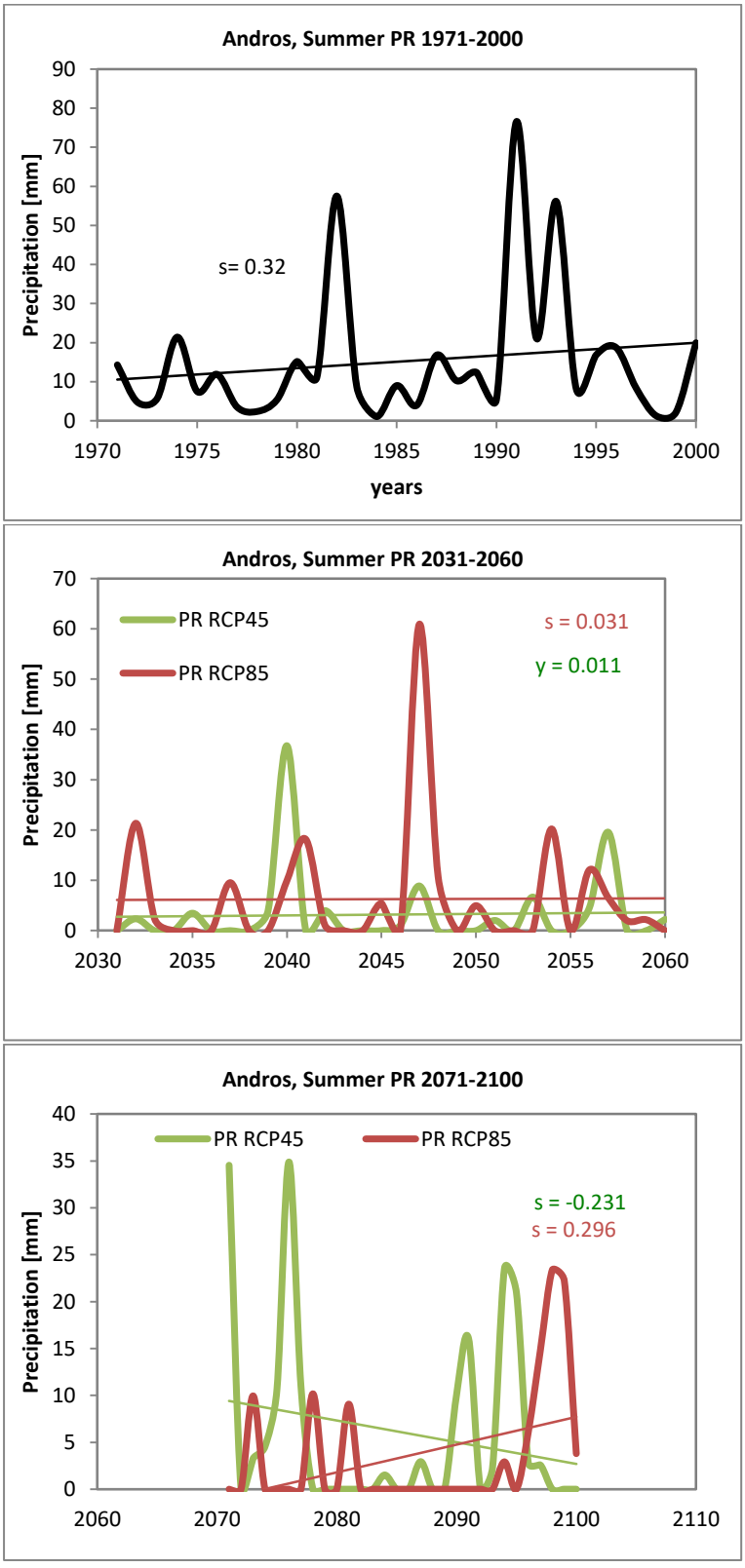

Figure 42 Total summer precipitation results for Andros Island during the historical period 1971-2000 (top panel), the near future period 2031-2060 (middle panel) and the distant future period 2071-2100 (bottom panel), under the future scenarios RCP4.5 (green line) and RCP8.5 (red line).

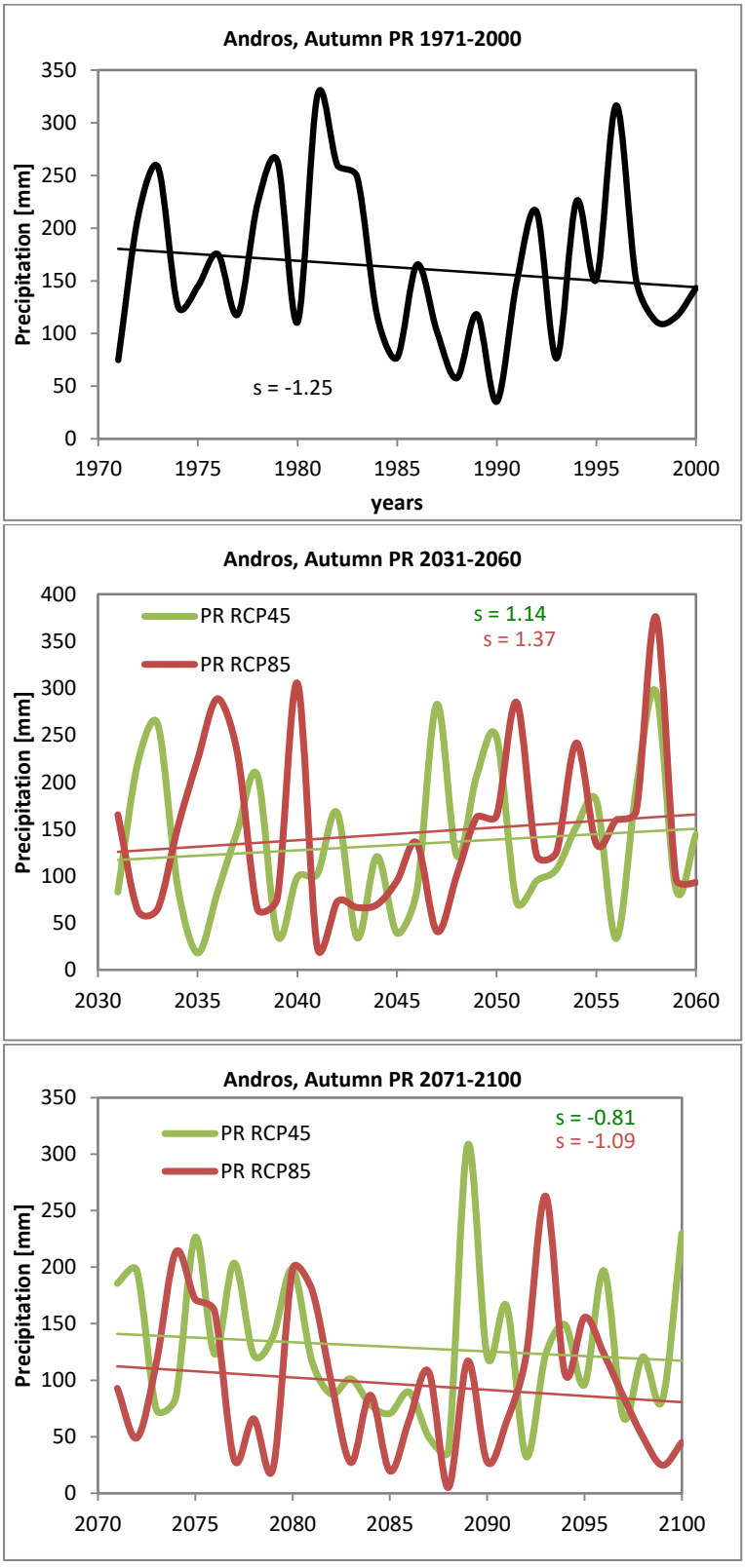

Figure 43 Total autumn precipitation results for Andros Island during the historical period 1971-2000 (top panel), the near future period 2031-2060 (middle panel) and distant future period 2071-2100 (bottom panel), under the future scenarios RCP4.5 (green line) and RCP8.5 (red line).

Extreme precipitation

Total annual precipitation is projected to decrease from 450mm/year to 350mm/year under both periods and climate scenarios (Fig. 39), while most of this decrease will take place over the "wet season", i.e. winter-spring (Figs. 40-43). However, extreme precipitation events are not showing much change in the near- to distant future. Heavy precipitation days (PR>10mm) decrease slightly from 11 to 10 days in the distant future (Fig. 44). The maximum 1-day precipitation of about 55mm does not change (Fig. 45), while the maximum 5-day precipitation falls from 90mm to about 80mm in the distant future (Fig. 46); the variability of these event becomes however much greater.

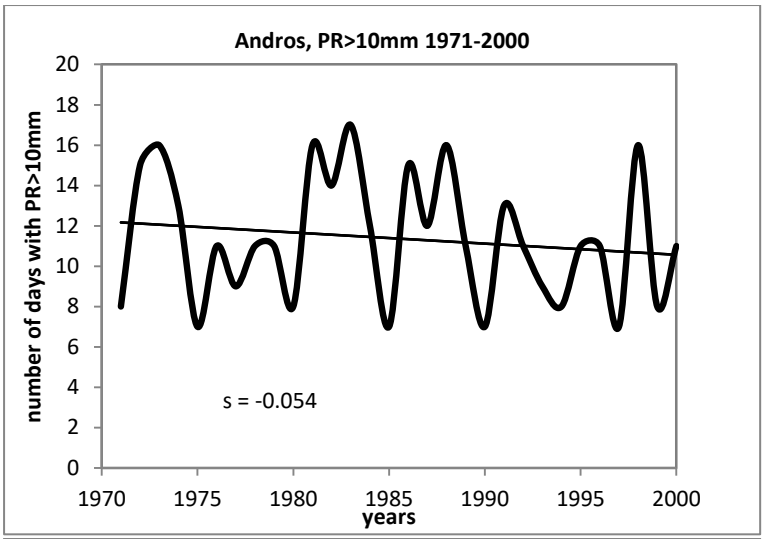

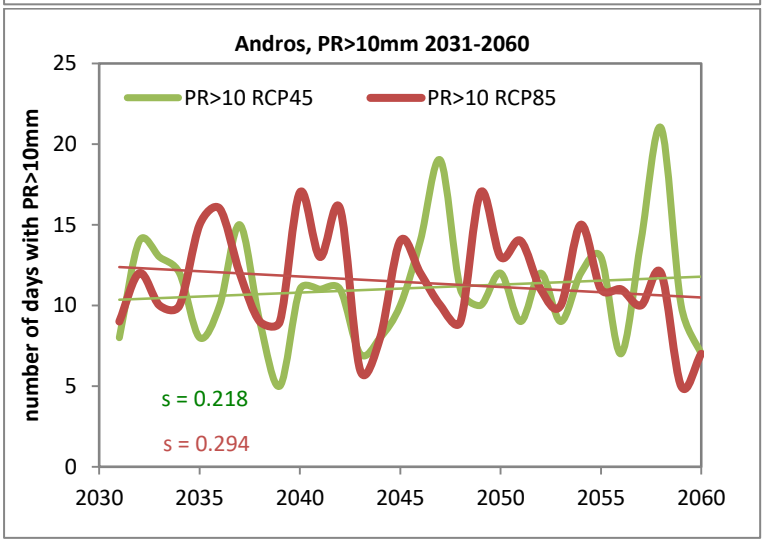

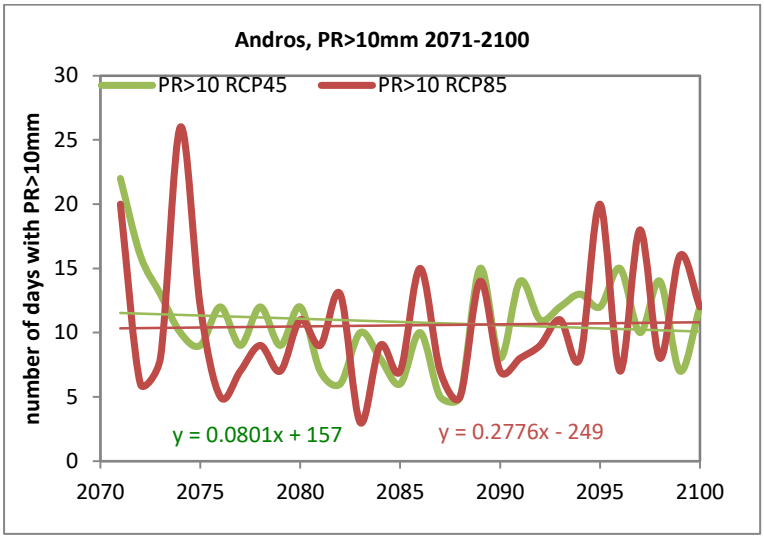

Figure 44 Annual trend for the number of days with precipitation >10mm for Andros during the historical period 1971-2000 (top panel), the near future period 2031-2060 (middle panel) and the distant future period 2071-2100 (bottom panel), under the future scenarios RCP4.5 (green line) and RCP8.5 (red line).

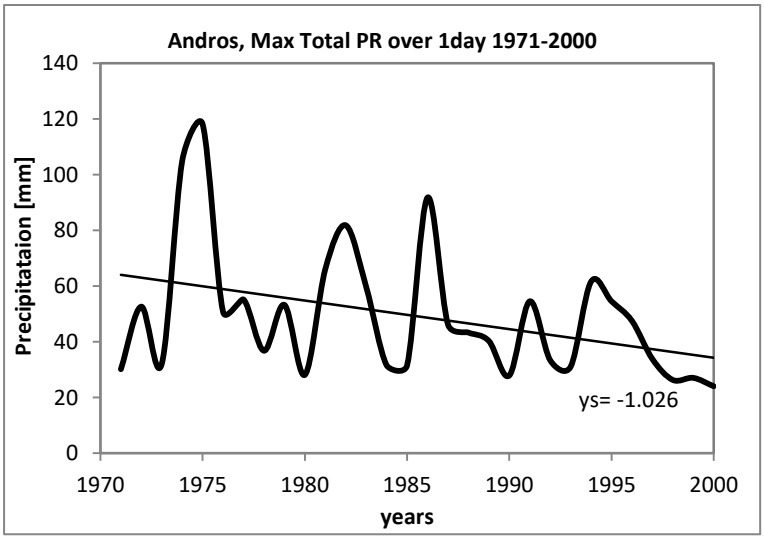

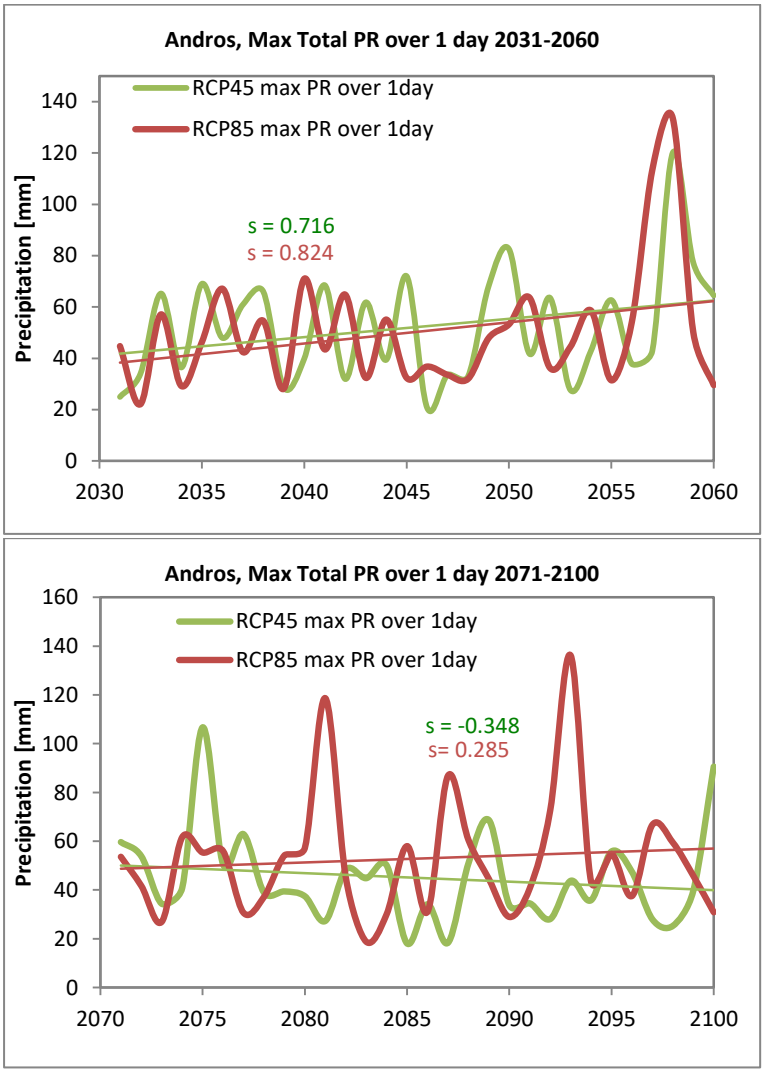

Figure 45 Annual trends for the maximum total precipitation sums over 1 day for Andros for Andros during the historical period 1971-2000 (top panel), the near future period 2031-2060 (middle panel) and the distant future period 2071-2100 (bottom panel), under the future scenarios RCP4.5 (green line) and RCP8.5 (red line).

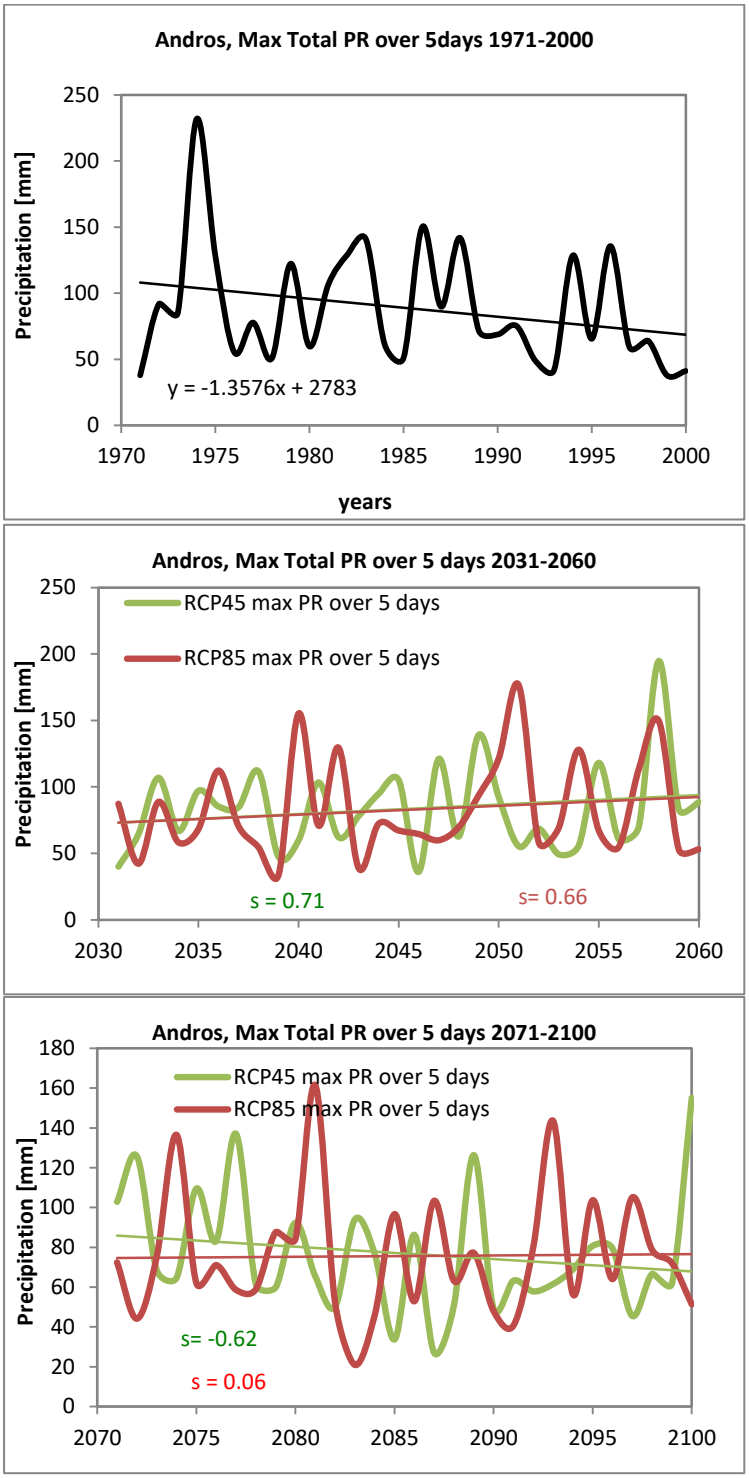

Figure 46 Annual trends for the maximum total precipitation sums over 5 days for Andros during the historical period 1971-2000 (top panel), the near future period 2031-2060 (middle panel) and the distant future period 2071-2100 (bottom panel), under the future scenarios RCP4.5 (green line) and RCP8.5 (red line).

Seasonal trends in extreme precipitation

Extreme precipitation events do not show much change on an annual basis in the near- to distant future (Figs. 44-46). When assessed according to season, it is apparent that heavy precipitation days (PR>10mm) occur mostly in winter and autumn, and to a lesser degree in spring, while rarely taking place during summer (Fig. 47). Overall, there are no changes to this distribution projected in the future. Similar patterns are displayed by the maximum 1-day precipitation and maximum 5-day precipitation over the different seasons: average events decrease in magnitude from winter, to autumn, to spring, and finally to summer (Figs. 48 & 49). The variability of these event becomes however much greater in the future.

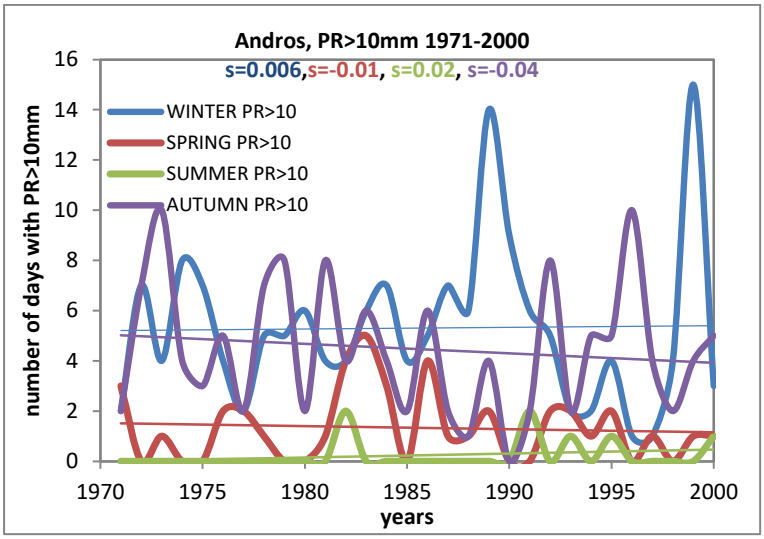

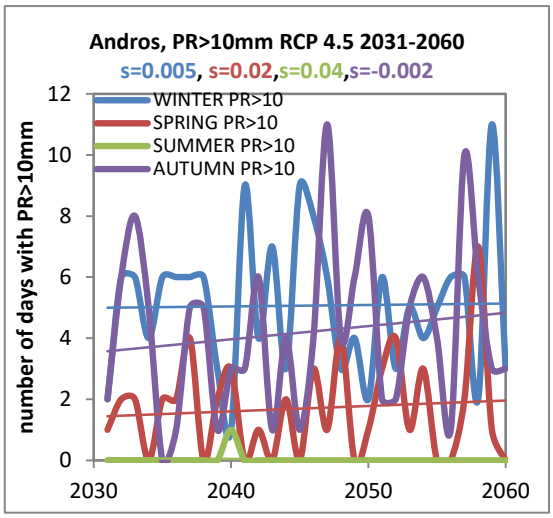

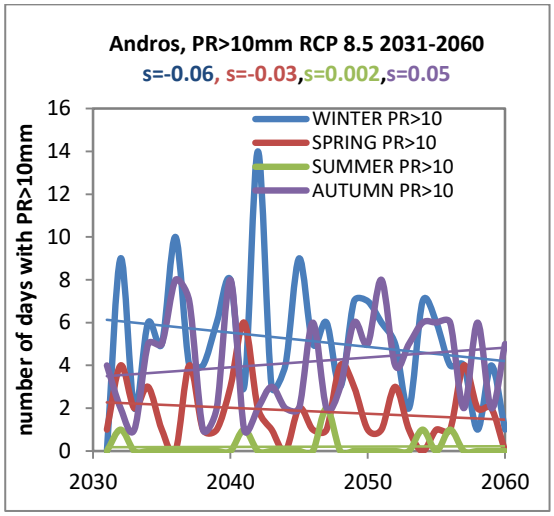

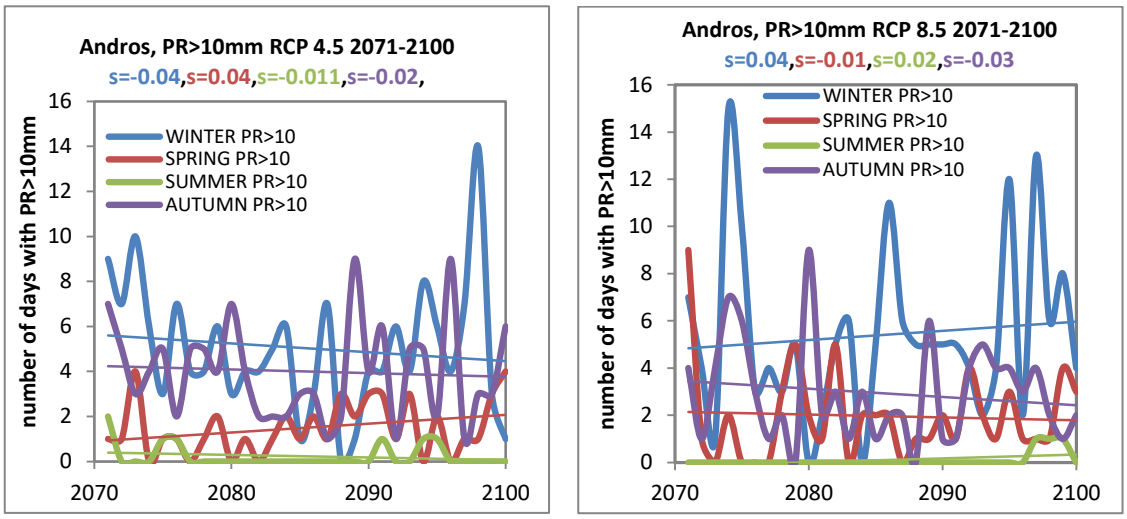

Figure 47 Seasonal trends for the number of days with precipitation amount greater than 10 mm for Andros during the historical period 1971-2000 (top panel), the near future period 2031-2060 (middle panels) and the distant future period 2071-2100 (bottom panels), under the future scenarios RCP4.5 and RCP8.5 (left and right panel, respectively). The colored numbers on the top indicate the calculated slopes for each one of the seasons.

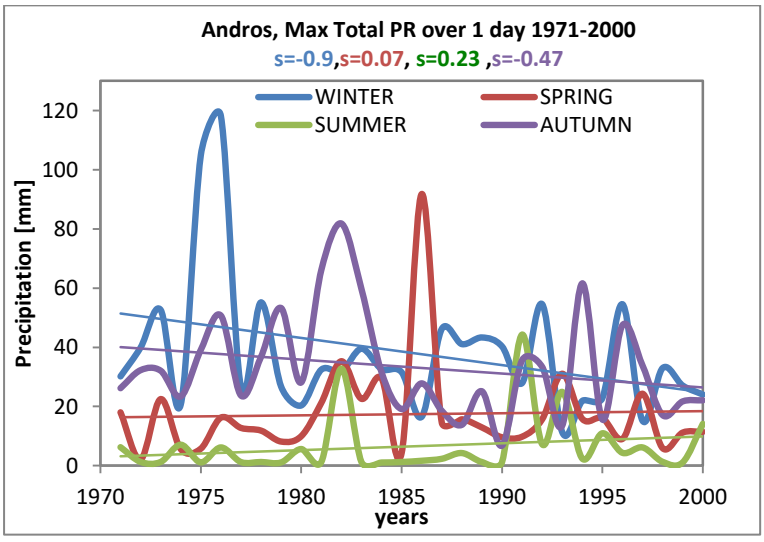

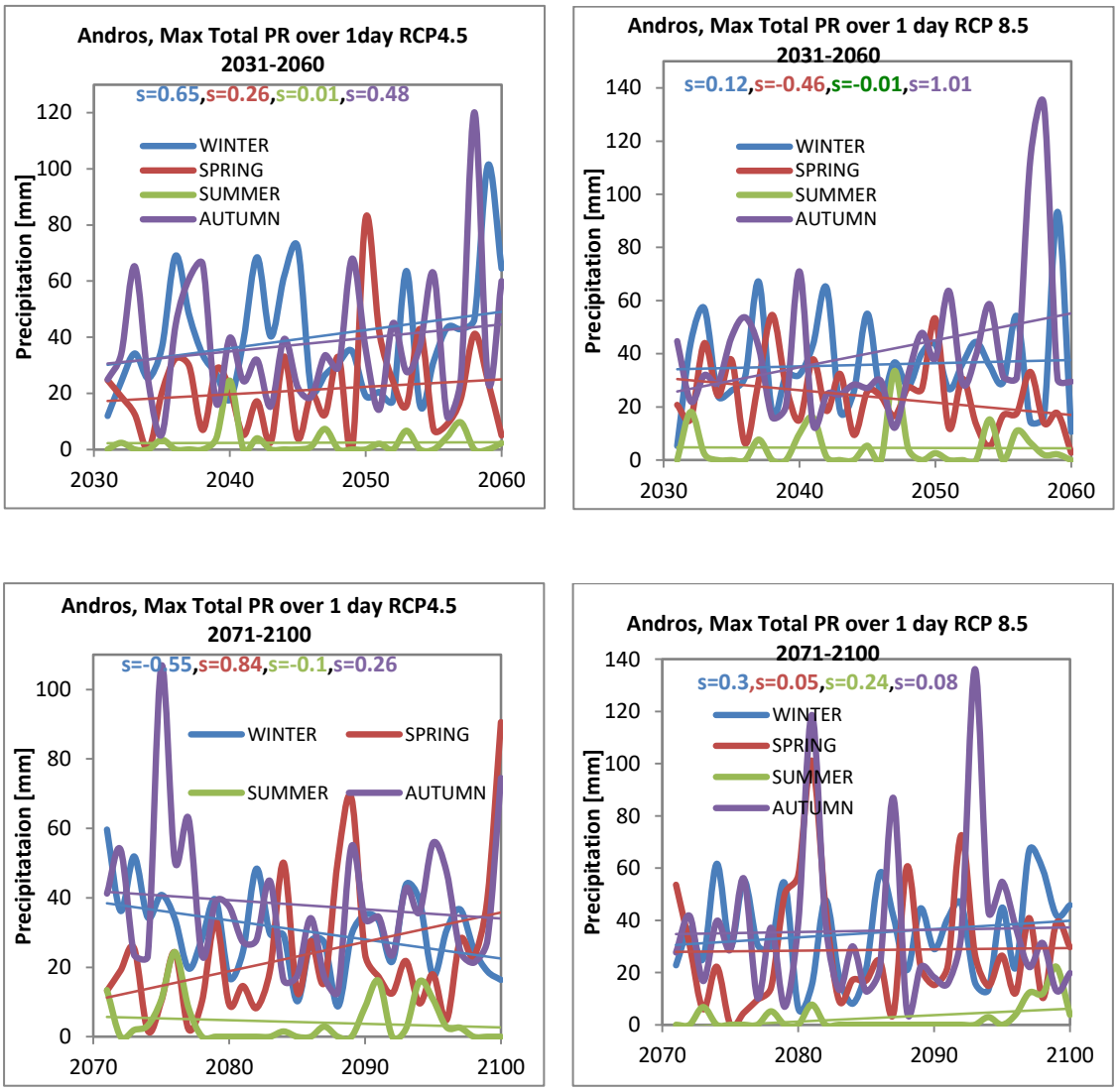

Figure 48 Seasonal trends for the maximum total precipitation sums over 1 day for Andros during the historical period 1971-2000 (top panel), the near future period 2031-2060 (middle panels) and the distant future period 2071-2100 (bottom panels), under the future scenarios RCP4.5 and RCP8.5 (left and right panel, respectively). The colored numbers on the top indicate the calculated slopes for each one of the seasons.

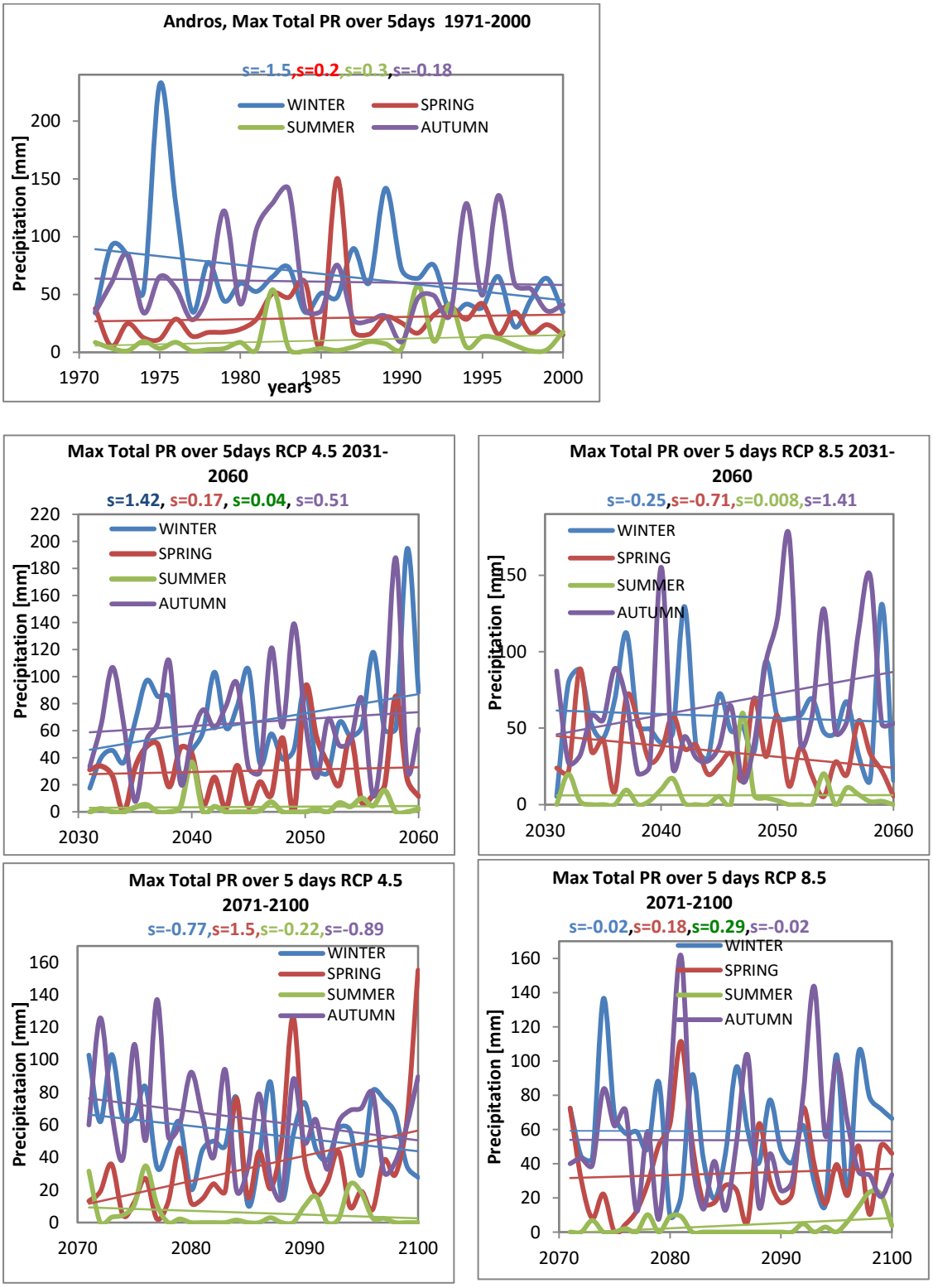

Figure 49 Seasonal trends for the maximum total precipitation sums over 5 days for Andros during the historical period 1971-2000 (top panel), the near future period 2031-2060 (middle panels) and the distant future period 2071-2100 (bottom panels), under the future scenarios RCP4.5 and RCP8.5 (left and right panel, respectively). The colored numbers on the top indicate the calculated slopes for each one of the seasons.

Maximum length of dry spell (PR<1mm)

Future simulations show large increases in the maximum length of dry spells (with precipitation-PR < 1mm). The maximum annual length of a dry spell was on average 59 days over the control (historical) period, increasing to 130 (RCP 4.5) – 110 (RCP 8.5) days in the near future and 135 (RCP 4.5) - 140 (RCP 8.5) days in the distant future (Fig. 50). When there is a seasonal breakdown of dry spells, there are 20 to 80 dry days in summer, and 5-30 days in all other seasons over the control period. In the near- and distant future period, dry spells lasts 90 days for almost all summers (i.e. the entire summer), while the length of dry spells in spring varies from 20-90 days, and 10-50 days over winter and autumn (Fig. 51). It should be noted that spring and summer dry spells are more severe in the near future under the RCP 4.5 scenario; in the distant future the maximum length of seasonal dry spells are large similar under both scenarios.

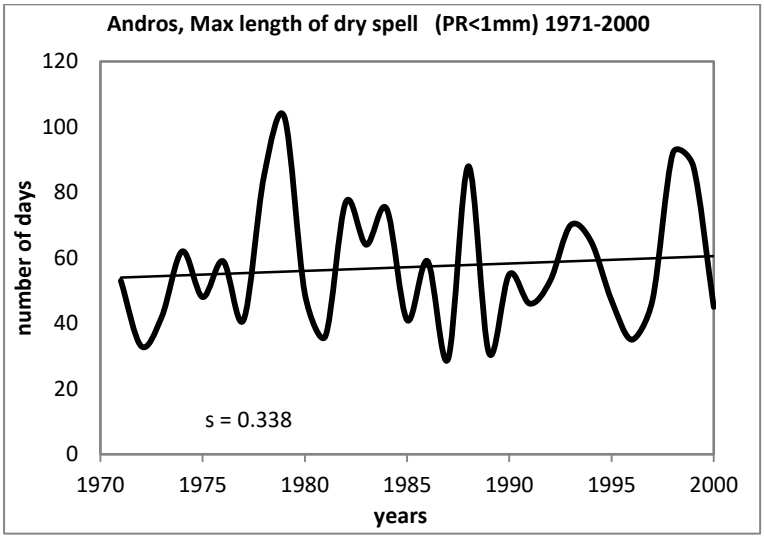

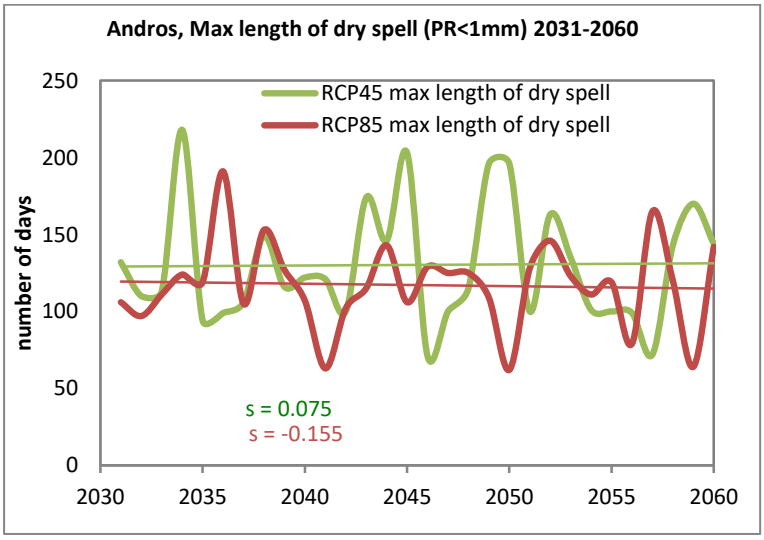

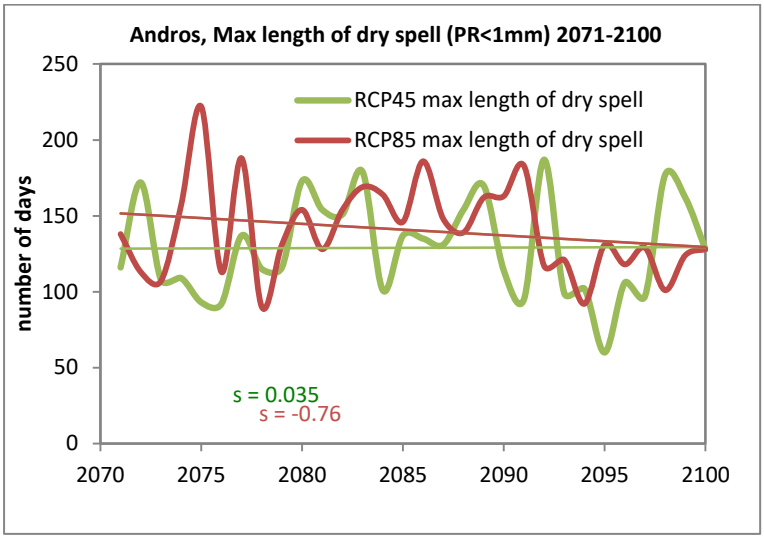

Figure 50 Maximum annual length of dry spell (days with precipitation <1mm) for Andros during the historical period 1971-2000 (top panel), the near future period 2031-2060 (middle panel) and the distant future period 2071-2100 (bottom panel), under the future scenarios RCP4.5 (green line) and RCP8.5 (red line).

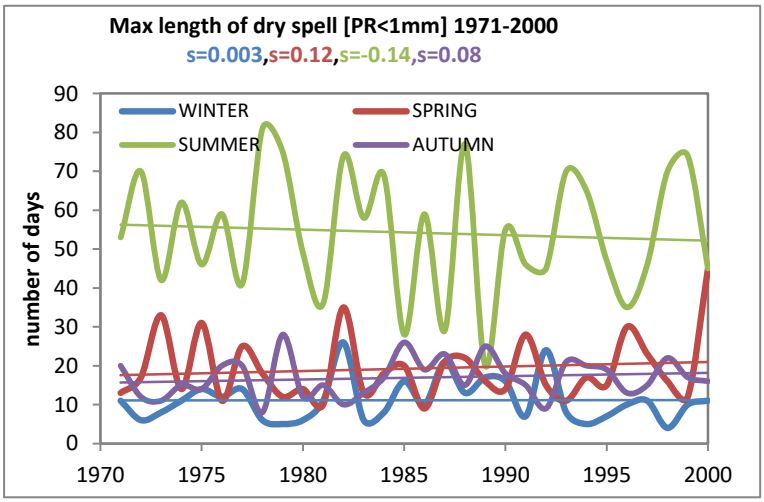

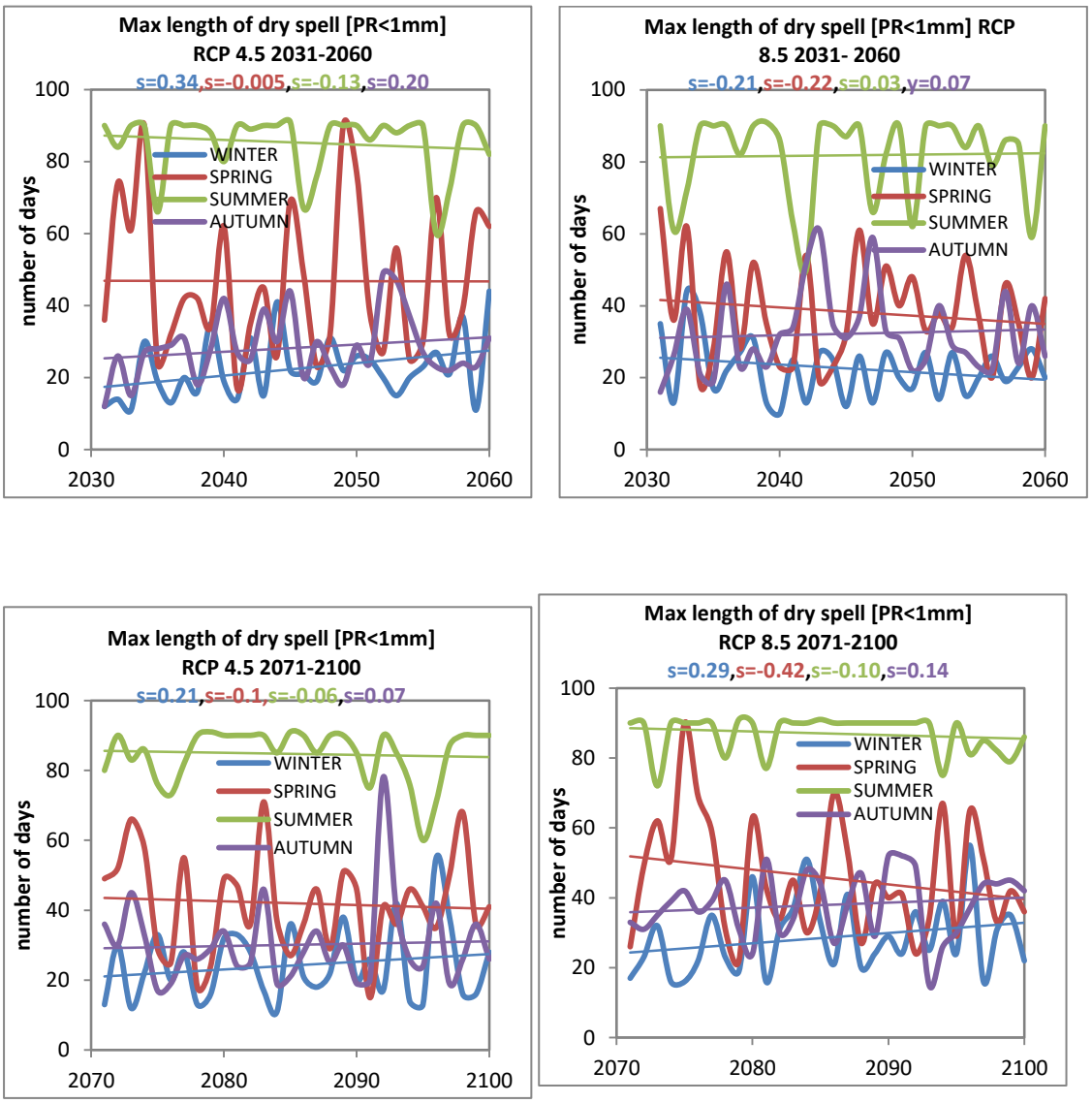

Figure 51 Seasonal trends for the maximum length of days with precipitation <1mm for Andros during the historical period 1971-2000 (top panel), the near future period 2031-2060 (middle panels) and the distant future period 2071-2100 (bottom panels), under the future scenarios RCP4.5 and RCP8.5 (left and right panel, respectively). The colored numbers on the top indicate the calculated slopes for each one of the seasons.

3.4 Statistically significant climate changes

Bootstrap analyses were applied to key climate indices to prove the statistical significance of simulated changes. Annual and seasonal temperature data all show a similar pattern of increasing values (section 3.3.1), while precipitation declines (section 3.3.2). For the purpose of this report, we focused on the statistical analyses of selected key indices to prove this overall pattern (Table 3). The following temperature indices are selected for bootstrap analyses: T_{max} (^{o}C), T_{min} (^{o}C), T_{max}>30^{o}C (hot days), and T_{min}>20^{o}C (tropical nights). Selected precipitation indices for bootstrap analyses are: Total precipitation – PR (mm), N^{o} of days with PR>10mm (heavy precipitation), max. 1-day precipitation (mm), and max. length of dry spell (days).

For each of the above indices, simulated values from the control period (1971-2000) were compared to the near- and distant future periods (2031-2060 and 2071-2100 resp.), for both selected climate scenarios (RCP4.5 and RCP8.5).

Table 3 shows that the temperature increases are statistically significant in the near- and distant future under both scenarios, with the largest increases projected under the RCP8.5 scenario. Annual mean maximum -T_{max} and minimum temperature- T_{min} is set to increase progressively over this century and amounts to, for example, in the distant future: T_{max} 2,89 – 4,41 ^{o}C (RCP 4.5 and RCP 8.5, resp.) and T_{min} 3,02-4,92 ^{o}C (RCP 4.5 and RCP 8.5, resp.). The amount of hot days (T_{max}>30^{o}C) and tropical nights (T_{min}>20^{o}C) also significantly increases in the near and distant future; for example, under the more extreme climate scenario (RCP8.5), there will be on average 82 more tropical nights in the distant future (!). Total annual precipitation is set to decrease significantly over the coming century under both climate scenarios, while the maximum length of dry spells is greatly increasing. However, extreme precipitation events (as indicated by N^{o} of days with PR>10mm and max. 1-day pr) are not set to change significantly in the near- to distant future, as was expected from visual analyses of the simulation results (section 3.3.2).

	T_{max} (increase in ^{o}C)	T_{min} (increase in ^{o}C)	T_{max}>30^{o}C (increase in days)	T_{min}>20^{o}C (increase in days)	PR TOTAL (%)	PR>10mm	PR1DAY	DRY SPELL (increase in days)
RCP4.5_1	1.99	2.15	22.80	42.73	-17.65	-	-	73.00
RCP4.5_2	2.89	3.02	44.50	56.93	-18.90	-	-	71.73
RCP8.5_1	2.39	2.67	32.00	50.70	-13.25	-	-	59.93
RCP8.5_2	4.41	4.92	74.60	81.93	-23.77	-	-	83.27

Table 3 Bootstrap analyses of simulated climate variables (T_{max}, T_{min}, T_{max}>30 ^{o}C, T_{min}>20 ^{o}C, Total precipitation-PR, Days with PR>10mm, max. 1-day PR (mm), max. length of dry spell): numbers in the table above signify statistically significant differences. The following scenarios and periods were analysed for statistically significant changes: RCP4.5_1 (2031-2060) vs ref (1971-2000), RCP4.5_2 (2071-2100) vs ref (1971-2000), RCP8.5_1 (2031-2060) vs ref (1971-2000), RCP8.5_2 (2071-2100) vs ref (1971-2000).

4. RESULTS: coarse resolution projections for the Aegean

This section presents geographical maps of current climate & future projections for the Aegean area. Maps for the Aegean area depict changes in climatic indices based on the projections of the state-of-the-art Regional Climate Model (RCM) simulations developed within the framework of EURO-CORDEX at a horizontal resolution of approximately 12km. Specifically, we examine the potential future climate changes for the Aegean islands, using the simulations of precipitation (PR), maximum- and minimum air temperatures (resp. Tmax and Tmin)from the RCA4 regional climate model SMHI with boundary conditions from the global HadGEM-ES model of the Met Office Hadley Centre (MOHC), which was found to give the best results for the Aegean region. Climate model data from this state-of-the-art RCM are available for the entire period spanning 1950 to 2098 and are used to assess the vulnerability of Aegean islands to climate change and prioritize future interventions in the most vulnerable regions.

Simulations covering the period 1971-2000 (control period) are used as reference for comparison with future projections for two future periods (2031-2060 and 2069-2098), under two new IPCC emissions scenarios: RCP4.5, representing a medium mitigation scenario, and RCP8.5, representing a high emission scenario with no climate mitigation policies. Geographical maps present the results for the control period (1971-2000), and the "near future" (2031-2060) and ''distant future'' (2069-2098) periods under the two aforementioned climate scenarios. Differences between control and future periods will be analysed in order to identify changes in climate indices, which directly or indirectly affect agriculture in the examined areas.

Changes related to temperature and precipitation were studied using the following climatic indices: [1] Mean max temperatures (absolute index), [2] Mean min temperatures (absolute index) [3] Number of days with maximum temperature Tmax > 30 ^{o}C (threshold index; hot days), [4] Number of days Tmax> 35 ^{o}C (threshold index; heatwave), [5] Number of days with minimum temperature Tmin> 20 ^{o}C (threshold index; tropical night), [6] Total Precipitation - PR (absolute index), [7] Highest 1-day precipitation amount (absolute index), [8] Heavy precipitation days (PR>10mm/day; threshold index), [9] Very heavy precipitation days (PR>20mm/day; threshold index), and [10] Maximum length of dry spell (consecutive days with PR<1mm; duration index).

4.1 Mean Annual Maximum Temperatures

The average maximum mean annual temperature for the control period (1971-2000) ranges between 14-20°C regarding the whole Aegean region (Fig. 1). The highest maximum average temperatures of around 20°C are detected for Dodecanese islands, while Tmax is between 14-19°C for Crete, and 16-20°C for Cyclades and North Aegean (Fig. 52). In the near future period average Tmax rises to ~22°C or ~23 °C for the Aegean region under the RCP4.5 and RCP8.5 scenarios, respectively; the highest temperatures are projected for Dodecanese Islands (Fig. 52 middle panel). In the distant future period (Fig. 52 bottom panel) Tmax rises to 24°C (RCP 4.5) or 25°C (RCP 8.5) for the whole Aegean area except for the mountainous areas of Crete (due to its high elevation).

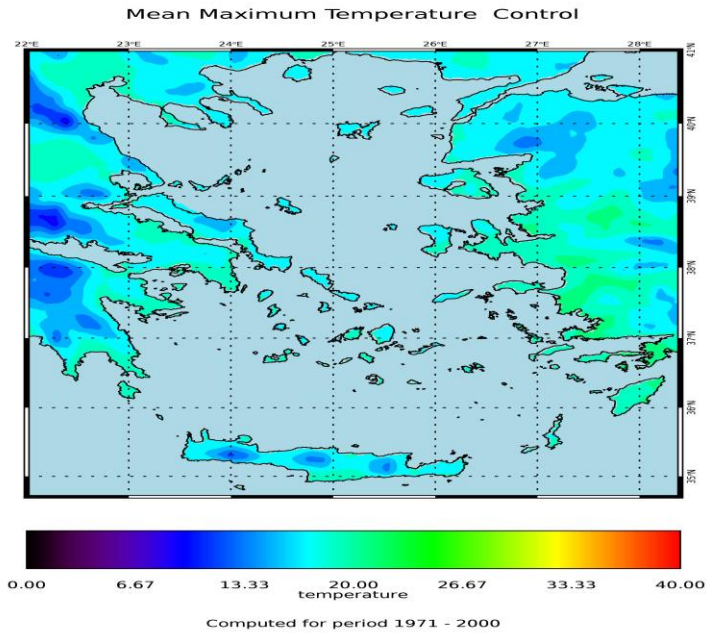
Mean Maximum Temperature Control
22°E
23°E
24°E
25°E
26°E
27°E
28°E
41°N
40°N
39°N
38°N
37°N
36°N
35°N
0.00
6.67
13.33
20.00
26.67
33.33
40.00
temperature
Computed for period 1971 - 2000

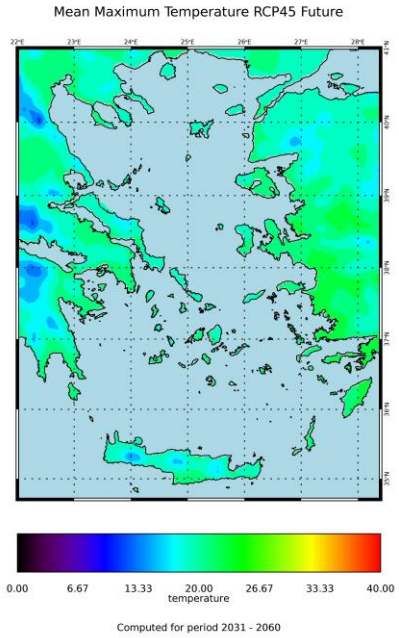
Mean Maximum Temperature RCP45 Future
0.00
6.67
13.33
20.00
26.67
33.33
40.00
temperature
Computed for period 2031 - 2060

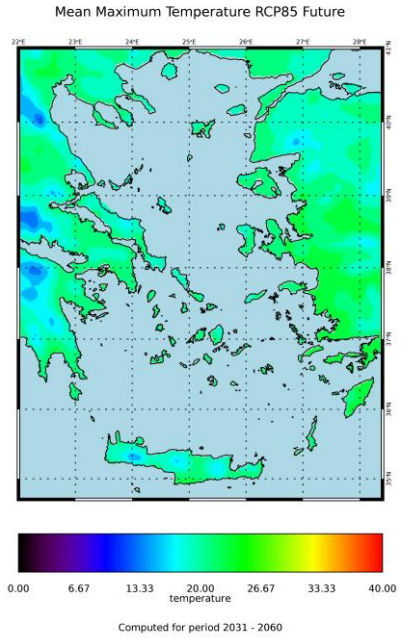
Mean Maximum Temperature RCP85 Future
0.00
6.67
13.33
20.00
26.67
33.33
40.00
temperature
Computed for period 2031 - 2060

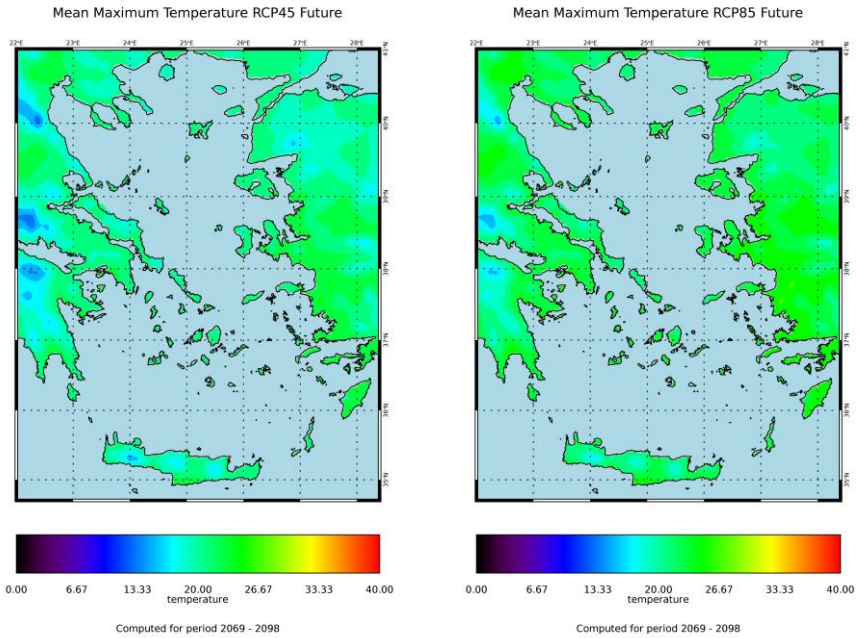

Figure 52 Average mean maximum annual temperature predictions for Aegean during the control period 1971-2000 (top panel), the near future period 2031-2060 (middle panel) and the distant future period 2069-2098 (bottom panel), under the future scenarios RCP4.5 (left column) and RCP8.5 (right column).

4.2 Mean Annual Minimum Temperatures

The average annual minimum temperature in the control period is ranging from around 9 - 11 °C at the central regions of Crete and the islands of North Aegean (Mitilini, Chios), while values up to 12°C are detected for Cyclades or Dodecanese (Fig. 53). Annual Tmin shows higher values over the near future period, with temperature averages of around 11-13 °C for Crete and North Aegean and 14°C or 15°C for Cyclades or Dodecanese, respectively under both climate scenarios (Fig. 53 middle panel). The results for the distant future period indicate that the minimum temperature remain almost the same under the RCP 4.5 climate scenario and will increase under the scenario RCP 8.5 to 17°C for the Aegean region (Fig. 53 bottom panel).

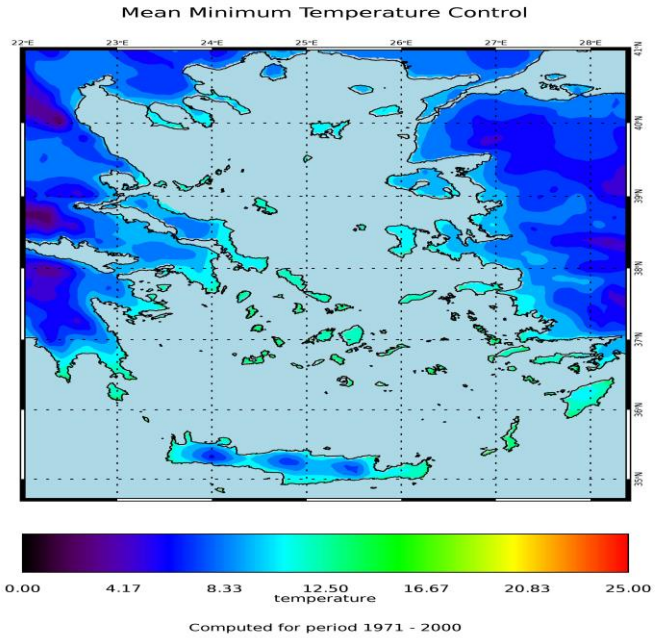
Mean Minimum Temperature Control
22°E
23°E
24°E
25°E
26°E
27°E
28°E
41°N
40°N
39°N
38°N
37°N
36°N
35°N
0.00
4.17
8.33
12.50
16.67
20.83
25.00
temperature
Computed for period 1971 - 2000

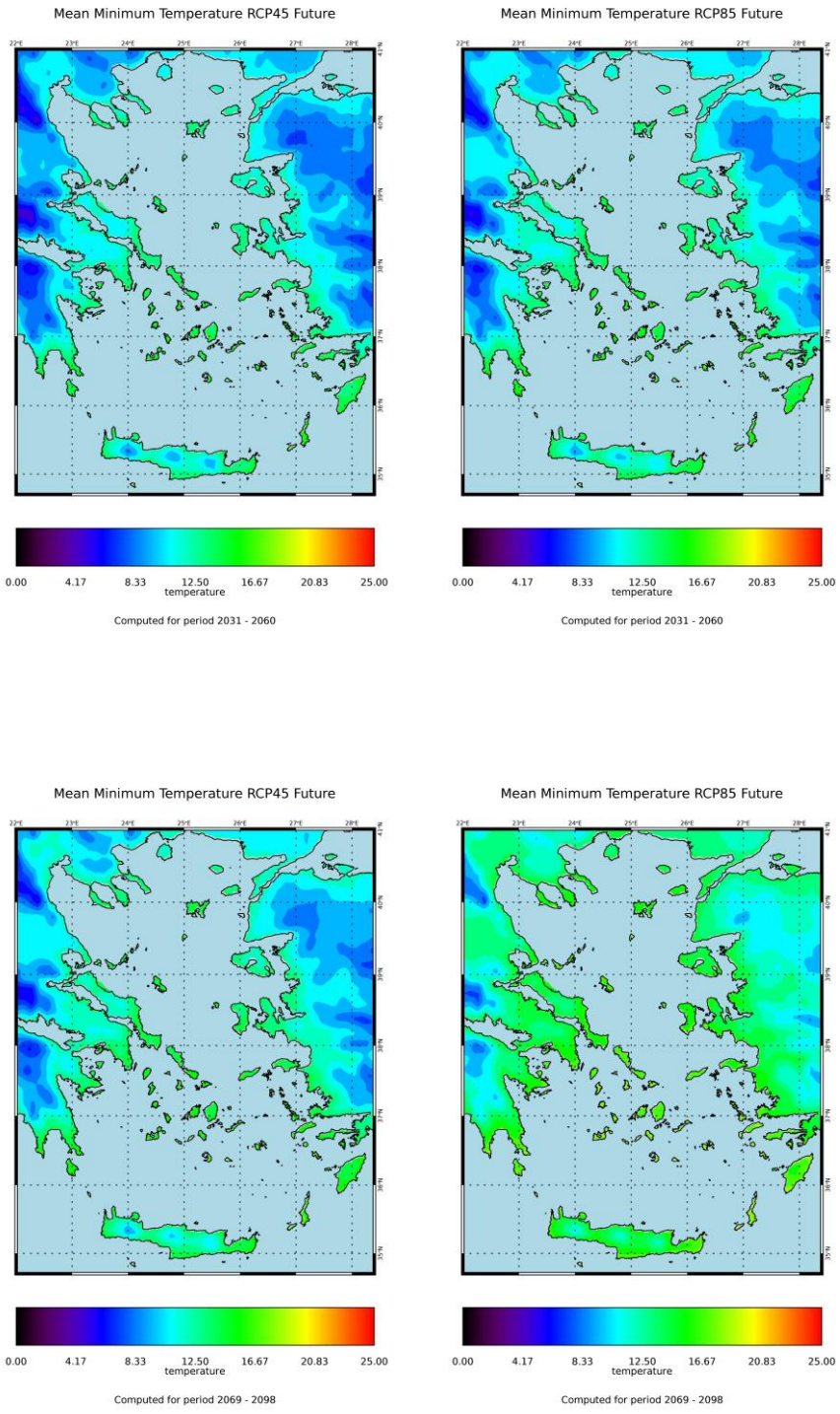

Figure 53 Average Mean annual minimum temperature predictions for Aegean during the control period 1971-2000 (top panel), the near future period 2031-2060 (middle panel) and the distant future period 2069-2098 (bottom panel), under the future scenarios RCP4.5 (left column) and RCP8.5 (right column).

4.3 Extreme temperature results

Extreme temperature indices show large increases in the near and distant future under both climate scenarios; the largest increases are projected under scenario RCP 8.5.

Hot days

The number of hot days (T_{max}>30^{o}C) are between 5 (mountainous areas of Crete) and 67 (Rhodes) during the control period 1971-2000 (Fig. 54). In the near future and for both climate scenarios, the average number of hot days increases from 13 days/year to 50 days/year for Cyclades and Crete and from 55 days/year to 75 days/year for the islands of North Aegean and Dodecanese (Fig. 54 middle panel).

In the distant future (Fig. 54 bottom panel) the average number of hot days per year is raising to 70 days/year for South Crete and Cyclades and 80 days/year for Dodecanese and North Aegean under the RCP4.5 scenario, while hot days are close to 80 under the RCP8.5 scenario.

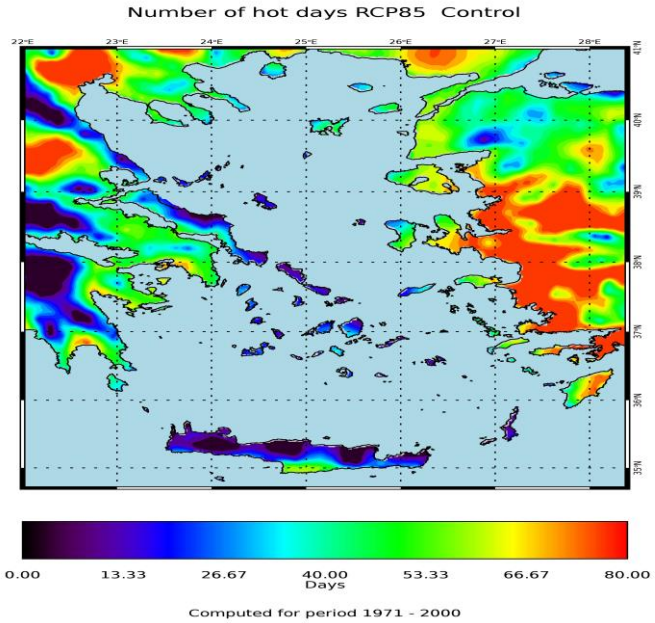

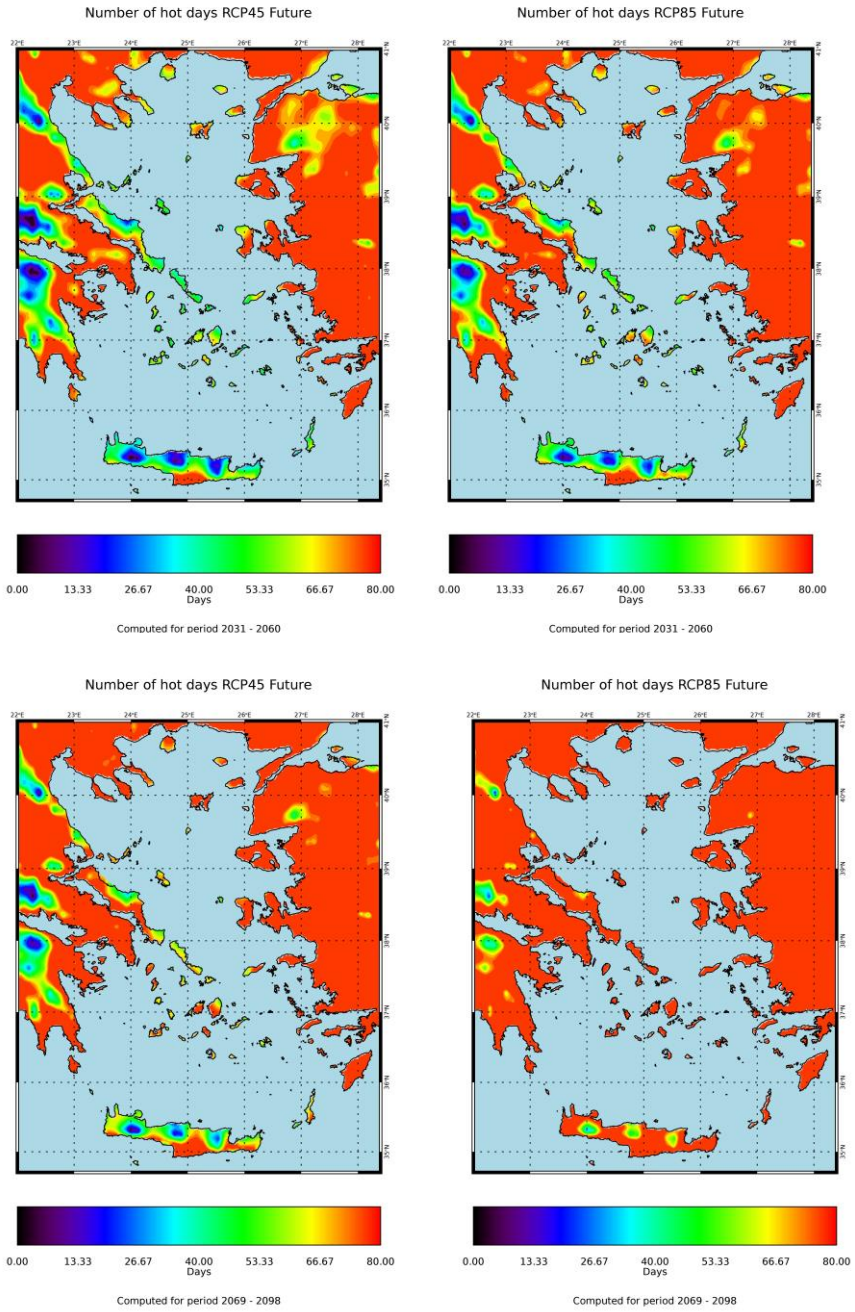

Figure 54 Average annual number of days with maximum temperature higher than 30^{O}C (hot days) for Aegean during the control period 1971-2000 (top panel), the near future period 2031-2060 (middle panel) and the distant future period 2069-2098 (bottom panel), under the future scenarios RCP4.5 (left column) and RCP8.5 (right column).

Heatwaves

When considering the average number of days with temperature greater than 35 ^{o}C (characterized as heatwaves), almost zero days of heatwaves were shown in Aegean area, except for some parts of Dodecanese and North Aegean (islands such as Mitilini, Chios, Samos) where about 10 days/year were shown, during the control period (Fig. 55). In the near future heatwaves are set to increase to 2-6 days/year and 15-30 days/year for Crete / Cyclades and Dodecanese / North Aegean, respectively, under both scenarios (Fig. 55 middle panel). Regarding the distant future period (Fig. 55 bottom panel), the greatest increases are shown under the RCP8.5 scenario, where the heatwave days/year reach 25-30 for Crete & Cyclades and 60 days/year for Dodecanese & North Aegean.

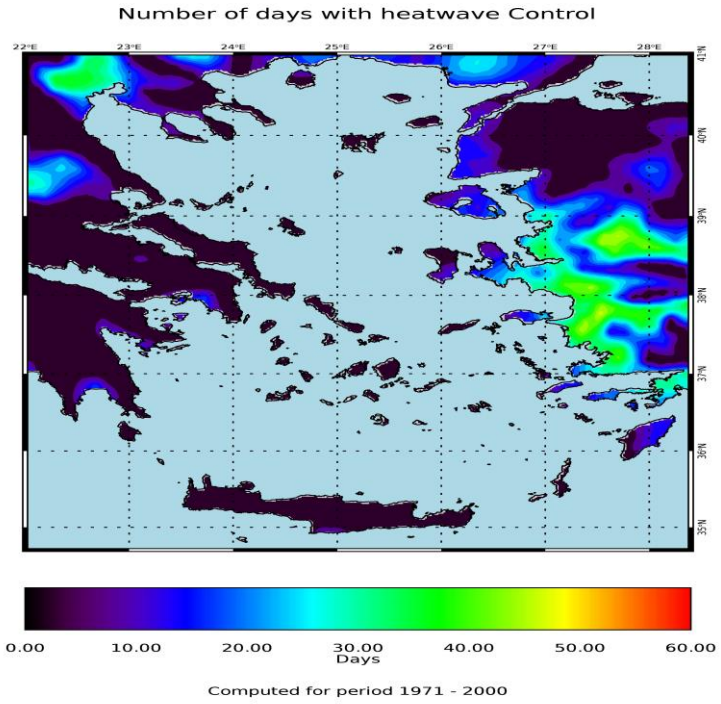

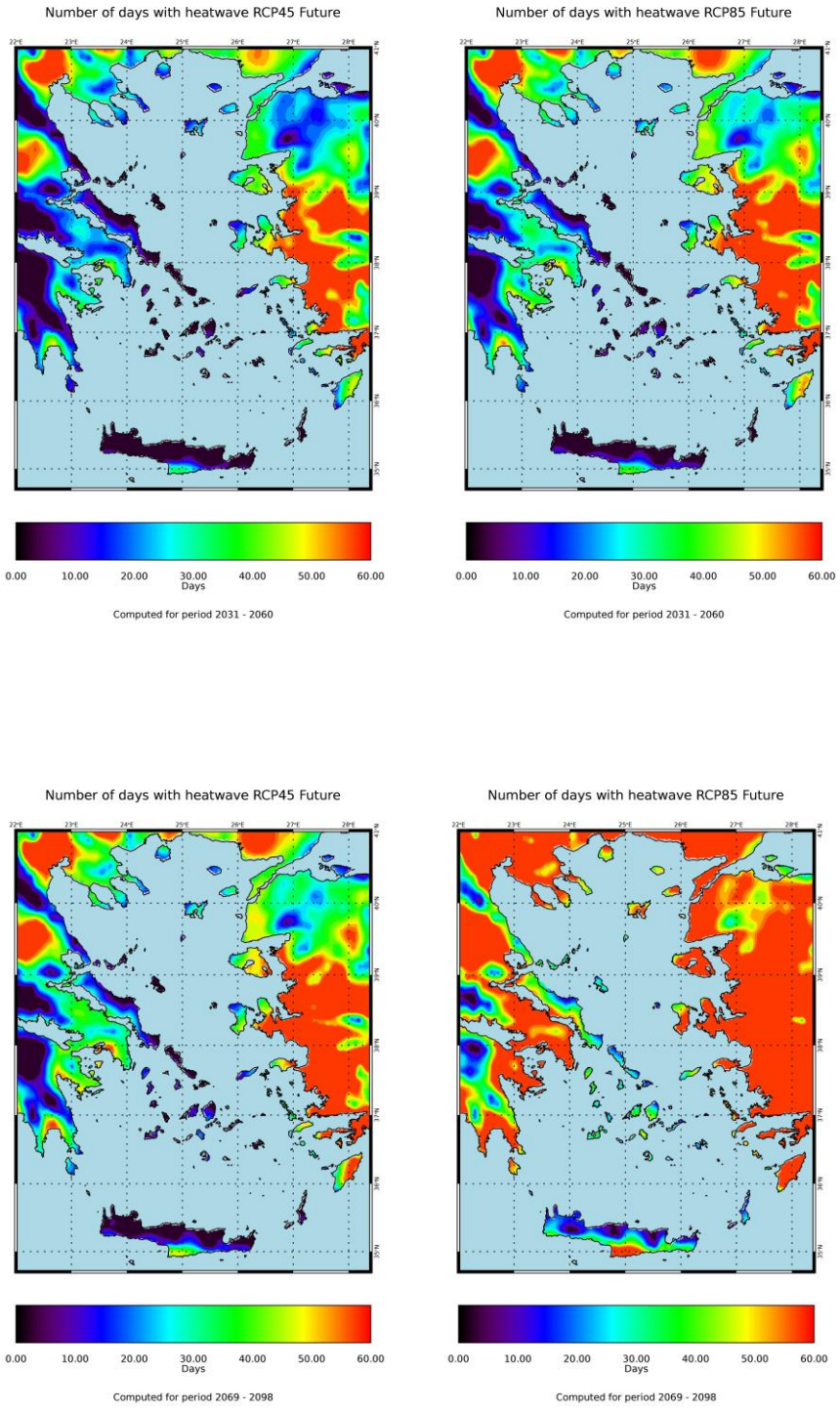

Figure 55 Average annual number of days with maximum temperature higher than 35^{O}C (heatwave) for Aegean during the control period 1971-2000 (top panel), the near future period 2031-2060 (middle panel) and the distant future period 2069-2098 (bottom panel), under the future scenarios RCP4.5 (left column) and RCP8.5 (right column).

Tropical nights (Tmin > 20°C)

The number of days with the minimum temperature greater than 20 °C (tropical nights) were computed for Aegean region. For the control period (Fig. 56), these number between 50 days/year (North Aegean, Crete) and 75 days/year (Dodecanese, South Cyclades). Tropical nights increase to 90 days/year (RCP4.5) or 100 (RCP8.5) for almost all Aegean islands in the near future (Fig. 56 middle panel). In the distant future the average number of tropical nights per year is rising to 110 (RCP4.5) and 140-160 (RCP8.5) (Fig. 56 bottom panel).

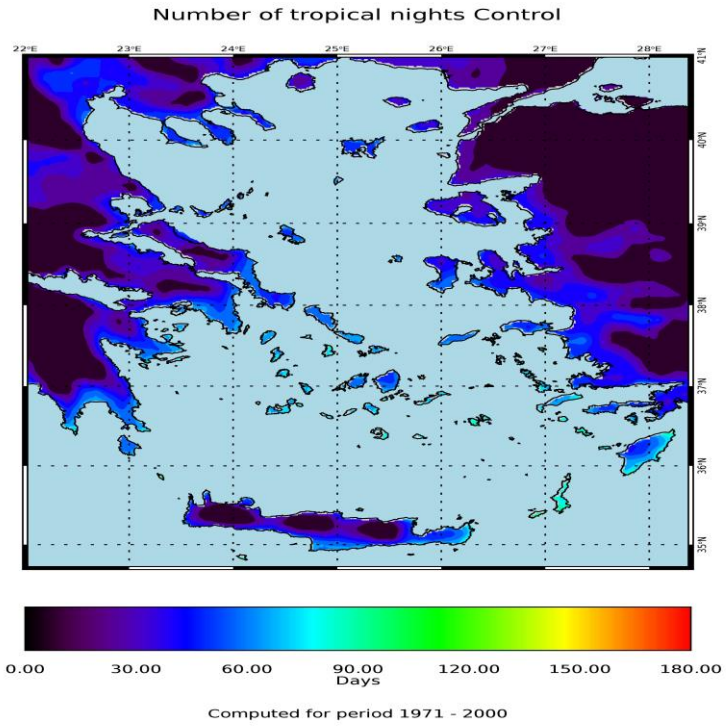

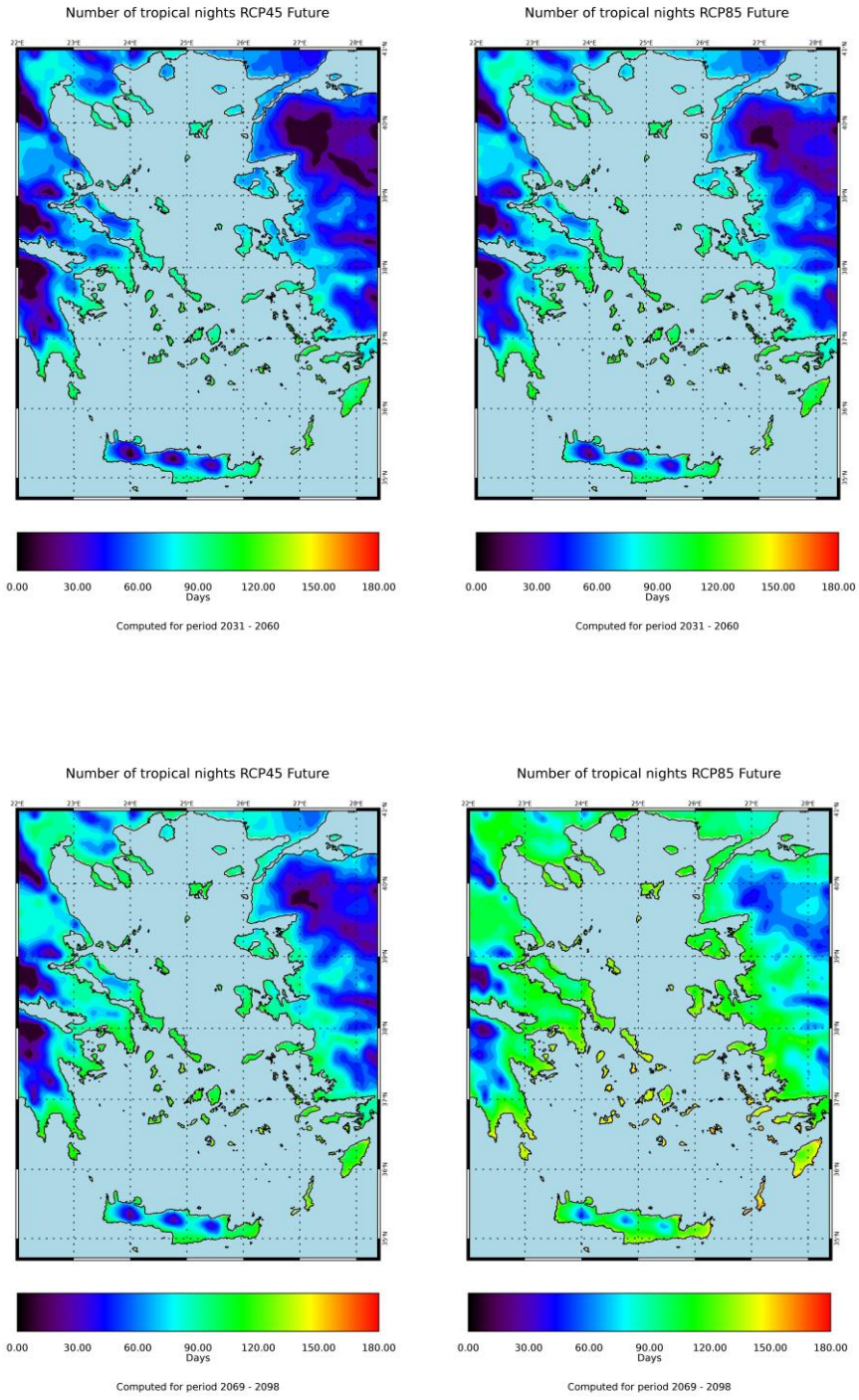

Figure 56 Average annual number of days with minimum temperature higher than 20°C (tropical nights) for Aegean during the control period 1971-2000 (top panel), the near future period 2031-2060 (middle panel) and the distant future period 2069-2098 (bottom panel), under the future scenarios RCP4.5 (left column) and RCP8.5 (right column).

4.4 Total Annual Precipitation

The average total annual precipitation (PR) over the control period is highly variable across the region, from ~350 mm/year (South Crete), to ~450 mm/year (Cyclades and North Aegean), and up to ~800 mm/year (parts of Central Crete, Eastern Aegean; Fig 57, top panel). The simulated precipitation variability continues with no great changes in average PR for the near future across the Aegean region (Fig. 57, middle panel). In the distant future total precipitation is projected to decrease to 350 mm/year (Cyclades) or 600 mm/year (Dodecanese) under both climate scenarios (Fig. 57, bottom panel).

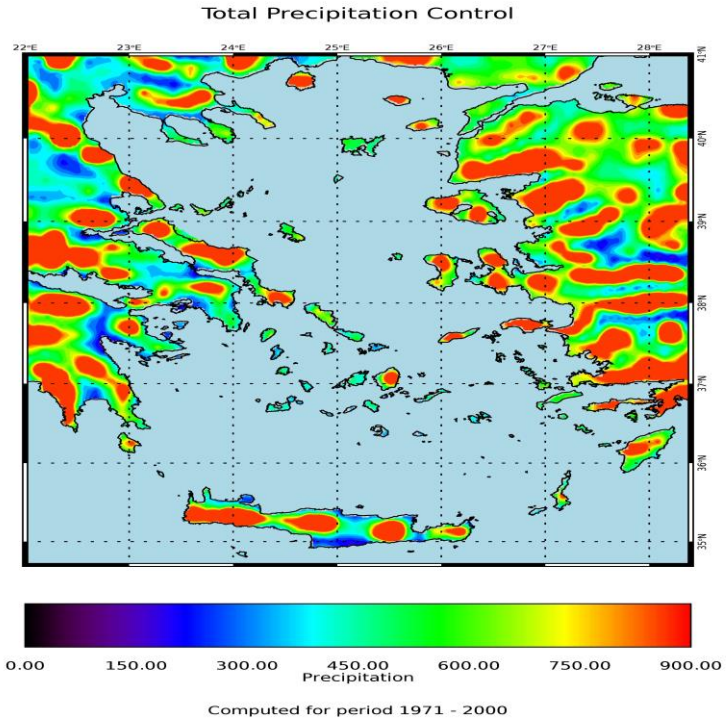

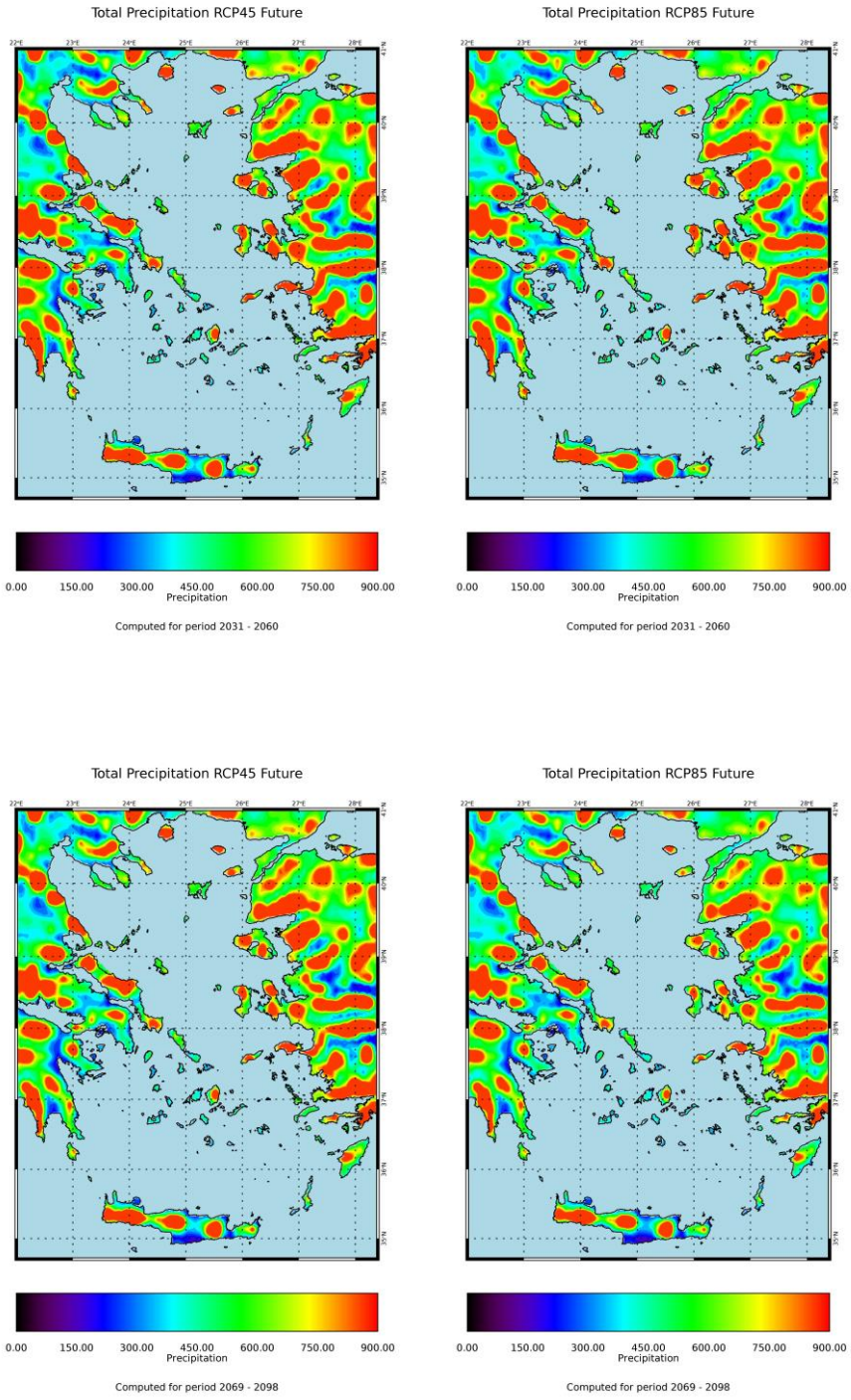

Figure 57 Average total annual precipitation for Aegean during the control period 1971-2000 (top panel), the near future period 2031-2060 (middle panel) and the distant future period 2069-2098 (bottom panel), under the future scenarios RCP4.5 (left column) and RCP8.5 (right column).

4.5 Extreme precipitation

Number of days with PR>10mm and PR>20mm

The average number of days with precipitation greater than 10mm (heavy precipitation) is variable across the Aegean, with about 16 days/year on average for the control period, except for mountainous areas (Crete, Naxos, Chios, Lesbos and Rhodes) where there may be up to 50 days/year (Fig. 58). This index shows almost no change in the near future compared to the control period (Fig. 58 middle panel). A small decrease of 5 days/year is noted for the Aegean area in the distant future period (Fig. 58 bottom panel).

Similarly, most Aegean islands show no change in very heavy precipitation days (number of days with precipitation greater than 20mm) in the near future, while slight decreases from 8 to 5 days are projected for the distant future (Fig. 59).

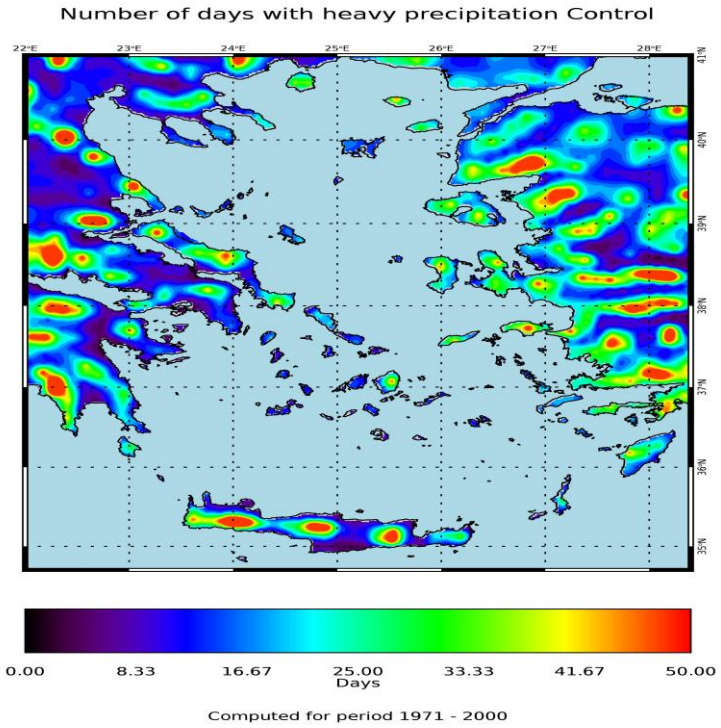

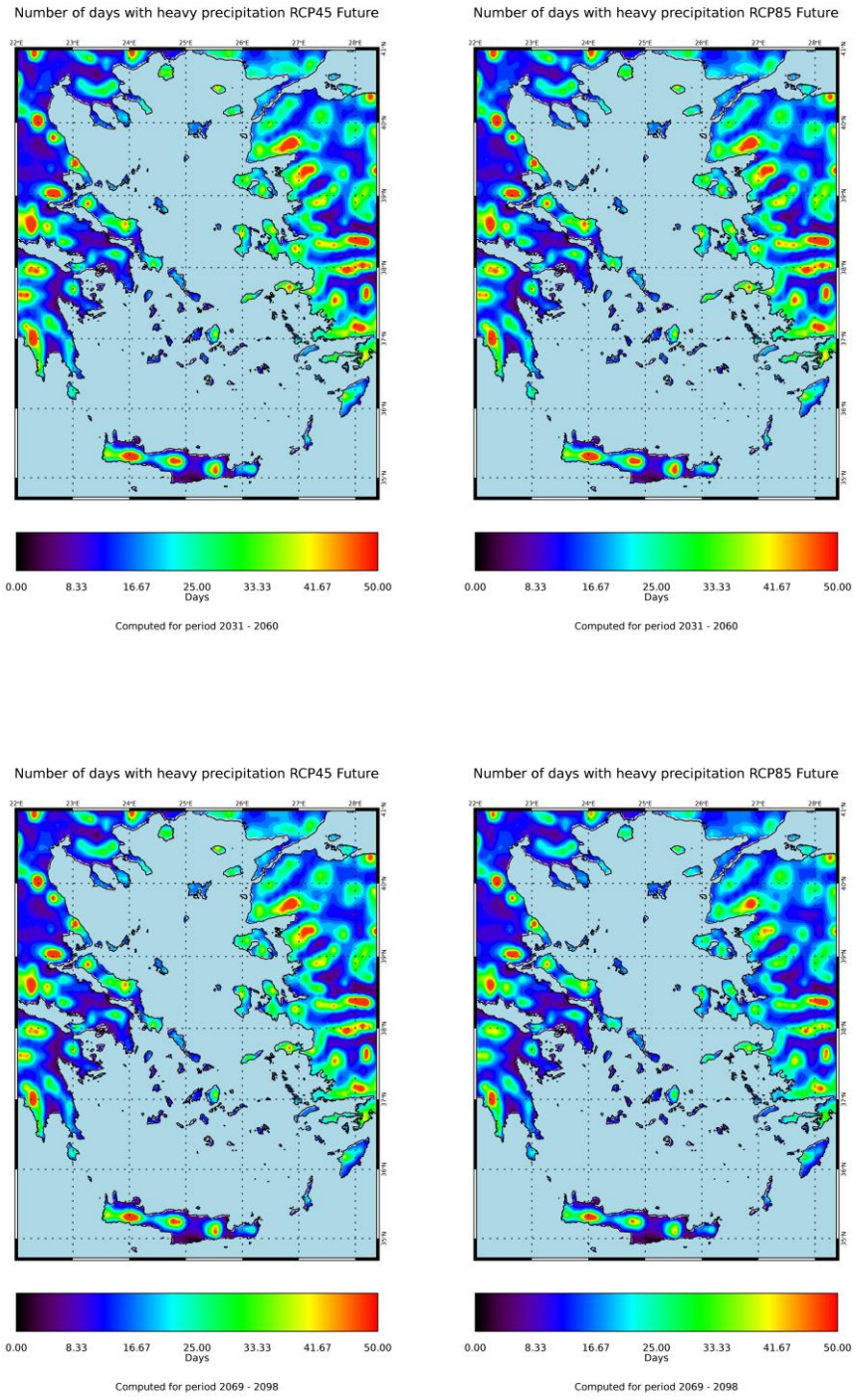

Figure 58 Average annual number of days with precipitation >10mm (heavy precipitation) for Aegean during the control period 1971-2000 (top panel), the near future period 2031-2060 (middle panel) and the distant future period 2069-2098 (bottom panel), under the future scenarios RCP4.5 (left column) and RCP8.5 (right column).

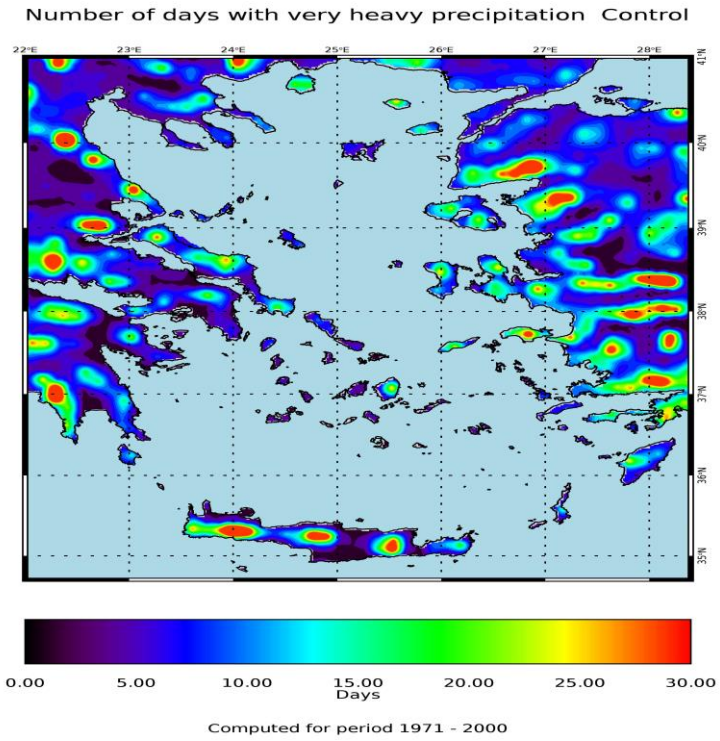
Number of days with very heavy precipitation Control
22°E
23°E
24°E
25°E
26°E
27°E
28°E
41°N
40°N
39°N
38°N
37°N
36°N
35°N
0.00
5.00
10.00
15.00
20.00
25.00
30.00
Days
Computed for period 1971 - 2000

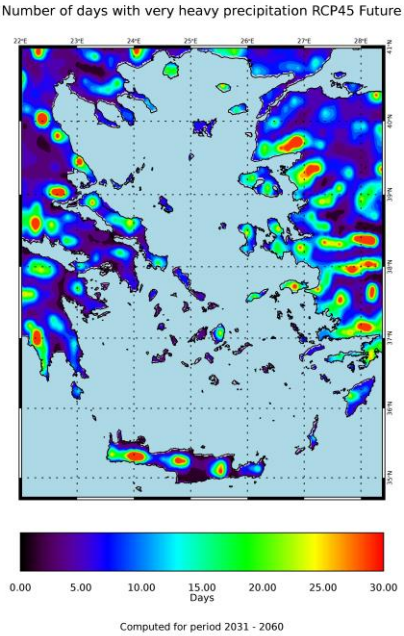
Number of days with very heavy precipitation RCP45 Future
0.00
5.00
10.00
15.00
20.00
25.00
30.00
Days
Computed for period 2031 - 2060

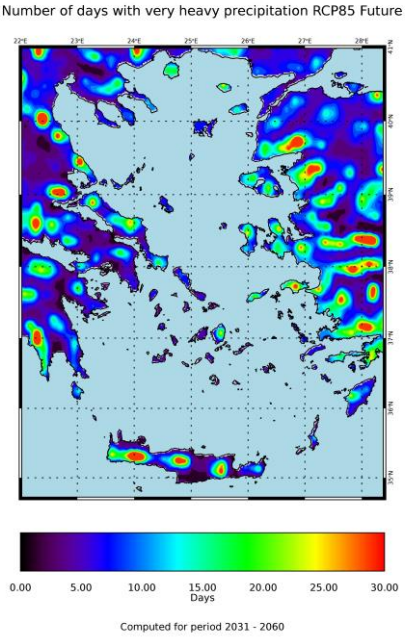
Number of days with very heavy precipitation RCP85 Future
0.00
5.00
10.00
15.00
20.00
25.00
30.00
Days
Computed for period 2031 - 2060

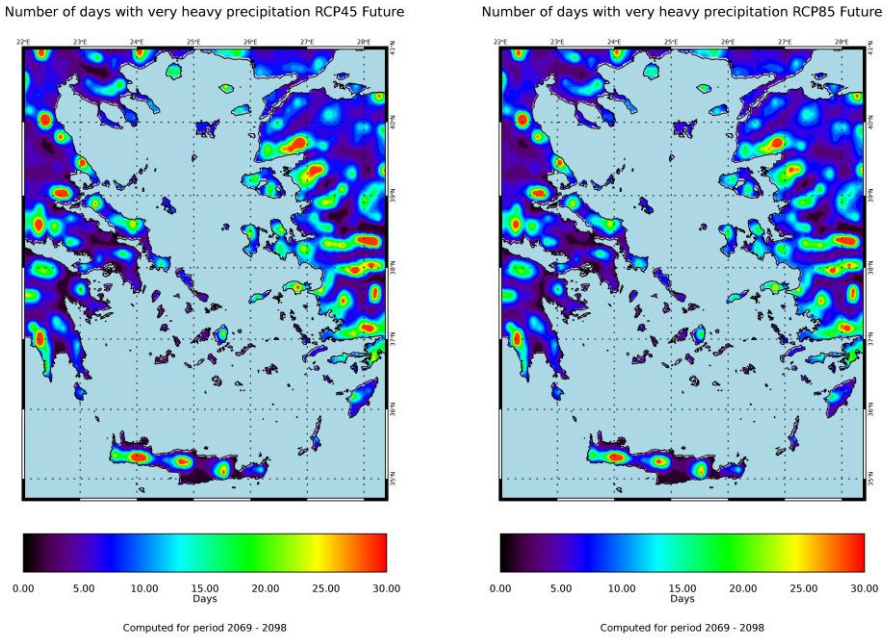

Figure 59 Average annual number of days with precipitation >10mm (heavy precipitation) for Aegean during the control period 1971-2000 (top panel), the near future period 2031-2060 (middle panel) and the distant future period 2069-2098 (bottom panel), under the future scenarios RCP4.5 (left column) and RCP8.5 (right column).

Precipitation extremes: Average maximum 1-day precipitation

The average maximum 1-day precipitation amount (precipitation sums for 1-day intervals) is about 35 mm/year (parts of Crete and South Cyclades) to 55 mm/year (rest of Aegean islands) over the historical (control) period (Fig. 60). Simulations show negligible changes in the near future. Increases are projected in the distant future, especially under the RCP 8.5 scenario, of 45 mm/year to 65 mm/year in the aforementioned areas respectively.

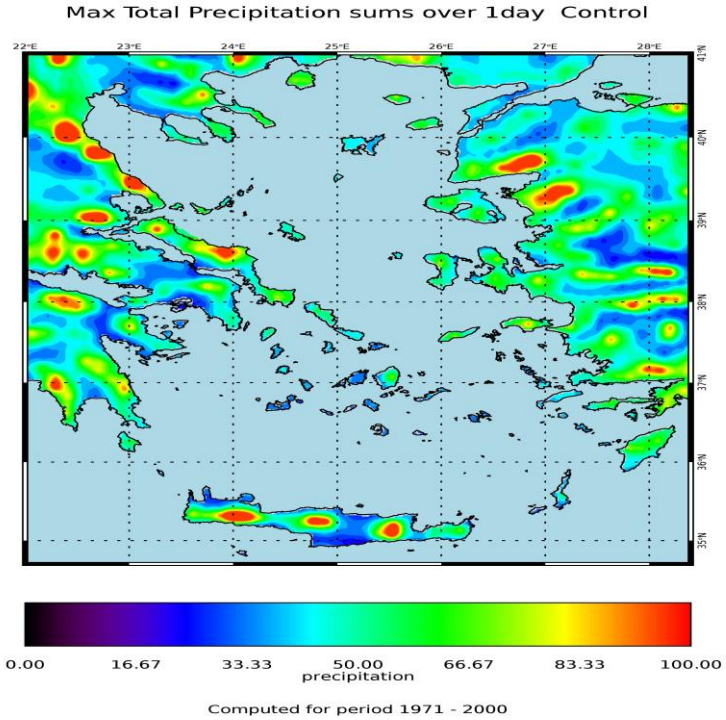
Max Total Precipitation sums over 1day Control
22°E
23°E
24°E
25°E
26°E
27°E
28°E
41°N
40°N
39°N
38°N
37°N
36°N
35°N
0.00
16.67
33.33
50.00
66.67
83.33
100.00
precipitation
Computed for period 1971 - 2000

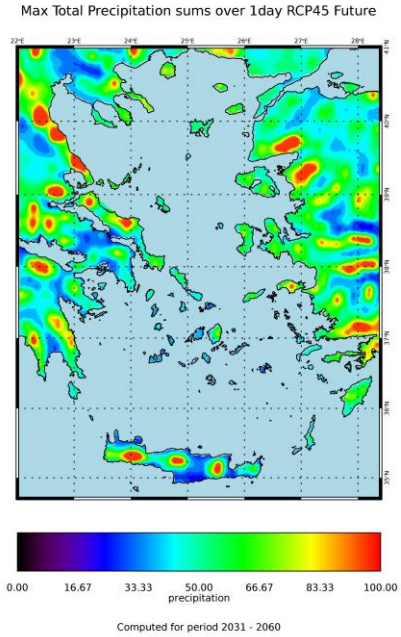
Max Total Precipitation sums over 1day RCP45 Future
0.00
16.67
33.33
50.00
66.67
83.33
100.00
precipitation
Computed for period 2031 - 2060

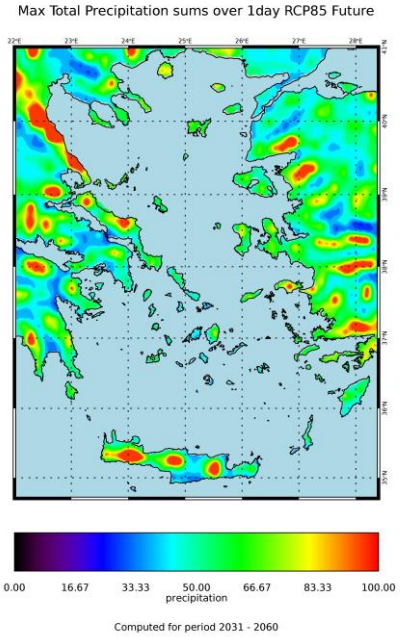
Max Total Precipitation sums over 1day RCP85 Future
0.00
16.67
33.33
50.00
66.67
83.33
100.00
precipitation
Computed for period 2031 - 2060

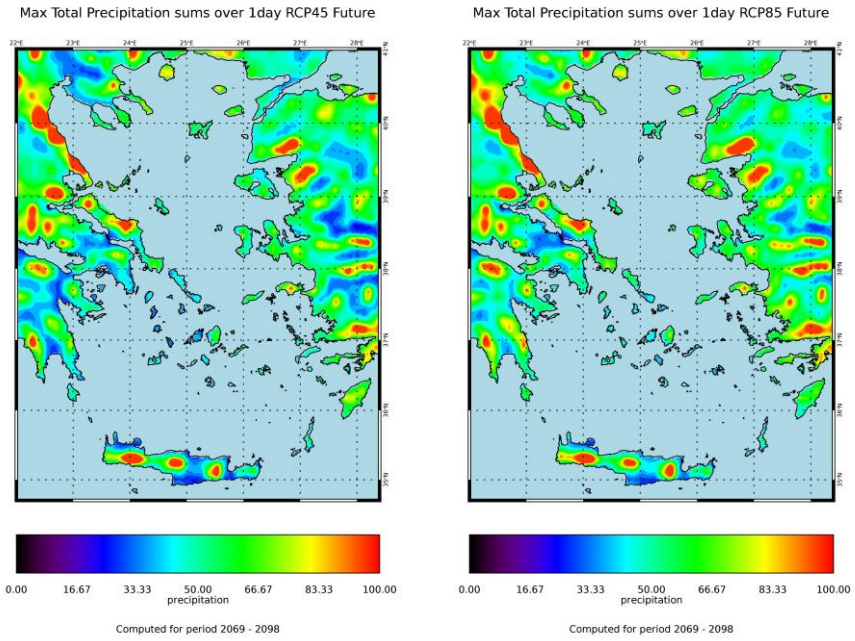

Figure 60 Annual trends for the maximum total precipitation sums over 1 day for the Aegean during the control period 1971-2000 (top panel), the near future period 2031-2060 (middle panel) and the distant future period 2069-2098 (bottom panel), under the future scenarios RCP4.5 (left column) and RCP8.5 (right column).

Maximum length of dry spell (PR<1mm)

Simulations of the maximum length of dry spells (Maximum length of consecutive days with precipitation; PR less than 1mm) show large future increases. The maximum annual length of a dry spell was on average ~66 days/year (North Aegean, Central Crete) to ~80 days/year (South Cyclades, Dodecanese) over the control period (Fig. 61). In the near future, maximum length of dry spell increases to ~90 days/year (North Aegean, Central Crete) to ~120 days/year (South Cyclades, Dodecanese) under the RCP 4.5 and to ~110 days/year for almost all Aegean area under the RCP 8.5 scenario (Fig. 61, middle panel). In the distant future period (Fig. 61, bottom panel), dry spells last for ~110 days/year across the Aegean area and reach ~130 days/year in South Crete (both scenarios).

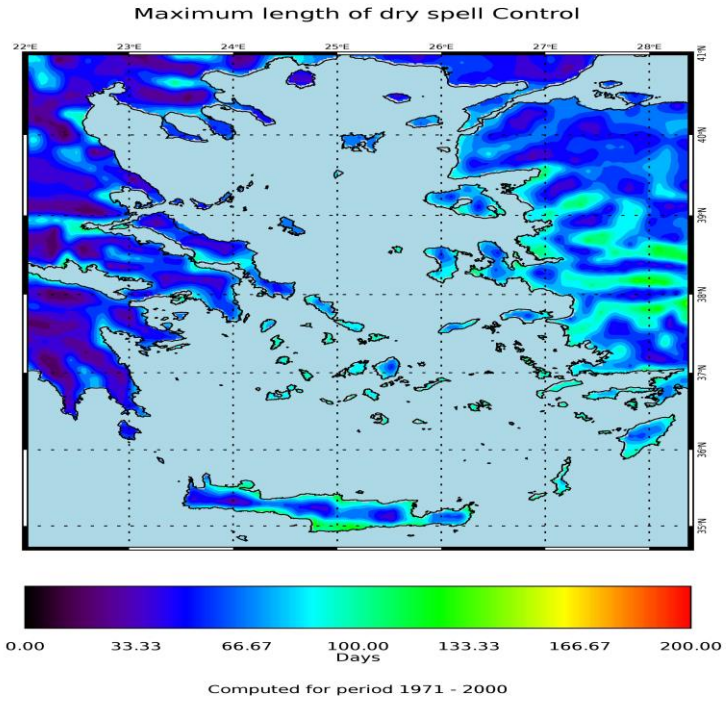
Maximum length of dry spell Control
22°E
23°E
24°E
25°E
26°E
27°E
28°E
41°N
40°N
39°N
38°N
37°N
36°N
35°N
0.00
33.33
66.67
100.00
133.33
166.67
200.00
Days
Computed for period 1971 - 2000

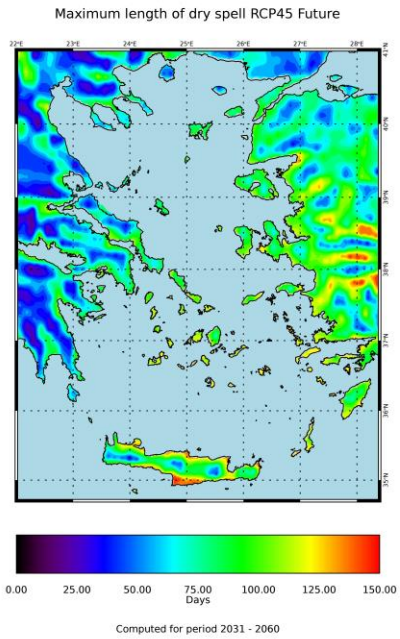
Maximum length of dry spell RCP45 Future
0.00
25.00
50.00
75.00
100.00
125.00
150.00
Days
Computed for period 2031 - 2060

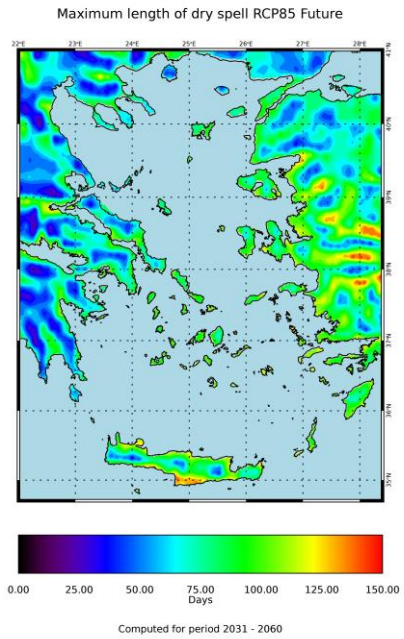
Maximum length of dry spell RCP85 Future
0.00
25.00
50.00
75.00
100.00
125.00
150.00
Days
Computed for period 2031 - 2060

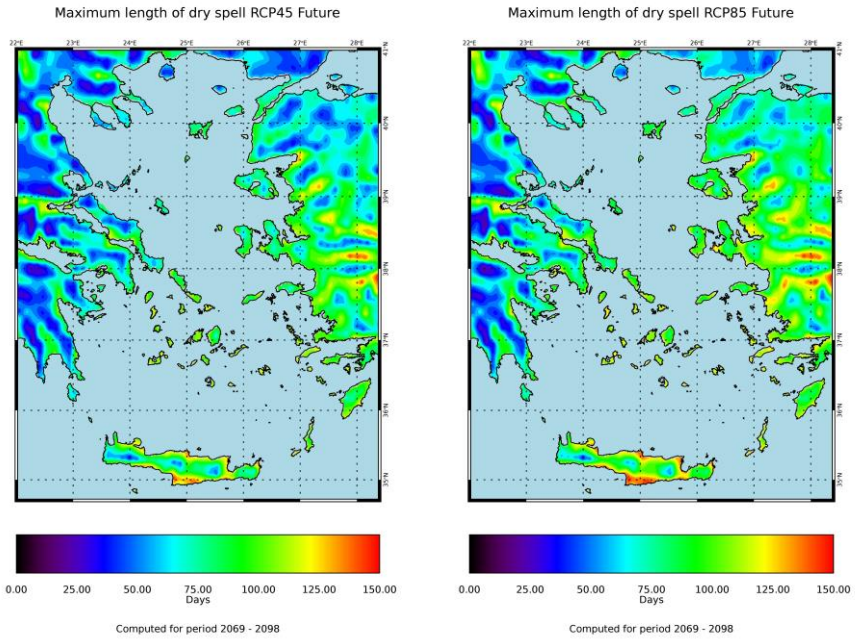

Figure 61 Average maximum length of dry spell (days with precipitation <1mm) for the Aegean region during the control period 1971-2000 (top panel), the near future period 2031-2060 (middle panel) and the distant future period 2069-2098 (bottom panel), under the future scenarios RCP4.5 (left column) and RCP8.5 (right column).

5. CONCLUSIONS

The RCA4 regional climate model SMHI with boundary conditions from the global HadGEM-ES model of the Met Office Hadley Centre (MOHC) was found to give the best results for the Aegean region following detailed evaluation.

We present first **fine-resolution simulation results** for the location of Andros Island, extracted from the SMHI-MOHC model, with daily data for the period 1971-2100. Results are presented for the control period (1971-2000) and the near future and distant future periods (2031-2060 and 2071-2100, respectively) under emission scenarios RCP4.5 and RCP8.5.

The bias-correction procedure of the climate model uses the general Cumulative Distribution Function transform method (CDFt). Long-term meteorological records are essential for this bias-correction procedure, which are lacking for Andros Island. We therefore compared the available meteorological record of Andros to long meteorological records from nearby stations. Assessment of meteorological station data of Elliniko (eastern Attika; 1964-2014), Naxos (1964-2014) and Andros Islands (2011-2017) show good correlation of [1] average monthly- and extreme air temperatures, and [2] long-term precipitation patterns. This correlation validates the use of the Naxos meteorological station data for the bias-correction procedure.

Simulations show that there are statistically significant temperature increases in the near- and distant future under both scenarios, with the largest increases projected under the RCP8.5 scenario. Annual mean maximum and minimum temperatures are set to increase progressively over the 21st century; here we summarise the main values, giving a pair of numbers with the first referring to RCP4.5 and the second to RCP8.5. These increases amount to 2-2,4 ^{o}C (near future) and 2,9-4,4 ^{o}C (distant future) for T_{max}, and to 2,2-2,7 ^{o}C (near future) and 3-4,9 ^{o}C (distant future) for T_{min}. The largest temperature increases are projected for summer and autumn, while increase for winter and spring are about 1 ^{o}C lower under both RCP scenarios.

The amount of hot days (T_{max}>30^{o}C) and tropical nights (T_{min}>20^{o}C) also incur statistically significant increases in the near and distant future. Hot days increase in the near future by 23-32 days/year, and by 45-75 days/year in the distant future. Tropical nights, meanwhile, increase in the near future by 43-51 days/year, and by 57-82 days/year in the distant future. Heatwaves (T_{max}>35^{o}C) increase from 0,5 days/year to 2-6 days/year in the near future and 4-15 days/year in the distant future. Extreme temperatures mainly occurred during summer over the historical (control) period. However, this is projected to change in the near- and distant future. The increase in heatwaves (T_{max}>35^{o}C) takes mainly place over the summer. About 10 days/year in summer are characterised as hot days (T_{max}>30^{o}C) over the control period; projected increases will mainly occur in summer, although 5-10 hot days/year may occur in autumn in the distant future. Of the about 85 tropical nights (T_{min}>20^{o}C) that occurred per year over the control period, 70 happened in summer and about 15 in autumn. In the near- and distant future, tropical nights will take place over the whole summer, and 10-20 days in spring to 40-60 days in autumn.

Total annual precipitation is set to decrease statistically significantly over the coming century under both climate scenarios, while the maximum length of dry spells (PR<1mm) is statistically increasing. However, extreme precipitation events (as indicated by the number

of days with PR>10mm and maximum 1-day precipitation in mm) are not set to change statistically significantly in the near- to distant future.

Total annual precipitation over the control period stands at about 450mm/year and is highly variable. Future precipitation variability is set to increase, while total precipitation is projected to decrease by 17,7-13,2% (RCP 4.5 and RCP8.5, respectively) in the near future, and by 18,9-23,8% (RCP 4.5 and RCP8.5, respectively) in the distant future. A seasonal breakdown of projected precipitation indicates that precipitation is set to decrease most over winter and autumn (the "wet season"), by up to 25-34%. Spring precipitation amounted to ~60mm in the historical period; this is projected to decrease by ~10mm, focusing on the distant future. Summer precipitations decreases from ~15mm to ~5mm in the near- and distant future, and becomes much more erratic.

Extreme precipitation events are not projected to change much in the near- to distant future. Heavy precipitation days (PR>10mm) decrease statistically non-significantly from 11 to 10 days in the distant future. Heavy precipitation days occur mostly in winter and autumn, and to a lesser degree in spring, while rarely taking place during summer. Overall, there are no changes to this distribution projected in the future. The maximum 1-day precipitation of about 55mm does not change, while the maximum 5-day precipitation falls statistically non-significantly from 90mm to about 80mm in the distant future. The seasonality of the maximum 1-day precipitation and maximum 5-day precipitation does not appear to change in the future. Average events decrease in magnitude in the following order: winter, autumn, spring and summer. The variability of extreme precipitation events becomes much greater in future, while the relative magnitude/frequency of such events is increasing given the overall decrease in annual / seasonal precipitation.

Future simulations show large, statistically significant, increases in the maximum length of dry spells (with PR < 1mm). The maximum annual length of a dry spell was on average 59 days over the control period, increasing by 73 (RCP 4.5) – 60 (RCP 8.5) days in the near future and by 72 (RCP 4.5) - 83 (RCP 8.5) days in the distant future. When there is a seasonal breakdown of dry spells, their length is 20 to 80 days in summer, and 5-30 days in all other seasons over the control period. In the near- and distant future period, dry spells in summer lasts ~90 days (i.e. the entire season). The length of dry spells varies from 20-90 days in spring, and 10-50 days in winter and autumn. It should be noted that spring and summer dry spells are more severe in the near future under the RCP 4.5 scenario.

Geographical maps for the **Aegean** depicting **coarse-resolution** changes in climatic indices at the horizontal resolution of ~12km were constructed based on model simulations. These model results could not be bias-corrected as the wider Aegean is not covered by the European gridded observational E-OBS database. Therefore, model data spanning 1950 to 2098 were split into a control period (1971-2000) and two future periods (2031-2060 and 2069-2098) under two IPCC emissions scenarios, namely the RCP4.5 and the RCP8.5, that were compared and evaluated.

Coarse-resolution simulation results show similar climate change trends as the fine-resolution study of Andros Island. The annual averaged **maximum** and **minimum temperatures** are set to increase across the wider Aegean region in the near- and distant

future, especially under the RCP8.5 climate change scenario. Temperature increases are in the range of 4-6^{o}C, and are largest in the E Aegean and least in the north. All extreme temperature indices are projected to increase considerably in the future. **Hot days** (T_{max}>30^{o}C) are to increase three- to six-fold, reaching up to 75-80 days/year in the E-N Aegean in the distant future. **Heatwave** days (T_{max} >35^{o}C) show also large increases, counting 30-50 days/year in the distant future; lowest values are registered for the Cyclades / Crete and the highest for the Dodecanese / N Aegean. **Tropical nights** (T_{min}>20^{o}C) are to double and triple in the near- to distant future for all Aegean Islands.

Total **annual precipitation** is to decrease significantly in the distant future across the region, by 15-25%, while large differences remain between- and within islands determined by geographical position and mountain height. **Extreme** precipitation indices only show minor decreases in the near- and distant future, while the maximum 1-day precipitation amount even records a minor increase in the distant future. The maximum **length** of **dry spells** (PR<1mm) shows large increases across the Aegean under both RCP scenarios. This length will double in the N Aegean / Crete and increase by 50% in the SE Aegean.

Based on these simulations, it is recommended that heat and drought-resistant varieties of crops without the need for irrigation should be prioritized and promoted in climate-proof island agriculture. The frequency and magnitude of floods triggered by extreme precipitation events should in principle not change as the relevant indices remain broadly similar. However, the future vegetation cover and composition is likely to change under influence of the declining annual precipitation and the increasing length of dry spells. In that case, flood frequency and magnitude may change as well, as land-cover and –use play important roles in their generation.

REFERENCES

Bellprat, O., Kotlarski, S., Lüthi, D., & Schär, C. (2012a). Exploring Perturbed Physics Ensembles in a Regional Climate Model. Journal of Climate, 25(13), 4582–4599. https://doi.org/10.1175/JCLI-D-11-00275.1

Clarke, L., J. Edmonds, H. Jacoby, H. Pitcher, J. Reilly, R. Richels., (2007) Scenarios of Greenhouse Gas Emissions and Atmospheric Concentrations. Sub-report 2.1A of Synthesis and Assessment Product 2.1 by the U.S. Climate Change Science Program and the Subcommittee on Global Change Research. Department of Energy, Office of Biological & Environmental Research, Washington, 7 DC., USA, 154 pp.

CYPADAPT. (2013). Report on the future climate change impact, vulnerability and adaptation assessment for the case of Cyprus. Deliverable 3.4, project CYPADAPT LIFE10 ENV/CY/000723. Available at http://uest.ntua.gr/cypadapt/wp-content/uploads/DELIVERABLE3.4.pdf

Diciccio, 1996. Bootstrap confidence intervals. *Statistical Science*, 11 (3), 189–228. doi:10.1214/ss/1032280214

Diffenbaugh, N.S., Pal, J.S., Giorgi, F., Gao, X., (2007). Heat stress intensification in the Mediterranean climate change hotspot. Geophys. Res. Lett. 34(11). http://dx.doi.org/10.1029/2007GL030000

Founda, D., Giannakopoulos, C., (2009). The exceptionally hot summer of 2007 in Athens, Greece—a typical summer in the future climate? Global Planet. Change 67(3), 227-236.

Giannakopoulos, C., Le Sager, P., Bindi, M., Moriondo, M., Kostopoulou, E., Goodess, C. M., (2009). Climatic changes and associated impacts in the Mediterranean resulting from a 2 C global warming. Global Planet. Change 68(3), 209-224.

Giorgi, F., (2006). Climate change hot-spots. Geophys. Res. Lett. 33(8). http://dx.doi.org/10.1029/2006GL025734

Giorgi, F., and X. Bi (2005). Updated regional precipitation and temperature changes for the 21st century from ensembles of recent AOGCM simulations, Geophys. Res. Lett., 32, L21715, doi:10.1029/2005GL024288.

Giorgi, F., Lionello, P. (2008). Climate change projections for the Mediterranean region. Global Planet. Change 63(2), 90-104.

González Hidalgo, J. C., De Luís, M., Raventós, J., & Sánchez, J. R. (2003). Daily rainfall trend in the Valencia Region of Spain. Theoretical and Applied Climatology, 75(1), 117-130. doi: 10.1007/s00704-002-0718-0

Goubanova, K., and L. Li (2007). Extremes in temperature and precipitation around the Mediterranean basin in an ensemble of future climate scenario simulations, Global Planet. Change, 57, 27–42, doi:10.1016/j.gloplacha.2006.11.012.

Hanel, M., & Buishand, T. A. (2012). Multi-model analysis of RCM simulated 1-day to 30-day seasonal precipitation extremes in the Czech Republic. Hydrology Conference 2010, 412–413 (Supplement C), 141–150. https://doi.org/10.1016/j.jhydrol.2011.02.007

Haylock, M. R., Hofstra, N., Klein Tank, A. M. G., Klok, E. J., Jones, P. D., & New, M. (2008). A European daily high-resolution gridded data set of surface temperature and precipitation for 1950–2006. Journal of Geophysical Research: Atmospheres, 113(D20). https://doi.org/10.1029/2008JD010201

Herrera, S., Fita, L., Fernández, J., & Gutiérrez, J. M. (2010). Evaluation of the mean and extreme precipitation regimes from the ENSEMBLES regional climate multimodel simulations over Spain. Journal of Geophysical Research: Atmospheres, 115(D21). https://doi.org/10.1029/2010JD013936

Hertig, E., Jacobeit, J., (2008). Downscaling future climate change: Temperature scenarios for the Mediterranean area. Global Planet. Change 63(2), 127-131.

Hofstra, N., Haylock, M., New, M., & Jones, P. D. (2009). Testing E-OBS European high-resolution gridded data set of daily precipitation and surface temperature. Journal of Geophysical Research: Atmospheres, 114(D21). https://doi.org/10.1029/2009JD011799

Hofstra, N., New, M., & McSweeney, C. (2010). The influence of interpolation and station network density on the distributions and trends of climate variables in gridded daily data. Climate Dynamics, 35(5), 841–858. https://doi.org/10.1007/s00382-009-0698-1

IPCC: Climate Change 2013: The Physical Science Basis. Contribution of Working Group I to the Fifth Assessment Report of the Intergovernmental Panel on Climate Change, Cambridge University Press, Cambridge, United Kingdom and New York, NY, USA, 1535 pp., 2013.

JRC (European Commission's Joint Research Centre). (2014). Climate impacts inEurope. The JRC PESETA II Project. JRC Scientific and Policy Reports, EUR 26586EN.

Kostopoulou, E., Giannakopoulos, C., Hatzaki, M., Karali, A., Hadjinicolaou, P., Lelieveld, J., Lange, M.A., (2014). Spatio-temporal patterns of recent and future climate extremes in the eastern Mediterranean and Middle East region. Nat. Hazards Earth Syst. Sci. 14(6), 1565-1577.

Kotlarski, S., Keuler, K., Christensen, O. B., Colette, A., Déqué, M., Gobiet, A., Wulfmeyer, V. (2014). Regional climate modeling on European scales: a joint standard evaluation of the EURO-CORDEX RCM ensemble. Geoscientific Model Development, 7(4), 1297–1333. https://doi.org/10.5194/gmd-7-1297-2014

Kuglitsch, F. G., A. Toreti, E. Xoplaki, P. M. Della-Marta, C. S. Zerefos, M. Türkeş, and J. Luterbacher (2010). Heat wave changes in the eastern Mediterranean since 1960, Geophys. Res. Lett., 37, L04802, doi:10.1029/2009GL041841.

Kyselý, J., & Plavcová, E. (2010). A critical remark on the applicability of E-OBS European gridded temperature data set for validating control climate simulations. Journal of Geophysical Research: Atmospheres, 115(D23). https://doi.org/10.1029/2010JD014123

Maraun, D., Osborn, T. J., & Rust, H. W. (2012). The influence of synoptic airflow on UK daily precipitation extremes. Part II: regional climate model and E-OBS data validation. Climate Dynamics, 39(1), 287–301. https://doi.org/10.1007/s00382-011-1176-0

Michelangeli, P. A., Vrac, M., and Loukos, H.: Probabilistic downscaling approaches: application to wind cumulative distribution functions, Geophys. Res. Lett., 36, L11708, doi:10.1029/2009GL038401, 2009.

Min, S.-K., Zhang, X., Zwiers, F. W., & Hegerl, G. C. (2011). Human contribution to more-intense precipitation extremes. Nature, 470, 378. doi: 10.1038/nature09763

Moberg, A., & Jones, P. D. (2005). Trends in indices for extremes in daily temperature and precipitation in central and western Europe, 1901–99. International Journal of Climatology, 25(9), 1149-1171. doi: doi:10.1002/joc.1163

Mudelsee, M., Börngen, M., Tetzlaff, G., & Grünewald, U. (2003). No upward trends in the occurrence of extreme floods in central Europe. Nature, 425, 166. doi: 10.1038/nature01928

Nastos, P. T. and Zerefos, C. S. (2007): On extreme daily precipitation totals at Athens, Greece, Adv. Geosci., 10, 59-66.

Oikonomou, C., Flocas, H. A., Hatzaki, M., Asimakopoulos, D.N., Giannakopoulos, C., (2008). Future changes in the occurrence of extreme precipitation events in eastern Mediterranean. Global NEST J. 10(2), 255-262.

Oki, T., & Kanae, S. (2006). Global Hydrological Cycles and World Water Resources. Science, 313(5790), 1068.

Pall, P., Aina, T., Stone, D. A., Stott, P. A., Nozawa, T., Hilberts, A. G. J., Allen, M. R. (2011). Anthropogenic greenhouse gas contribution to flood risk in England and Wales in autumn 2000. Nature, 470, 382. doi: 10.1038/nature09762

Rajczak, J., Pall, P., & Schär, C. (2013). Projections of extreme precipitation events in regional climate simulations for Europe and the Alpine Region. Journal of Geophysical Research: Atmospheres, 118(9), 3610–3626. https://doi.org/10.1002/jgrd.50297

Riahi, K., A. Gruebler and N. Nakicenovic., (2007) Scenarios of long-term socio- economic and environmental development under climate stabilization, Technological Forecasting and Social Change 74, 7, 887-935.

Smith, S. J., Wigley, T.M.L., (2006) MultiGas forcing stabilization with minicam. The Energy Journal Special issue, 3, 373–392.

Tank, A. M. G. K., & Können, G. P. (2003). Trends in Indices of Daily Temperature and Precipitation Extremes in Europe, 1946–99. Journal of Climate, 16(22), 3665-3680. doi: 10.1175/1520-0442(2003)016

Thomson, A. M., Calvin, K. V., Smith, S. J., Kyle, G. P., Volke, A., Patel, P., Delgado-Arias, S., Bond-Lamberty, B., Wise, M. A., Clarke, L. E. et al., (2011) RCP4.5: a pathway for stabilization of radiative forcing by 2100. Climatic Change. 109, 77. https://doi.org/10.1007/s10584-011-0151-4.

Tolika, K., Maheras, P., Tegoulias, I., (2009). Extreme temperatures in Greece during 2007: Could this be a 'return to the future'?. Geophys. Res. Lett. 36(10).

van der Schriek, T. and Giannakopoulos, C. (2017), Determining the causes for the dramatic recent fall of Lake Prespa (SW Balkan). Hydrological Sciences Journal 7: 1131-1148.

van Vuuren, D.P., Edmonds, J., Kainuma, M. et al., (2011) The representative concentration pathways: an overview. Climatic Change, 109, 5-31. https://doi.org/10.1007/s10584-011-0148-z.

Varotsos *et al*., 2013. Statistical estimations of the number of future ozone exceedances due to climate change in Europe. *Journal of Geophysical Research of the Atmosphere*, 118, 6080–6099. doi:10.1002/jgrd.50451

Vrac, M., Drobinski, P., Merlo, A., Herrmann, M., Lavaysse, C., Li, L., & Somot, S. (2012). Dynamical and statistical downscaling of the French Mediterranean climate: uncertainty assessment. Natural Hazards and Earth System Sciences,12, 2769-2784.

Wise, M., Calvin, K., Thomson, A., Clarke, L., Bond-Lamberty, B., Sands, R., Smith, S. J., Janetos, A., Edmonds, J. (2009). Implications of limiting CO2 concentrations for land use and energy. Science, 324, 1183–1186.

Zanis, P., Kapsomenakis, I., Philandras, C., Douvis, K., Nikolakis, D., Kanellopoulou, E., Zerefos, C. and Repapis, C. (2009). Analysis of an ensemble of present day and future regional climate simulations for Greece. Int. J. Climatol., 29: 1614–1633. doi:10.1002/joc.1809.

Zolina, O., 2012. Change in intense precipitation in Europe, in: Kundzewicz, Z.W. (Ed.), Changes in Flood Risk in Europe. Special Publication No.10. IAHS Press, Wallingford, Oxfordshire, UK